Effect of annealing on physicochemical properties of quinoa, amaranth, taro, potato and maize starch

Zifan Su

(479122529)

A thesis submitted in fulfillment of the requirements for the degree

of Master of Science in Food Science

The University of Auckland

September 2022

Abstract

Native starch has the characteristics of a high swelling effect and low gelatinization temperature, which cannot meet the needs of some industries. As a physical modification, annealing treatment is mild and non-polluting. In order to study the effect of annealing treatment on starch from different plant sources, small-granular starch quinoa, amaranth and taro starch, large-granular starch potato and maize starch were selected according to the size of starch granules for annealing treatment under the same conditions. The granule morphology, swelling, gelatinization, pasting, gelling and rheological properties of starch before and after treatment were carried out. The results show that the effect of annealing on starch depends on the physicochemical properties of starch.

Key words: starch, annealing, small-granular starch, quinoa starch, amaranth starch, taro starch, potato starch, maize starch, gelatinization, rheology.

Acknowledgements

First, I would like to express my sincere thanks to my mentor Dr Fan Zhu. Thank him for cultivating me in my teaching and research work, providing me with help and support, and answering my questions. Second, I would like to thank Dr Li Guantian for his help, thank him for helping me solve the problems I encountered in the experiment and for guiding me on the right path. Then I would like to express my gratitude to the Sreeni Pathirana technician for training me on how to use the instrument, helping me solve many problems on the instrument, and supporting my experiments. Thanks to my food science teacher for educating and guiding me. At the same time, I would also like to thank the team members for their help and care. Finally, I sincerely thank my parents for their care and encouragement. Thank you all for your help and support.

Table of Contents

List of Figures

List of Tables

List of Abbreviations

BD	Breakdown (Pa·s)
Cpv	Cool paste viscosity (Pa·s)
d (0.5)	Numerical median diameter
D [3,2]	Surface area moment mean diameter
D [4,3]	Mass moment mean diameter
DSC	Differential scanning calorimetry
g	Gram
g	Gravity
G'	Storage modulus
G''_{25}	The loss modulus at 90°C (Pa)
G'_{25}	The storage modulus at 25°C (Pa)
G''_{90}	The loss modulus at 90°C (Pa)
G'_{90}	The storage modulus at 90°C (Pa)
G''_{max}	The maximum loss modulus (Pa)
G'_{max}	The maximum storage modulus (Pa)
G''	Loss modulus (Pa)
h	Hour
Hpv	Hot paste viscosity (Pa·s)
K	Consistency coefficient ($Pa \cdot s^n$)
K_0	Yield stress (Pa)
MC%	Moisture content
mg	Milligram
min	Minute
N	Flow behavior index
n	Liquidity behavior index
Pt	Pasting temperature (°C)
Pv	Peak viscosity (Pa·s)
R	Retrogradation (%)

R^2	Coefficient of determination
SB	Setback (Pa·s)
SEM	Scanning electron microscopy
SP	Swelling power (g/g)
tan δ 25	The ratio of the loss modulus and the storage modulus at 25°C
tan δ 90	The ratio of the loss modulus and the storage modulus at 90°C
tan δ max	The ratio of the maximum loss modulus and the maximum storage modulus
T_c	Conclusion temperature (°C)
$T_{G'' max}$	The time of maximum loss modulus (°C)
$T_{G' max}$	The time of maximum storage modulus (°C)
T_o	Onset temperature (°C)
T_p	Peak temperature (°C)
WSI	Water solubility (%)
$\dot{\gamma}$	Shear rate (s^{-1})
ΔH	The change of enthalpy (J/g)
ΔT	Gelatinization temperature range (°C)

Chapter 1. Introduction

1.1 Background

Starch, as one of the basic ingredients of food, has the characteristics of pure nature, low price, wide distribution and is widely used in the production of raw industries (Zhu, 2018; Sadeghi et al., 2017). The plant source of starch affects its physicochemical properties, such as particle size, which are determined by the genotype of plants (Jayakody & Hoover, 2008). Starch granules are usually between 1 and 100 μm, while small-granular starch is less than 10 μm in size (Lindeboom, Chang & Tyler, 2004). Potato starch and maize starch are two common types of large-grained starches used in comparison with the three small-grained starches of quinoa, amaranth and taro. Modification can make starch meet more demands, and annealing is a physical modification with little impact on the human body and environment (Fonseca et al., 2021; Wang et al., 2017b). Previous studies on starch annealing were mostly focused on a certain starch, comparing two annealed starches and the effects of different treatment conditions on starch annealing. Annealing makes the starch more stable (Jayakody & Hoover, 2008). After Scanning electron microscopy, particle size distribution, gelatinization characteristics, X-ray diffraction, rheological behavior and gel characteristics of starch, it was found that the annealing treatment made the surface of most starches more rugged, the particle size increased slightly, and the paste Enthalpy and gelatinization temperature increase, relative crystallinity increases, swelling decreases and viscosity increases (Xu et al., 2018a; Hu et al., 2020; Sui & Kong, 2018; Marboh et al., 2022; Zhang et al., 2015). Annealing conditions also affect the effect of annealing (Jayakody & Hoover, 2008). Generally, the longer the annealing time, the closer the temperature is to the starting temperature of gelatinization, and the higher the water content, the more obvious the effect of annealing (Jayakody & Hoover, 2008; Xu et al., 2018b).

1.2 Research objectives

There are few studies on the annealing properties of quinoa, amaranth, and taro, and few have compared the effect of annealing on large-grained and small-grained starches. In this study, the three small-granular starches of quinoa, amaranth and taro were compared with the two large-granular starches of potato and maize under the same annealing conditions. Comparing the differences in particle state, crystalline morphology, thermal properties, swelling properties and rheological properties of starch between different plant sources and granule sizes. Independent samples t-tests were performed on the results to determine the significance of differences between the results.

1.3 Thesis structure

The first chapter of the dissertation briefly introduces the research background and presents the goals of the entire research. The second chapter is a literature review, detailing the structure, properties and characteristics of quinoa, amaranth, taro, potato and maize starch. The introduction and rationale of the annealing process is also included in this chapter, as well as the results of studies conducted by other researchers on the properties of annealed starch. The third chapter is about the materials, instruments, and specific operation methods of the experiment. The fourth chapter is the results and analysis of the physicochemical properties of the five starches before and after annealing, and the possible reasons are discussed. The fifth chapter is the summary and generalization of the whole article, and at the same time, the future research direction is assumed.

Chapter 2. Literature review

2.1 Introduce starch

2.1.1 Basic introduction to starch

Starch is one of the essential components of food (Zhu, 2018). Humans eating food containing starch has a long history (BeMiller & Whistler, 2009). Starch is produced through plant photosynthesis and widely exists in roots, stems, leaves, flowers, fruits and seeds (Alcázar-Alay & Meireles, 2015; Ai & Jane, 2015). In nature, starch exists in granular form (Wani et al., 2012). However, it can be modified and has a wide range of applications due to its high biocompatibility, safety, and low cost (Sadeghi et al., 2017).

Starch has many applications in the food industry, including baked goods, convenience foods, food packaging, and convenience foods (Fonseca et al., 2021). Starch used in flavor packaging materials can provide food with a longer shelf life and faster flavor recovery speed (Wang, Yuan & Yue, 2015). In addition to its main application in food, starch is also widely used in papermaking, materials, textiles, Pickering emulsion, medicine and other fields (Kulshreshtha et al., 2017; Ji et al., 2019; Fonseca et al., 2021).

The starch of higher plants contains amylose and amylopectin two polysaccharides (Wang, 2017; Jayakody & Hoover, 2008), and they account for more than 98% of the starch quality (Tester, Karkalas & Qi, 2004). In most starch, the amylose content is less than amylopectin (Kulshreshtha et al., 2017). Amylose and amylopectin (Figure 2.1.1.1) differ in structure and properties (Tester, Karkalas & Qi, 2004). Among them, amylose is a kind of linear polymer connected by α-(1,4) glycosidic bonds, and

amylopectin is a kind of bundle structure with many branches connected by α-(1,4) glycosidic bonds and α-(1,6) glycosidic bonds (Li et al., 2021; Wang, Jin & Yu, 2013). In general, the molecular weight of amylose is less than that of amylopectin (Wang et al., 2019). The molecular weight of the former is between 10^5 and 10^6, and the molecular weight of the latter is from 10^7 to 10^9 (Zhu, 2019b).

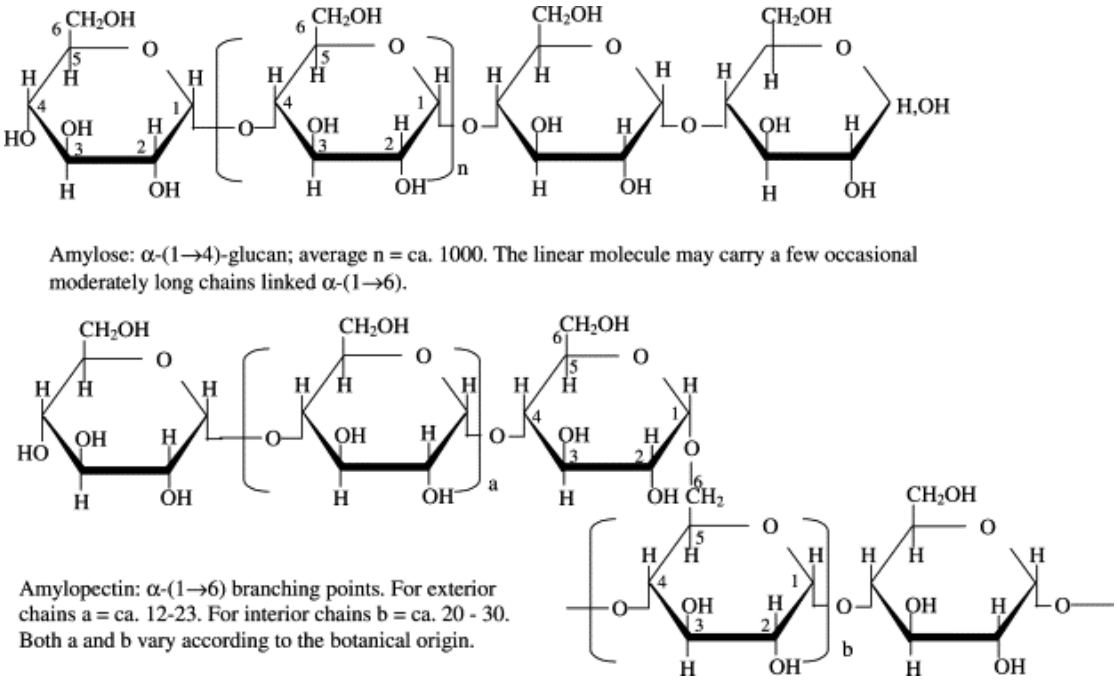

Figure 2.1.1.1 Structure of amylose and amylopectin. Adapted from Sui & Kong (2018)

Amylose and amylopectin macromolecules form semi-crystalline aggregated granules of various sizes, which ultimately constitute starch (Zavareze & Dias, 2011). The true amylose content usually is the apparent amylose, which differs from the measured amylose content because the measurement can be influenced by external amylopectin (Zavareze & Dias, 2011). Amylose is present in different amounts in different plant-derived starches (Sui & Kong, 2018). Starches such as maize, rice and wheat are high in amylose (Zavareze & Dias, 2011). Amylose is essential for the structural stability of starch granules (Wang et al., 2014). Therefore, amylose greatly influences the functional properties of starch, including thermal properties, gel

strength, swelling power and gelatinization (Sui & Kong, 2018). Amylopectin, on the other hand, has an effect on starch retrogradation. (Wang et al., 2021).

In nature, starch granules have a semi-crystalline structure formed by alternating concentric rings of crystalline and amorphous regions (Figure 2.1.1.2) (Carlstedt et al., 2015; Lavoisier & Aguilera, 2019). Among them, the semi-crystalline region is mainly amylopectin, and the amorphous region is composed of amylose and non-crystalline amylopectin (Carlstedt et al., 2015; Wang, Jin & Yu, 2013). There are different types of crystallization areas, which are determined by the length of the amylopectin short chains (Carlstedt et al., 2015). Amylose differs from amylopectin and is mainly distributed in the amorphous core of starch granules, while a small amount of amylose is also present in amylopectin clusters towards the outer surface of the granule (Wang, Jin & Yu, 2013). Amylopectin chains include three kinds of chains that form links with other chains, chains that form links with other chains and carry other chains, and long chains with reducing end groups in the molecule (Sui & Kong, 2018). Its structure can be determined by high-performance anion exchange chromatography and high-performance liquid chromatography (Sui & Kong, 2018).

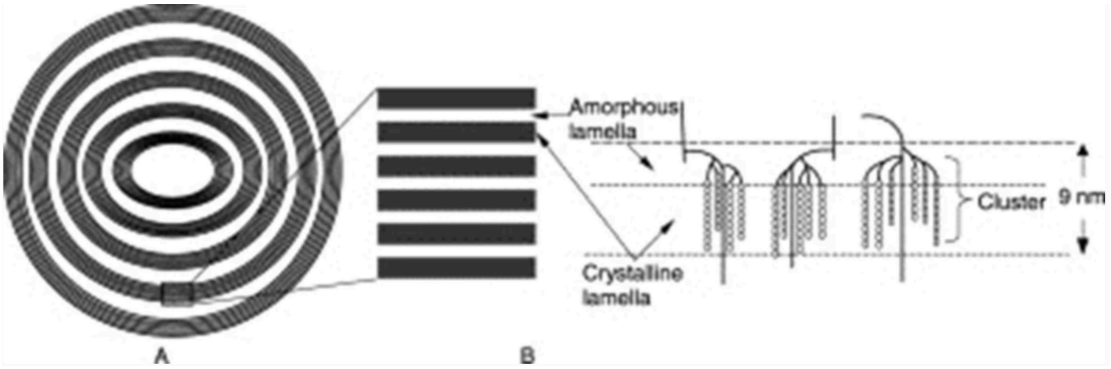

Figure 2.1.1.2 Structure of semi-crystalline. Adapted from Sui & Kong (2018)

Starch also contains trace components such as protein, ash, lipid, and phosphorus-containing compounds (Vamadevan & Bertoft, 2015; Sui & Kong, 2018). Table 2.1.1.1 shows that the content of trace substances in different types of starch is different. The composition is also affected by factors such as the separation technique

used to identify trace components and the growing season of the plants (Sui & Kong, 2018). Although the concentrations of these trace elements are low, they have a certain degree of influence on the properties of starch (Sui & Kong, 2018). Higher phosphorus content can result in higher strength of starch gels, while grain firmness increases due to higher protein content inside and on the surface of starch granules (Sui & Kong, 2018; Tester, Karkalas & Qi, 2004).

Starches are generally classified into three types. High amylose content, lenticular or disk-shaped starch with a diameter greater than 10 μm are classified as A-type starch granules (Li et al., 2016). B-type starch has a high amylopectin content, granule size smaller than 10 μm, and a polygonal or spherical shape (Li et al., 2016). C-type starch contains amylopectin, forming both A and B-type crystals (Buléon et al., 1998).

Table 2.1.1.1 Trace components in different starches

Starch	Lipids (%)	Proteins (%)	Phosphorus (%)	Ash (%)	Reference
Maize	0.6 - 0.8	0.3 - 0.4	0.03		Vamadevan & Bertoft, 2015
Wheat	0.3 - 0.8	0.3	0.06		Vamadevan & Bertoft, 2015
Barley	0.6 - 0.9	0.1	0.05 - 0.06		Vamadevan & Bertoft, 2015
Tapioca	0.03 - 0.1	0.2	0.01		Vamadevan & Bertoft, 2015
Potato	0.02 - 0.2	0.1 - 0.4	0.04 - 0.09		Vamadevan & Bertoft, 2015
Amorphophallus	0.088	0.21	0.045	0.95	Zhu, 2016

2.1.2 Glass transition temperatures

The glass transition temperature is an important parameter affecting the physical properties of starch and refers to the temperature at which the glassy polymer system in the amorphous region transforms into a rubbery state during the heating process (Biliaderis et al., 1986; Sui & Kong, 2018). Among them, the glass state has high chain stability, and the rubber state contains high energy (Sui & Kong, 2018). Glass transition temperatures can usually be measured by high sensitivity differential scanning calorimetry (Mizuno, Mitsuiki & Motoki, 1998). Water content greatly influences starch glass transition temperatures (Tester & Debon, 2000). The glass transition temperatures of starch decrease with increasing water content, falling to room temperature at about 25% water (Tester & Debon, 2000).

2.2 Introduce those five kinds of starch

2.2.1 Taro starch

Taro is a tuber crop that is widely grown worldwide (Dai et al., 2015). It grows mainly in tropical and subtropical regions and is a staple food source for many people (Pachuau et al., 2018; Lu et al., 2008; Simsek & El, 2012). The dry matter of taro contains 70 - 80% starch (Lu et al., 2008; Agama-Acevedo et al., 2011). Taro starch is also widely used in the packaging and pharmaceutical industries. Taro starch nanoparticles can be added to the starch films to improve their thermal stability and mechanical properties (Dai et al., 2015). Taro starch also can increase the dissolution efficiency of medicines and improve their bioavailability (Pachuau et al., 2018). The application of taro starch is determined by its physicochemical properties. Taro starch has a small diameter and is a small granule starch with polygonal and irregular shapes (Agama-Acevedo et al., 2011). Different varieties of taro starch, containing different amylose and amylopectin contents, have different physicochemical properties (Agama-Acevedo et al., 2011). In addition, the planting season and region where the taro is grown affect the physicochemical properties of taro starch (Agama-Acevedo et al., 2011).

2.2.2 Amaranth starch

In recent years, amaranth has regained popularity (Zhu, 2017). Amaranth is cultivated in Asia and America, and some varieties of amaranth have strong adaptability to the environment (Chandla, Saxena & Singh, 2017; Zhu, 2017). Amaranth is a good source of protein, vitamins and minerals (Chandla, Saxena & Singh, 2017; Gorinstein et al., 2002). Amaranth starch can be used in foods to replace part of its fat content without making significant differences in sensory evaluation (Malinski et al., 2003). Amaranth starch can also be used as a filler to prepare low-density polyethylene,

which can give the film higher performance, allowing it to be used in packaging applications (Ahamed et al., 1996).

2.2.3 Quinoa starch

Quinoa, a pseudocereal native to South America, has attracted attention for its high nutritional value (Ray et al., 2021). It contains all essential amino acids, rich in vitamins, minerals, and does not contain cholesterol or gluten (Gordillo-Bastidas et al., 2016). The starch content of quinoa seed is 32 - 69.2% (James, 2009). Quinoa starch can be used in packaging, catalysis reactions, and the pharmaceuticals industry (Steffolani, León & Pérez, 2013). A film can be prepared using quinoa starch, giving good barrier and mechanical properties (Araujo-Farro et al., 2010). Pickering emulsion prepared with modified quinoa starch has strong stability and emulsification properties (Li et al., 2019). In addition, due to the small size of quinoa starch, Pickering emulsion can provide a larger interface area when used for catalysis (Rayner et al., 2012; Zhu, 2019a). Quinoa has a low amylose content (~10%), a short average chain length, and more branches, while its amylopectin has a large number of short chains (Li, Xu & Zhu, 2019). This contributes to the physicochemical properties of quinoa starch which exhibits slower retrogradation, lower gelatinization temperature, and higher enzyme sensitivity and swelling power than other starches (Li, Xu & Zhu, 2019).

2.2.4 Potato starch

As the fourth largest global food crop, the potato has high dry matter and nutrient production efficiency (Ezekiel et al., 2013). Potato has been cultivated all around the world (Ezekiel et al., 2013). Its starch has the characteristics of high gel transparency, low gelatinization temperature, high viscosity, large swelling power , and less retrogradation (Xu et al., 2018a). Potatoes are rich in polyphenol compounds such as

chlorogenic acid, which has the effects of lowering cholesterol, lowering blood sugar, anti-oxidation and anti-cancer (Friedman, 1997). Potato starch can also be used in film preparation (Wilpiszewska & Czech, 2014). The glucose production rate caused by potato starch is low, so its dextrin can be used in the preparation of soft drinks, not only to replace part of the sugar but also to improve human intestinal flora (Kapusniak, & Nebesny, 2017; Xu et al., 2018a). Karlsson and Eliasson (2003) showed that the physicochemical properties of potato starch are affected by the size of the potato tubers used. The larger the tuber, the higher the amylose content of potato starch and the larger the starch granules (Karlsson & Eliasson, 2003). The potato starch's trace elements phosphorus content was higher than other starches, which is consistent with the results shown in Table 2.1.1 (Xu et al., 2018a). Those phosphate groups esterified to the amylopectin of starch improved the freeze-thaw stability and gel clarity of potato starch (Xu et al., 2018a; Sui & Kong, 2018).

2.2.5 Maize starch

Nowadays, maize is the main crop grown worldwide, with a wide growth range, strong adaptability to temperature, and high yield (Chaudhary, Kumar & Langyan, 2014). Maize is rich in vitamins, essential fatty acids and antioxidants, which can protect organs and the immune system, regulate blood pressure, and fight cancer (Rouf Shah, Prasad & Kumar, 2016). Maize is the most important global source of starch (Teli et al., 2009). Maize starch has the advantages of low cost, abundant quantity and biodegradability (Giuri et al., 2018). It is widely used in the production of polymer films (Giuri et al., 2018). It can also be used as a concrete admixture to increase the strength of concrete and reduce deformation (Akindahunsi, 2019).

2.3 The size of starch granules

Starch particle size depends on the plant source (Jayakody & Hoover, 2008). Small granular starch is starch with an average diameter of less than 10 μm (Lindeboom, Chang & Tyler, 2004). It can be seen from Table 2.3.1 that quinoa starch, amaranth starch and taro starch are small granular starches. Compared with general starch granules, they have a larger specific surface area (Lindeboom, Chang & Tyler, 2004). The granule size of starch is related to the physical and chemical properties of starch, such as amylose content, light transmittance, and swelling power (Singh et al., 2003).

Table 2.3.1 The starch granules size

Kinds	Granular size (diameter)	Reference
Taro starch	1 - 5 μm	Lu et al., 2008
	2 - 3 μm	Lindeboom, Chang & Tyler, 2004
	1.182 - 1.431 μm	Chandla, Saxena & Singh, 2017
Amaranth starch	0.5 - 2.0 μm	Kong et al., 2012
	1 - 2 μm	Lindeboom, Chang & Tyler, 2004
	0.5 - 3 μm	Rayner et al., 2012
Quinoa starch	0.5 - 3 μm	Li et al., 2019
	0.5 - 3 μm	Lindeboom, Chang & Tyler, 2004
	2 - 4 μm	Velásquez-Barreto et al., 2021
Potato starch	5 - 100 μm	Vamadevan & Bertoft, 2015
	From < 1 to 100 μm	Ek, Brand-Miller & Copeland, 2012
Maize starch	2 - 30 μm	Vamadevan & Bertoft, 2015

2.4 Annealing

It is difficult for native starch to fully meet the standards required in industrial production due to its high swelling effect and low gelatinization temperature (Sui & Kong, 2018; Majzoobi et al., 2012). In order to impart the desired properties to starch, the starch is modified. Chemical modification, physical modification, enzymatic modification and genetic modification are four modification methods for starch (Sui & Kong, 2018). Annealing is a kind of physical modification that can affect the starch's thermal properties by improving its crystallinity (Ji et al., 2019; Stute, 1992; Shen et al., 2021). Between the glass transition temperature and the gelatinization temperature, water and heat are simultaneously combined with starch for a while (Sui & Kong, 2018). Heat moisture treatment is very similar to annealing (Sui & Kong, 2018). Annealing and hydrothermal treatment are differentiated by the temperature and moisture content at the time of treatment. The temperature of heat moisture treatment (90 - 120°C) is higher than that of annealing, and its water content (10 - 30%) is lower than annealing (50 - 90%) (Tester & Debon, 2000; Zavareze & Dias, 2011)

Natural starch has a crystalline region and an amorphous region. The crystalline region is mainly composed of amylopectin chains with a compact and ordered helical structure, while the amorphous region is composed of amylose with a loose and random structure (Sui & Kong, 2018). Annealing of starch is a sliding diffusion supported by the movement of molecular sequences within the crystal lattice, the fusion of crystals, and the recrystallization of molten material (Martuscelli & Pracella, 1974; Jayakody & Hoover). The principle of this action is that annealing can hydrate the amorphous region of starch (Ji et al., 2019). The amorphous region of starch granules is susceptible to water uptake (Jayakody & Hoover, 2008). While annealing is carried out at higher water content and temperature, the mobility of the amorphous region increases, causing the amorphous and crystalline regions to vibrate (Jayakody & Hoover, 2008). Therefore, the double helix can do limited side-by-side motion,

forming a smectic structure, the order of the double helix is enhanced, and the molecules are tightly packed (Jayakody & Hoover, 2008; Tester et al., 1999). During the annealing process, the number of imperfect crystallites is reduced, and the remaining crystallites fuse and recrystallize, increasing their perfection (Jayakody & Hoover). Since the annealing process only involves water and heat, it is considered to be a clean modification method (Guo et al., 2020). Annealing has the benefits of being low-cost, safe, environmentally friendly and effective (Fonseca et al., 2021; Wang et al., 2017b). Annealed starch is now widely used in improving product qualities such as appearance, stability, and emulsification (Ji et al., 2019). In yogurt, low-digestible foods, and potato chips, it has a better performance than natural starch (Guo et al., 2020).

When annealing, the temperature, water content of starch and time should be controlled (Zavareze & Dias, 2011). However, the water content should be moderate and above (usually more than 40%, w/w), and the processing temperature should be lower than the starch gelatinization temperature (usually lower than 60°C) but higher than glass transition temperatures (Zavareze & Dias, 2011; Guo et al., 2020). Therefore, annealing will not cause gelatinization and swelling (Wang et al., 2014).

Table 2.4.1 Annealing of different starches

Starch	Condition	Result	Reference
Pea starch	45°C 24 and 72 hours	The starch granules slightly swell irreversibly, and the amylose molecules are slightly leached	Wang, Jin & Yu, 2013
Sorghum starch	50°C 24 hours	Starch granule size, peak viscosity and swelling power decreased, retrogradation increased	Singh et al., 2011
Maize starch	50°C 24 hours	The surface of starch granules becomes rough, the amylose content,	Liu et al., 2016 a

		the relative crystallinity and thermal stability increase, the hardness decreases and there are more resistant starch in it	
Wheat starch	30,40,50°C 24 hours	Annealing at 50°C destroyed part of the wheat starch microcrystals, resulting in a decrease in starch crystallinity	Wang et al., 2017 b
Potato starch	30,40,50°C 24 hours	Annealing has slight effect on the morphology and structure of starch granules, but annealing greatly increases the viscosity	Wang et al., 2017 b
Yam starch	30,40,50°C 24 hours	Annealing has slight effect on the morphology and structure of starch granules, but the viscosity increases	Wang et al., 2017 b
Rice starch	55°C 36 hours	Compared to amylopectin, amylose is more sensitive to annealing	Guo et al., 2020
Buckwheat starch	50°C 24 hours	Annealing treatment makes starch granules higher relative crystallinity, rougher surface and higher amylose content, increases thermal stability and reduces solubility	Liu et al., 2015
Native wheat starch	35 - 50°C 0.5 - 48 hours	A longer annealing time improves the stability of wheat starch. When there is a low annealing temperature, the annealing time has a more significant influence on the degree of retrogradation.	Yu et al., 2016

Different sources of starch affect annealing (Guo et al., 2020). Comparing the results of different researchers found that they used slightly different annealing media and starch drying methods. Annealing treatments are often water-based (Waduge et al., 2006). For long-term annealing treatment, some researchers added sodium azide as a bacteriostatic agent to prevent the growth of microorganisms such as bacteria (Hu et al., 2020; Xu et al., 2018b; Su et al., 2020).

Annealing is usually performed in a water bath or constant temperature oven (Wang, Jin & Yu, 2013; Majzoobi et al., 2012; Zhang et al., 2015; Dias et al., 2010; Yadav, Guleria & Yadav, 2013; Liu et al. al., 2015; Adebowale et al., 2009). After annealing, annealed starch is usually obtained by oven drying and grinding (Song et al., 2014; Dias et al., 2010; Yadav, Guleria & Yadav, 2013; Liu et al., 2015; Adebowale et al., 2009). In addition, the dried form of starch is freeze-dried, washed with alcohol, dried, and vacuum-filtered (Wang, Jin & Yu, 2013; Yu et al., 2015; Zhang et al., 2015). These types of equipment and steps can impact the starch annealing results. Freeze-drying has an impact on the crystallization properties, molecular structure and gelatinization properties of the starch (Wang et al., 2017b). For example, Wang et al. (2017b) found that freeze-drying changed the crystallinity and crystal form of potato starch.

In addition, starch can be processed by repeated annealing (Shen et al., 2021). Xu et al. (2018a), Zhang et al. (2019), and Xu et al. (2018b) experimentally found that under the same treatment time, repeated annealing can change starch properties more than continuous annealing. However, the morphological structure change of the granule depends on the starch type (Xu et al., 2018a; Zhang et al., 2019; Xu et al., 2018b). They explained that this may be due to the faster rate at which continuous annealing reaches equilibrium and that repeated annealing gives starch more opportunity to rearrange its molecules, thereby changing its structure (Zhang et al., 2019). Shi (2008) treated grain starch through multi-step annealing while controlling the temperature and time of each annealing step. They found that the annealing effect of starch was

different after different annealing times and annealing temperatures (Shi, 2008). Some researchers perform physical or chemical treatment on starch before annealing to study the effect of annealing on it, such as cross-link (Majzoobi et al., 2012; Fonseca et al., 2021). This also provides insight into the application of starch in food and industry (Xu et al., 2018a).

Modified starch used in products and plastics can provide new features (Zhu, 2016). From Table 2.4.1 above, it can be seen that annealing treatment improves the thermal stability of starch and reduces swelling power and hardness. It can be applied to different products according to the desired change of characteristics. Hormdok & Noomhorm (2007) found that using annealed starch in noodles can make noodles with better viscosity, hardness and chewiness characteristics, improving product quality and saving costs. Zhang et al. (2015) concluded that annealing enhances the stability of starch granule structure and improves thermal stability while reducing starch retrogradation, swelling power and solubility, which helps solve quality problems in canned and frozen food (Hu et al., 2020). Furthermore, Yadav, Guleria & Yadav (2013) indicated that annealing makes starch gels stronger and easier to form, so annealed starch may have applications in sauces.

2.5 Physical and chemical properties

2.5.1 Morphology

The morphology of starch granules can be accessed by scanning electron microscopy (SEM). The surface condition and distribution of starch granules can be clearly seen through SEM micrographs. The surface properties of starch and its granule morphology affect the application of starch (Majzoobi et al., 2012). Different plant sources have different starch shapes and surface conditions. Natural sweet potato starch granules have various shapes, including polygonal, spherical and irregular (Hu et al., 2020). Sohphlang starch granules are spherical, polygonal and elliptical (Marboh et al., 2022). Sorghum starch granules are elongated, spherical and irregular in shape (Singh et al., 2011). The shapes of buckwheat starch granules are irregular polygonal or spherical (Liu et al., 2015). The distribution is different for different types of starch. For example, quinoa starch forms aggregate because it is a small-granular starch (Steffolani, León & Pérez, 2013), while buckwheat starch granules only slightly aggregate (Liu et al., 2015). The distribution of potato starch granules is dispersed, and there is little contact between granules (Wang et al., 2017b). Annealing treatment hardly affects the distribution of starch granules (Xu et al., 2018b).

Majzoobi et al. (2012) indicated that annealing treatment results in pores on the surface of rice starch, while the pore size of barley starch became larger after treatment. Nevertheless, at the same time, some starches, such as potato, yam, and lentil, do not significantly change in granule morphology of starch after annealing treatment (Majzoobi et al., 2012). Pea starch showed cracks on the surface after treatment (Wang, Jin & Yu, 2013). Zhang et al. (2015) reported that more grooves and pores appeared on the surface of C-type kudzu starch after annealing. Annealing treatment made the surface of sweet potato, wheat, and sohphlang starch granules

rougher (Hu et al., 2020; Marboh et al., 2022), while adzuki bean starch showed pores or cracks on the surface of granules after treatment (Xu et al., 2018b). These changes in the surface of starch granules can make the structure of starch granules more fragile and more susceptible to erosion (Sui & Kong, 2018).

Annealing conditions, including annealing time and temperature, also affect the morphology of starch granules (Shen et al., 2021). Hu et al. (2020) annealed potato starch at 75% moisture content at 50°C for 1 - 5 days and found that the surface of sweet potato starch annealed for five days was smoother than that of starch annealed for three days. Su et al. (2020) showed that surface cracks and dents in wheat starch increased with increasing annealing time. Annealing at 50°C resulted in the fusion and destruction of wheat starch granules, but annealing at 30°C showed no significant difference between wheat starch granules and native starch (Wang et al., 2017b).

Annealing treatment had different effects on the granule size of starch from different plant sources. The particle size of starch granules can be determined by a particle size analyzer (Li & Zhu, 2018). Wang, Jin & Yu (2013) found that annealing treatment slightly increased the average diameter of pea starch in different varieties, and C-type kudzu wheat starch also had the same results (Zhang et al., 2015; Jayakody & Hoover, 2008). Sohphlang starch, Prata banana starch, and potato starch showed no significant change in starch granule size after annealing (Marboh et al., 2022; Almeida et al., 2020; Xu et al., 2018b), while Singh et al. (2011) indicated that the granule size of annealed sorghum starch was smaller than that of native starch.

2.5.2 Crystallinity

The crystalline region of starch granules is composed of a double helix, which consists of amylose and its outer chain and amylopectin, of which the outer chain of amylopectin is the main component (Tester, Karkalas & Qi, 2004). Starches are

classified into three types, A, B, and C, according to their crystalline polymeric forms (Sui & Kong, 2018; Singh et al., 2003). Among them, A-type starch has the highest proportion of A-chain amylopectin that forms links with other chains, and B-type starch has the highest proportion of B-chain amylopectin that forms links with other chains and carries other chains (Sui & Kong, 2018). It can be seen from Figure 2.5.2.1 that the A-type crystal is more compact in structure than the B-type crystal and does not contain a hydrated helical core (Hsien-Chih & Sarko, 1978).

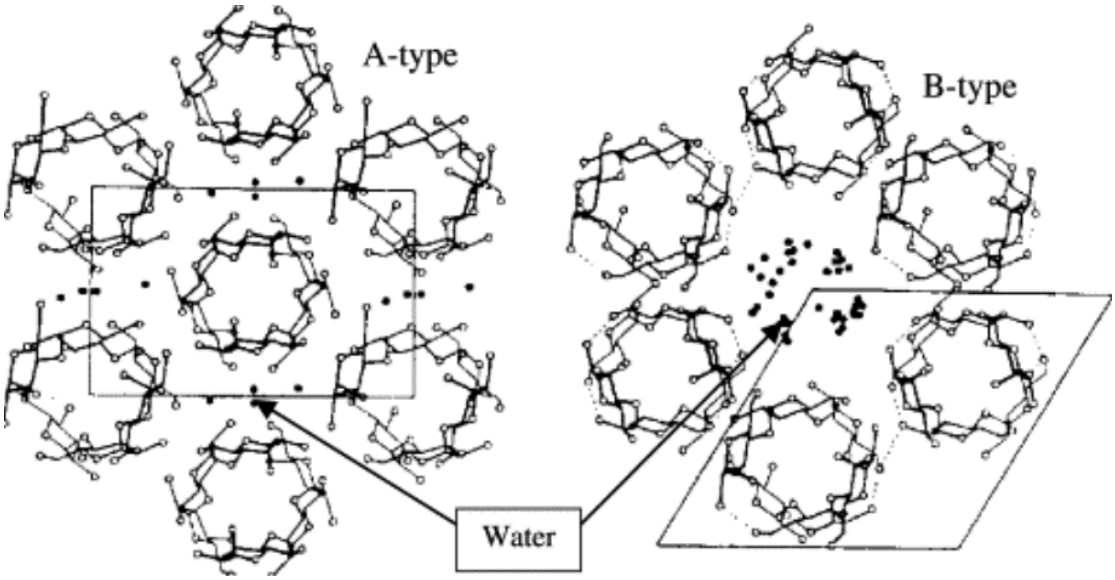

Figure 2.5.2.1 The unit cell of A-type starch and B-type starch. Adapted from Hsien-Chih & Sarko (1978).

The crystallinity of starch is usually assessed using an X-ray diffraction pattern obtained with an X-ray diffractometer (Wang, Jin & Yu, 2013). In the pattern, the position of the main peak shows the crystalline type of starch (Yu et al., 2016; Wang et al., 2017a). Type A crystals have significant diffraction peaks at Bragg angle (2θ) = 15°, 23°, double peaks at Bragg angle (2θ) = 17°, 18°, and weak peaks at Bragg angle (2θ) =19° (Hu et al., 2020; Marboh et al., 2022; Singh et al., 2011; Liu et al., 2016; Dias et al., 2010). Type B crystals have clear diffraction peaks at Bragg angle (2θ) =

5°, 15°, 17°, 22°, and 24° (Xu et al., 2018a). There are both A-type crystals and B-type crystals in C-type starch, so there will be clear diffraction peaks around the Bragg angle (2θ) = 5°, 15°, 17°, 23° (Zhang et al., 2016; Xu et al. al., 2018b; Adebowale et al., 2009).

In addition to the type of starch crystals and the calculated relative crystallinity, the X-ray diffraction pattern can also reveal other crystalline structures in starch (Waduge et al., 2006). For example, there is a weak peak at Bragg angle (2θ) = 20°, indicating that starch contains V-amylose–lipid complexes (Waduge et al., 2006).

Most researchers report that the annealing treatment does not change the crystallization pattern of starch (Xu et al., 2018a; Zhang et al., 2016; Liu et al., 2016b; Xu et al., 2018b). Some researchers have found that the annealing process increases the diffraction intensity (Liu et al., 2016b). In a study of barley starch, Waduge et al. (2006) found that annealing treatment caused the disappearance of B-type crystals in starch. Annealing also had an effect on relative crystallinity, resulting in increased crystallinity of red adzuki bean and African yam bean starch (Xu et al., 2018b; Adebowale et al., 2009). Rocha et al. (2011) obtained experimental results showing that annealing increased the relative crystallinity of potato starch and Peruvian carrot starch. However, the relative crystallinity of tapioca starch did not change after annealing. The relative crystallinity of waxy maize starch increased after annealing, whereas the relative crystallinity of common maize was almost unchanged (Rocha et al., 2012). Dias et al. (2010) showed that the relative crystallinity and peak intensity of annealed rice starch decreased. Therefore, the effect of annealing treatment on the change of crystallinity of different starches is different.

Different annealing conditions have different effects on crystallization. Zhang et al. (2016) found that the relative crystallinity and peak intensity of C-type kudzu starch increased with annealing time. Xu et al. (2018a) and Zhang et al. (2019) obtained the same results in the annealing of potato starch and sweet potato starch. However, Hu

et al. (2020) showed that as annealing progressed, the relative crystallinity of sweet potato starch decreased slightly at one and three days but increased on the fifth day. The effect of moisture content during annealing on X-ray diffusion pattern and crystallinity is that the peak intensity of starch after annealing increases with increasing water content (Marboh et al., 2022).

2.5.3 Gelatinization

Starch granules are insoluble in cold water, but starch will swell in excess water (Srichuwong & Jane, 2007). The principle of starch gelatinization is that the semi-crystalline structure of the starch granules is transformed into an amorphous form in the situation with appropriate water and a high enough temperature higher, the gelatinization temperature (Sui & Kong, 2018). This means starch may gelatinize when it encounters sufficient heat and moisture, which will affect product quality (Carlstedt, et al., 2015; Zhu et al., 2016). The gelatinized starch granules form a viscous solution (Carlstedt et al., 2015). Once the starch granules swell and rupture from absorbing water, crystallographic order collapse and their structure will not recover (Carlstedt et al., 2015; Singh et al., 2003). After gelatinization, the molecular order, birefringence and semi-crystalline structure of starch granules are lost irreversibly (Srichuwong & Jane, 2007).

Differential scanning calorimetry (DSC) is used for the determination of starch gelatinization (Ji et al., 2019). During the heating process, this method is used to record the melting enthalpy, onset temperature, peak temperature, and conclusion temperature (Ji et al., 2019). In addition to DSC, there are other techniques to monitor structural and thermodynamic changes during gelatinization, such as viscometry measurement, Fourier transform infrared spectroscopy (FTIR) and X-ray diffraction (XRD) (Ratnayake & Jackson, 2009).

Different types of starch have different gelatinization onset temperatures and gelatinization enthalpy. The onset temperature of gelatinization for most starches is between 50 - 80 ºC (Sui & Kong, 2018). It is also affected by starch crystal form, amylose content, and starch molecular structure (Sui & Kong, 2018).

Table 2.5.3.1 The gelatinization onset temperature and gelatinization enthalpy of starch

Starch	T_o (ºC)	ΔH(J/g)	Reference
Pea	52.3	8.5	Wang, Jin & Yu, 2012
C-type kudzu	59.7	6.5	Zhang et al., 2015
Sweet potato	66.6	8.9	Hu et al., 2020
Wheat	55.6	10.3	Wang et al., 2017 b
Yam	60.0	13.2	Wang et al., 2017 b
Potato	55.0	13.0	Wang et al., 2017 b
sohphlang	60.3	13.2	Marboh et al., 2022
sorghum	66.7	9.26	Singh et al., 2011
Peruvian carrot	57.0	16.8	Rocha et al., 2012
Water chestnut	66.8	12.0	Yadav, Guleria & Yadav, 2013

T_o: Gelatinization onset temperature

Annealing leads to an increase in the onset and peak temperature of starch gelatinization and a decrease in the range of gelatinization temperature, which improves the thermal properties of starch for a wider range of applications (Jayakody & Hoover, 2008; Su et al., 2020; Su et al., 2020; Wang, Jin & Yu, 2012; Yadav, Guleria & Yadav, 2013). However, the effects of annealing on the gelatinization enthalpy of starch from different plants are different. Some researchers have found that annealing increases starch gelatinization enthalpy (Wang, Jin & Yu, 2012; Zhang et al., 2015; Marboh et al., 2022; Singh et al., 2011; Su et al., 2020; Rocha et al., 2012;

Yadav, Guleria & Yadav, 2013). Others have found that annealing does not change the gelatinization enthalpy of starch (Waduge et al., 2006; Larsson & Eliasson, 1991).

Different treatment temperatures affect the thermal properties of annealed starch. Although the annealing treatment can be performed at 0 - 15°C below the onset temperature, the closer the treatment temperature is to the onset temperature, the more pronounced the annealing effect will be (Tester & Debon, 2000; Almeida et al., 2020). Jayakody and Hoover (2008) pointed out that if the annealing temperature is too close to the onset temperature of gelatinization, starch will gelatinize during the annealing process. As the annealing temperature increases, the gelatinization onset temperature increases, and the gelatinization enthalpy also increases (Yu et al., 2016; Zhang et al., 2015). Wang et al. (2017b) found that with the increase in annealing temperature, the gelatinization onset temperature of wheat starch continues to increase, and the gelatinization enthalpy first increased and then decreased. The same results were obtained after performing the same experiment with yam starch and potato starch at 30 - 50°C (Wang et al., 2017b).

Annealing time is a factor that affects the starch's thermal properties. When increasing the annealing time, the gelatinization onset temperature and gelatinization enthalpy of starch also increase (Su et al., 2020). Hu et al. (2020) illustrated that different annealing times are of different effects on the gelatinization enthalpy of sweet potato starch. Short-time (1 - 3 days) annealing reduced the gelatinization enthalpy of starch but increased on the fifth day, exceeding that of native starch (Hu et al., 2020). The moisture content of annealing also affects the gelatinization properties of annealed starch (Marboh et al., 2022). The gelatinization enthalpy and thermal transition temperature of the starch increased with increasing water content during annealing (Marboh et al., 2022).

In addition, the gelatinization properties of starch are also affected by other factors. Xu et al. (2022) illustrated that protein content also affected annealing results.

Karlsson and Eliasson (2003) tested the gelatinization kinetics of potato starch from different varieties and different tissue parts. They indicated that the gelatinization temperature of potatoes of different varieties was different, and the gelatinization characteristics of potatoes differed in different harvest years and tuber sizes (Karlsson & Eliasson, 2003).

2.5.4 Retrogradation

Retrogradation is when the starch, after gelatinization, undergoes partial rearrangement and recrystallization during storage (Sui & Kong, 2018). Starch retrogradation is measured using the same technique as gelatinization. Singh et al. (2003) stated that during storage, there is hydrogen bond movement within the gelatinized starch. During retrogradation, amylose forms a double helix, and amylopectin crystallizes in association (Singh et al., 2003). The starch's retrogradation enthalpy is much lower than that of starch before gelatinization because of its weaker crystallinity (Baker & Rayas-Duarte, 1998). Retrogradation is of great significance for the application of starch in food because retrogradation affects the hardness, viscosity and digestibility of food (Sui & Kong, 2018).

Annealing treatment can reduce starch retrogradation (Hoover & Vasanthan, 1994; Adebowale et al., 2005; Jayakody & Hoover, 2008). However, different annealing conditions will affect the retrogradation of starch. Annealing time, water content and annealing temperature affect the degree of starch retrogradation (Yu et al., 2016). Yu et al. (2016) indicated that the retrogradation rate was higher with increased annealing time and moisture content but decreased when it approached the gelatinization temperature. When the annealing temperature and water content are constant, the starch with a shorter annealing time has the highest retrogradation rate, so the longer the annealing time, the more stable the starch (Yu et al., 2016). When the annealing temperature and annealing time are constant, the lower the moisture

content, the lower the retrogradation rate of the starch, and the more stable the starch is (Yu et al., 2016).

2.5.5 Starch Swelling

Heating starch in excess water causes it to expand (Sui & Kong, 2018). Starch swelling generally includes swelling power and water solubility (Sui & Kong, 2018; Li & Zhu, 2018). In food, swelling power and water solubility affect the disintegration of tablets in the pharmaceutical industry and the taste of food to a certain extent, so it is an essential feature for the application of starch in food and medicine (Sui & Kong, 2018). Both the swelling power and water solubility of starch are positively correlated with temperature (Lawal & Adebowale, 2005; Zhang et al., 2015; Liu et al., 2016b). The swelling performance of starch is determined by the type of starch, and annealing treatment will reduce the swelling power while the water solubility of starch (Wang, Jin & Yu, 2013; Zhang et al., 2015; Liu et al., 2016b; Waduge et al., 2006; Yadav, Guleria & Yadav, 2013; Nakazawa & Wang, 2004).

Annealing treatment conditions also have an influence on starch swelling properties. The annealing time of starch affects its swelling power and water solubility (Shen et al., 2021). Some researchers found experimentally that the longer the annealing time, the lower the solubility and swelling power of starch (Zhang et al., 2019; Zhang et al., 2015; Xu et al., 2018b). Shen et al. (2021) found that as annealing progressed, the swelling power and water solubility of maize starch first increased and then decreased.

2.6 Rheological properties of starch

2.6.1 Pasting

Pasting properties are essential properties of starch heated with water that affect its application in the industry (Sui & Kong, 2018). A rapid viscosity analyser (RVA) can be used to determine the pasting properties of starch (Song et al., 2014). The measurement process is divided into heating and cooling stages, during which the starch suspension is stirred (Majzoobi et al., 2012). The probe measures starch viscosity at different times during stirring (Xu et al., 2018a). With heating and stirring, starch granules lose their granular structure because of the swelling, breaking down when the swelling reaches a certain point (Sui & Kong, 2018). Among them, when the starch paste's viscosity is the largest, the starch granules are the most swollen (Sui & Kong, 2018). Then during the cooling stage, the starch forms a network structure, forming a gel (Ai & Jane, 2015).

The pasting properties of different starches differ because the pasting properties of starch granules are affected by particle size, amylopectin content, and impurities (Sui & Kong, 2018). Ai & Jane (2015) found that maize starch, rice starch, and wheat starch have different paste temperatures, and their peak viscosity and final viscosity are also different. Liu et al. (2016b) also demonstrated that the pasting properties of buckwheat and sorghum starches are different.

The effects of annealing treatment on starch pasting properties differ. Generally, annealing treatment can enhance the thermal stability of starch, increase the pasting temperature of starch and reduce the peak viscosity and final viscosity, but it has no significant influence on the overall shape of the gelatinization curve. (Majzoobi et al., 2012; Zhang et al., 2015; Singh et al., 2011; Almeida et al., 2020; Yadav, Guleria & Yadav, 2013). However, in pea starch, the peak viscosity and trough viscosity

increased significantly after annealing (Wang, Jin & Yu, 2013), while Marboh et al. (2022) stated that annealing increased the paste temperature of Sohphlang starch, reducing the peak viscosity and increasing its final viscosity.

Different annealing conditions also affect starch pasting properties. The annealing time affects starch pasting properties (Wang, Jin & Yu, 2013; Xu et al., 2018b). With the increase in annealing time, the peak viscosity, trough viscosity and final viscosity of starch continue to decrease, the paste temperature increases steadily, and the thermal stability also increases (Zhang et al., 2015; Xu et al., 2018b). Hu et al. (2020) illustrated that the peak viscosity and final viscosity of sweet potato starch decreased with the increase of annealing time and were lower than those of natural starch, but the trough viscosity first decreased and then increased, and finally was higher than that of natural starch. Wang, Jin & Yu (2013) found that the peak viscosity and trough viscosity of pea starch first increased sharply during long-term annealing and then decreased slowly, but which was still higher than that of native starch after 72 hours of treatment.

Different annealing temperatures have different effects on starch pasting properties. Wang et al. (2017b) illustrated that the peak viscosity and trough viscosity of yam starch annealed at 30°C increased, but they decreased after annealing at 40 and 50°C. On the other hand, after annealing at 30 and 40°C, the paste temperature decreased while the trough viscosity, peak viscosity, and final viscosity all increased. After annealing at 50°C, the viscosity decreased, but the paste temperature (Wang et al., 2017b). Almeida et al. (2020) found that in the annealing treatment of Prata banana starch at 45 - 55°C, the paste temperature increased steadily with the treatment temperature. However, the peak viscosity and trough viscosity increased at first and decreased later (Almeida et al., 2020).

Marboh et al. (2022) found that the water content during the annealing treatment affects the pasting properties of annealed starch. With the increase of water content

(70 - 80% wet basis), the pasting temperature of Sohphlang starch first increased, then decreased, and finally increased. Meantime, the peak viscosity first decreased, then increased and finally decreased, while both were lower than that of native starch (Marboh et al., 2022).

2.6.2 Gel texture

Starch gels are formed by the interaction of amylose and amylopectin, which form a water-holding network in swollen granules (Ai & Jane, 2015). Amylose gels at excessively high temperatures, so starches with higher amylose content have stronger gels that form faster (Ai & Jane, 2015). The gel properties of starch, including hardness, adhesiveness and cohesiveness, can be tested by a texture profile analyzer, and compression evaluation can be done using a probe (Singh et al., 2011). The test results have a large impact on the application of starch in food and non-food applications (Iftikhar & Dutta, 2019). Therefore, it is of great significance for the application of starch to adjust the starch gel texture through modification.

Different starches have different gel textures. Yu et al. (2016) indicated that the hardness and cohesiveness are affected by the gel concentration. In starch gels with higher concentrations, some amylose molecules are parallel, increasing the hardness and cohesiveness of starch gels. They also indicated that starch concentration might also affect the amount of amylose leached and, thus, the form of the gel (Yu et al., 2016). Molavi and Razavi (2018) stated that the properties of the starch gel are also affected by the preparation method of starch gel, storage temperature and time, physicochemical properties of starch itself, and measuring instruments and procedures. Yu et al. (2016) proved experimentally that different types and concentrations of additives could modify the gel properties of starch gels.

Annealing treatment leads to a higher hardness of starch (Singh et al., 2011; Yadav, Guleria & Yadav, 2013; Molavi & Razavi, 2018; Iftikhar & Dutta, 2019). In addition, adhesiveness decreases after annealing treatment (Iftikhar & Dutta, 2019). Annealing also reduces the cohesiveness of starch (Iftikhar & Dutta, 2019). Furthermore, it increases the minimum concentration required for starch to form a gel. The network structure is formed during gelatinization, with leached amylose as the main binder (Almeida et al., 2020). However, annealing reduces the leaching of amylose, so the annealed starch requires a higher concentration to form a gel (Almeida et al. et al., 2020).

2.6.3 Flow

The flow behavior of starch can be measured by a rheometer, which measures the relationship between starch shear rate and shear force (Li & Zhu, 2018; Sui & Kong, 2018). The flow behavior of starch can be expressed by Herschel-Bulkley, Robertson-Stiff, power law, Heinz Casson and Mizrahi-Berk models (Kong et al., 2010; Li & Zhu, 2021). As a non-Newtonian elastic fluid, starch exhibits pseudo-plasticity and shear-thinning behavior (Kong et al., 2010; Malumba et al., 2009). The concentration of starch paste, temperature, and the amylose content of starch have a significant effect on the viscosity of starch paste (Sui & Kong, 2018; Ai & Jane, 2015). There are also differences in the flow properties of starch from different plant sources, which are related to the chain length of amylopectin (Kong et al., 2010).

Pseudoplasticity and shear-thinning behavior remain after starch annealing (Devi & Sit, 2019). However, annealing treatment increases the coefficient of flow behavior, so the pseudoplasticity and shear-thinning behavior of starch after annealing are weakened (Devi & Sit, 2019).

2.6.4 Oscillation

The oscillating properties of starch show that starch's structure and molecular structure change during processing, which significantly impacts product sensory properties, product development and design, and quality control (Molavi & Razavi, 2018). Dynamic rheological analysis of starch can be achieved by rheometer and continuous modulus analysis, showing the viscoelastic properties of starch (Singh et al., 2003). The advantage is that starch gels can be continuously evaluated at various temperatures and shear rates (Ai & Jane, 2015). By measuring these, one can determine the storage modulus G′ which measures the deformation energy recovered per deformation cycle and loss modulus G″, which is the energy lost in the deformation cycle (Ai & Jane, 2015; Sui & Kong; Molavi & Razavi, 2018). As well as the ratio of loss modulus and storage modulus, the loss tangent indicates the degree of deformation recovery (Ai & Jane, 2015; Sui & Kong; Molavi & Razavi, 2018). The larger the loss tangent, the stronger the gel, the greater the hardness, and the more difficult it is to recover from deformation (Singh et al., 2003; Li & Zhu, 2018; Ai & Jane, 2015). Annealing treatment reduces starch loss tangent and reduces elasticity (Molavi & Razavi, 2018).

Chapter 3. Materials and methods

3.1 Materials

Quinoa：Countdown supermarket

Amaranth: GoodFor, New Zealand

Taro: Pink taro

Potato starch: GoodFor, New Zealand

Maize starch: GoodFor, New Zealand

Table 3.1 Chemicals

Chemical	Supplier
Sodium dodecyl sulfate	Sigma-Aldrich, USA
Sodium hydroxide (NaOH)	Sigma-Aldrich, USA
Sodium metabisulfite ($Na_2S_2O_5$)	Sigma-Aldrich, USA
Total Starch assay kit (AA/AMG)	Megazyme International, Ireland
Calcium chloride ($CaCl_2$)	Sigma-Aldrich, USA
Sodium acetate ($C_2H_3NaO_2$)	Sigma-Aldrich, USA
Milli-Q water (H_2O)	Millipore Corporation, USA
Hydrogen chloride (HCl)	ECP, Ltd, New Zealand
Sodium acetate ($C_2H_3NaO_2$)	Sigma-Aldrich, USA
Rice bran oil	Countdown, New Zealand
Ethanol (C_2H_5OH)	Ecp-Laboratory Reagent

3.2 Instruments

The instruments involved in the experiment are shown in Table 3.2.

Table 3.2 Equipment

Equipment	Model	Manufacturer
Balance	Mettler Toledo XS 205	Mettler-Toledo Ltd., Australia
Hot plate	RCT B S104	IKA, Germany
Shaking water bath	W28, Grant	Barrington, England
Centrifuge	Thermofisher Scientific Sorvall Lynx 4000 Centrifuge	Thermo Fisher Scientific, USA
Centrifuge	ThermoFisher, Heraeus™ Labofuge™ 400 Centrifuges	Thermo Fisher Scientific, USA
Air-force oven	Model MOV-112P Program Oven	Sanyo Electric Co, Ltd., California
UV spectrophotometer	Spectronic 200	Thermo Fisher Scientific, USA
Aluminum pan	-	Two dollars shop, New Zealand
Differential scanning calorimeter	Q1000 Series	TA Instruments, USA
Freezer	Freezer	Freezer
Fridge	Model SRS 535NW	Samsung, Korea
Vortex mixer	Vortex Mixer VF2	IKA Laboratory, Germany
Particle size analyzer	Mastersizer 2000	Malvern Instruments Ltd, UK
Gel texture analyzer	TA–XT plus	Stable Micro Systems Ltd., UK
Ph meter	Schott Instrument pH Metre, Lab 850	Xylem Inc, Germany
X-ray diffractometer	-	Almelo, The Netherlands
Scanning electron microscope	SU-70	HITACHI, Tokyo, Japan
Rheometer	Physica MCR 301 Stressed Controlled Rheometer	Anton-Paar, Austria
Rheometer	Physica MCR 302 Stressed Controlled Rheometer	Anton-Paar, Austria

3.3 Methods

3.3.1 Quinoa starch extraction

The extraction method of quinoa uses the procedure of Li, Wang & Zhu (2016) with some modifications. After freezing the quinoa seeds in a container with liquid nitrogen for two minutes, place them in a coffee ginder (Breville, Coffee ginder, BCG200) and grind them for one minute to obtain quinoa flour. Soak quinoa flour in sodium borate buffer (12.5mM, pH10 solution consisting of 0.5% Sodium metabisulfite [w/v] and 0.5% SDS [w/v] in a ratio of 100 grams of quinoa flour in one liter of buffer. Stir with a hot plate for 30 minutes to remove lipids and proteins from the quinoa flour. The residue was centrifuged at 6000 × g for ten minutes. Use deionized water in a ratio of 100 grams of quinoa flour in one liter of deionized water wash and recover by centrifugation at 6000 × g for ten minutes. Stir the residue in distilled water overnight. The starch suspension was passed through a cheesecloth (4 layers) and nylon mesh to remove impurities. Then centrifuge the starch suspension at 6000 × g for ten minutes, pour off the liquid and remove the brown layer that formed on the top of the starch with a spatula. Repeat this six times to make sure SDS and the brown impurities have been removed. Dried the remaining starch in an air-forced oven at 40°C for 48 hours. The dried starch was grounded into powder in a mortar, sealed in a sealed plastic container and stored in a desiccator.

3.3.2 Amaranth starch extraction

The extraction method of amaranth uses the procedure of Li, Wang & Zhu (2016) with some modifications. After freezing the amaranth seeds in a container with liquid nitrogen for two minutes, place them in a coffee ginder (Breville, Coffee ginder, BCG200) and grind them for one minute to obtain amaranth flour. Soak amaranth flour in sodium borate buffer (12.5mM, pH10 solution consisting of 0.5% Sodium

metabisulfite [w/v] and 0.5% SDS [w/v] in a ratio of 100 grams of amaranth flour in one liter of the buffer. Stir with a hot plate for 30 minutes to remove lipids and proteins from the amaranth flour. The residue was centrifuged at 6000 × g for ten minutes. Use deionized water in a ratio of 100 grams of amaranth flour in one liter of deionized water wash and recover by centrifugation at 6000 × g for ten minutes. Stir the residue in distilled water overnight. The starch suspension was passed through a cheesecloth (4 layers) and nylon mesh to remove impurities. Then centrifuge the starch suspension at 10000 × g for ten minutes, pour off the liquid and remove the brown layer that formed on the top of the starch with a spatula. Repeat this six times to make sure SDS and the brown impurities have been removed. Dried the remaining starch in an air-forced oven at 40°C for 48 hours. The dried starch was grounded into powder in a mortar, sealed in a sealed plastic container and stored in a desiccator.

3.3.3 Taro starch extraction

The extraction method of taro starch was adapted from Jane et al. (1992). Cut the peeled taro into one-centimeter pieces and put them in the blender. After beating for two minutes, pour the slurry into the NaOH solution (0.05%) and stir for two minutes. The ratio is 1L NaOH solution per 100g of taro. Pass through four layers of cheesecloth after stirring well. The remaining solid was added to the NaOH solution, stirred for one hour, and re-passed through cheesecloth. The solution was centrifuged at 3000 x rpm for 20 minutes and then removed impurities from the upper and lower layers. This step was repeated four times to obtain starch, dried the remaining starch was in an air-forced oven at 40°C for 48 hours. The dried starch was grounded into powder in a mortar, sealed in a sealed plastic container and stored in a desiccator.

3.3.4 Moisture content (MC)

The determination of starch moisture content was according to Li, Wang & Zhu (2016) with some modifications. Use preheated 120°C air oven to dry the aluminum pans to

constant weight and weigh (W) after cooling in a desiccator. 200 mg (W_0) of starch was put in an aluminum pan and placed in the oven to dry to constant weight for at least 24 hours. The dried aluminum pan and starch were cooled to room temperature in a desiccator and weighed (W_1). MC is calculated by Equation 1.

$$MC=(W_1-W)/W_0 \qquad \text{Equation 1.}$$

3.3.5 Total starch

The starch content was tested according to Megazyme's procedure manual. 100 mg sample was weighed into Corning culture tubes and the weight was recorded in duplicate. Tap the tube to make sure the sample is at the bottom of the tube. 0.2 ml of 80% v/v ethanol in water was added to the test tube, and a vortex mixer was used to mix well. 2ml of 1.7M sodium hydroxide solution was added to the tube, and the tube was stirred in an ice-water bath on a hot plate for fifteen minutes, during which time it was vortexed two to three times to prevent the sample from agglomeration. 8 ml of sodium acetate buffer (600 mM, pH 3.8) plus calcium chloride (5 mM) were added and vortexed to homogenize. Added 0.1 ml α-amylase and 0.1 ml amyloglucosidases (AMG), and 0.2 ml sodium acetate buffer (600 mM, pH 3.8) plus calcium chloride (5 mM) for the control group and vortexed for three seconds with the lid on. The tubes were incubated in a 50°C water bath for thirty minutes. After cooling to room temperature, the tube was inverted several times to ensure a homogenous solution. 2.0 ml of the solution was placed in a centrifuge tube and centrifuged at 13000 rpm for five minutes. Transferred 1.0 ml of the supernatant to tubes containing 4 ml of sodium acetate buffer (600mM, pH 3.8) plus calcium chloride (5 mM) and mixed well. Transferred 0.1 ml of the solution to new Corning culture tubes, added 3.0 ml glucose oxidase/peroxidase (GOPOD) reagent, incubated in a 50°C water bath for 20 minutes, and measured the absorbance at 510 nm.

3.3.6 Kjeldahl determination

The Kjeldahl method was derived by summarizing the method of Sáez-Plaza et al. (2013). 0.3 g of starch samples were taken in duplicate, and 0.2 g of gelatin and a blank control group were set. 10 g potassium sulfate and 0.1 g titanium dioxide copper sulfate (1:1) mixture were weighted and mixed well and added to digestion Tube. 20 ml of concentrated sulfuric acid was added to the digestion Tube. Cover the suction module on the digestion Tube. Turn on the scrubber, speed digester, and basin water pumps to ensure that the NaOH is bubbling. After the liquid turns light green, continue heating for ten minutes, turn off the main switch, take out the digestive tube, and let it cool down. Conical flasks were prepared and added 60ml of 2% boric acid solution and ten drops of methyl red indicator. Kjeldahl distillation was carried out by means of a K-350 distillation apparatus. 0.1M HCl was used to titrate the solution in the Erlenmeyer flask, record the required volume of hydrochloric acid, and calculate the nitrogen content in the sample by Equation 2.

$$\%\text{protein} = (F \times 14 \times (\text{ml of HCl})) / \text{sample weight} \times 0.1\text{M HCl} / 1000\text{ml} \times 100$$

Equation 2.

ml of HCl: sample reading - blank reading

F: conversion factor

3.3.7 Annealing

The annealing temperature is 0 - 15°C lower than the onset temperature of gelatinization, however, being too close to the starting temperature of gelatinization may affect the pasting properties of starch or even lead to starch gelatinization. The pre-experiment was performed to select the treatment temperature, time and water content. The temperature was 14°C lower than the starting temperature of starch gelatinization, the treatment time was five days (120 h), and the starch and water

content were 1:4 (dry basis). The annealing method is based on the method of Wang et al. (2017b) with improvements. Starch was placed in a 500ml Thermo centrifuge bottle and accurately weighed. Milli-Q water was added to the centrifuge bottle at four times the dry weight of the starch minus the water weight of the starch itself. The centrifuge bottle was sealed after the starch-water suspension was mixed until there were no lumps. Immerse the centrifuge bottle in a water bath at a temperature of 14°C below the onset of starch gelatinization. The samples were incubated in a water bath with shaking for five days (120 h) to ensure that the starch was fully dispersed and contacted with Milli-Q Water during processing. Centrifuge the samples (6000 g, 20 min) after annealing is complete and decant the supernatant. Deionized water was used to wash the remaining lower pellet and centrifuged (6,000 g, 20 min), the supernatant was decanted, and the above operation was repeated twice. The starch was dried in a 35°C air-forced oven for 48h, ground to powder and passed through a 250-mesh screen. The resulting samples were stored, sealed in plastic containers and placed in a desiccator.

3.3.8 Control group

The starch of the control group was natural starch washed with water. Starch and Milli-Q water were added to a 500 ml Thermo centrifuge bottle, and the starch-water suspension was mixed until there was no clumping and the centrifuge bottle was tightly capped. Centrifuge the samples (6,000 g, 20 min) and pour off the supernatant. Deionized water was used to wash the remaining lower pellet and centrifuged (6,000 g, 20 min), the supernatant was decanted, and the above operation was repeated twice. The starch was dried in a 35°C air-forced oven for 48h, ground to powder and passed through a 250-mesh screen. The resulting samples were stored, sealed in plastic containers and placed in a desiccator.

3.3.9 Particle size

The starch particle size was measured using the method of Li and Zhu (2017a). Before measuring the particle size distribution of starch, the starch suspension (1%, w/w) was sonicated in an ultrasonic cleaner for 90 min to ensure no sticking between starch granules. The starch suspension was slowly added to the dispersing unit of a Malvern Mastersizer 2000 particle size analyzer (Malvern Instruments Ltd, UK). The stirring speed of the dispersing unit is 2000rpm, and the solution is added until the shading degree is 10 - 20%. The results D [4,3], d (0.5), and D [3,2] are obtained, which are the mean diameter of mass moment, median diameter and surface area moment mean diameter, respectively.

3.3.10 Scanning electron microscopy (SEM)

A scanning electron microscope (HITACHI SU-70, Tokyo, Japan) was used to analysis the morphology of starch. The accelerating voltage during the whole process was 10 kV.

3.3.11 Thermal analysis

Thermal properties of control and annealed starch were measured according to Li and Zhu (2017a) with some modifications. Samples were determined by a Differential scanning calorimeter (DSC) machine (TA Instruments Q1000, New Castle, DE). 6 - 8mg starch sample was weighted in an aluminum pan and mixed with double Milli-Q water. The aluminum crucible was sealed and left to equilibrate at room temperature for one hour. An empty aluminum crucible was sealed as a control before starting the test. In this process, the quinoa and amaranth sample was heated from 25 to 90°C in a nitrogen atmosphere at a rate of 10°C/min, and then cooled to 30°C. The temperature range for the taro, potato and maize samples was 25 - 100°C. After cooling, the samples were refrigerated in a 4°C freezer for four weeks and then

subjected to the same conditions for retrogradation analysis. Parameters include onset temperature (T_o), peak temperature (T_p), conclusion temperature (T_c) and the change of enthalpy (ΔH) can be directly derived from the figure by Universal Analysis 2000 software (version 4.1D, T A Instruments, New Castle, USA). The parameter gelatinization temperature range (ΔT) is obtained by subtracting the onset temperature from the conclusion temperature ($\Delta T=T_c-T_o$). R is the retrogradation rate of starch.

3.3.12 Swelling power and water solubility index

The swelling power and water solubility index of starch were determined using a previous procedure of Zhang, Li, Wang, Yao & Zhu (2017) with some modifications. Weigh the 15ml centrifuge tube. Dry weight 150 mg starch (W_0) was weighed into a centrifuge tube and 10 ml Milli-Q Water was added. The starch-water suspension was mixed well on a vortex mixer prior to incubation in an 85°C water bath for 1 hour. Alternate vortex for 5 seconds for the first twenty minutes of incubation and 5 seconds every 10 minutes for the next 40 minutes. After the incubation, the centrifuge tubes were placed in an ice-water bath to cool for 5 minutes. Centrifugation at 3000 x g for 30 min. The aluminum pans were dried in an air-forced oven at 120°C to constant weight and taken out and placed in a desiccator to cool and then weighed. The supernatant was poured vertically into the aluminum pan and the process was held for 30 seconds. All poured fractions were considered as supernatants, and the remaining fractions adhering to the centrifuge tubes were considered as pellets. Weigh the sediment weight (Ws). The supernatant was dried in an air-forced oven at 120°C for 24 h and weighed (W1). WSI and SP are calculated according to the following formula

$$WSI = (W1 / W0) \times 100\% \quad \text{Equation 3.}$$

$$SP = Ws / (W0 \times (100\% - WSI)) (g/g). \quad \text{Equation 4.}$$

3.3.13 Pasting analysis

Pasting properties of starch were determined using a method described by Li, Wang & Zhu (2016) and Li, Lin & Corke (1997). 2.0 g (dry basis) starch was weighted in a centrifuge tube, 20 ml of Milli-Q Water was added, vortexed to mix well, and then added it to the starch cell. The pasting properties was measured using an MCR 301 Rheometer (Anton Paar, GmbH, Ostfildern, Austria) and the probe that equipped was ST24-2D. In program, the starch solution was held at 50°C for 5 min before climbed to 95°C in 7.5 min. Then held this temperature for 5 min. Held at 50°C for 2 min after cooling to 50°C in 7.5 min. In pasting analysis, pasting temperature (PT), hot paste viscosity (HPV), peak viscosity (PV), peak temperature (PKT) and cool paste viscosity (CVP) can be read directly from the result data. The rest are derived parameters. Setback (SB = CPV − HPV), setback ratio (BR = CPV/HPV), breakdown (BD = PV − HPV) and stability ratio (SR = 100 × HPV/PV).

3.3.14 Gel texture analysis

The gel structure analysis was based on Li, Wang & Zhu (2016) with some modifications. After pasting, starch gels formed. Transfer the gel to a 10 mL Teflon-faced rubber liner glass canister with a three-mL pipette in triplicate. Centrifuge the glass canister at 1000 × g for five minutes. The gel structure test was carried out after refrigerating at 4°C for 24 h. The gel texture properties were analyzed by a TA-XT Texture Analyzer (Stable Micro Systems Ltd., Surrey, UK). The mode is Texture Profile Analysis (TPA) mode. Tested gel under the condition of distance 15 mm, with a trigger force of 0.03 N and speed 0.5 mm/s by a diameter 5 mm cylinder probe. Hardness (HD), adhesiveness (AD) and cohesiveness (COH) were recorded from the resulting graph. Among them, the hardness is the maximum force peak at the first compression, the adhesiveness is the negative area of the probe when the probe is contracted for the first time, and the ratio of the positive force area of the second compression to the positive force area of the first compression is the cohesiveness.

3.3.15 Wide-angle X-ray diffractometry

Wide-angle X-ray diffractometry was measured using the method of Li & Zhu (2017b). Samples were packed into open plastic containers that were sealed and equilibrated for four weeks in a desiccator with saturated sodium carbonate solution (20°C, 43% relative humidity) at the bottom. The samples were scanned by X-ray diffractometer (Almelo, The Netherlands). The operating conditions were voltage 24 kV current 40 mA, the angle between 5 and 40 º, the step size was 0.0131303, and the time per step was 99.450 s. The following formula calculated the crystallinity of starch.

Degree of crystallinity (%) = Ac x 100/ (Ac + Aa) Equation 5.

Ac: the total area of the crystalline peaks

Aa: the amorphous area of the diffractogram

3.3.16 Flow

The Flow experiment is based on the method described by Li and Zhu (2018) with some modifications. Weigh 0.402 g of dry starch into a 15ml centrifuge tube, add water and vortex to make a 5% (w/v) starch suspension. The suspension was heated in a 90°C water bath for thirty minutes with frequent vortexing for the first ten minutes. The paste was analyzed using an Anton Paar rheometer (Physica MCR 301, Anton Paar GmbH, Graz, Austria) parallel plate geometry (pp50). The analysis conditions were parallel plate geometry with a 1 mm gap between the bottom plate of the rheometer, shearing from 0.1 to 1000 s^{-1} and shearing from 1000 to 0.1 s^{-1} after incubating the sample for 5 min at 25°C. The relationship between shear rate and shear stress was characterized by Herschel-Bulkley gel rheological behavior.

$\tau = K_0 + K \cdot (\dot{\gamma})^n$ Equation 6.

τ: Shear stress (Pa)

K_0: Yield stress (Pa)

K: Consistency coefficient ($Pa \cdot s^n$)

$\dot{\gamma}$: shear rate (s^{-1})

n: liquidity behavior index

3.3.17 Oscillation

The Dynamic oscillation procedure was performed as described by Zhu, Bertoft and Li (2016) with some modifications. Weigh 0.22 - 0.23 g of starch in a 1.5 ml centrifuge tube and add Milli-Q water to a concentration of 20% (w/w). The starch suspension was vortexed to homogenize with a vortex mixer. Then precisely 0.515 mL of the solution was transferred to the bottom plate of an Anton Paar rheometer (Physica MCR 301, Anton Paar GmbH, Austria) with a pipette. Vegetable oil was added dropwise to the surface of the sample in contact with the air to prevent the evaporation of water. The dynamic oscillation properties of starch were determined using a heating and cooling program. Heating ranges from 40 to 90°C and cooling from 90 to 25°C. The relationship of Storage modulus (*G')* and loss modulus (*G''*) to temperature, frequency and amplitude is thus determined. When changing samples, thoroughly clean the rheometer base plate and probe with detergent, Milli-Q water and alcohol and wipe dry to avoid residual oil, starch and moisture affecting the results.

Chapter 4. Result and discussion

4.1 The basic situation of starch

The MC of starch has a great influence on the physical and chemical properties of starch annealed starch and the effect of annealing, including relative crystallinity and gelatinization characteristics (Sui & Kong, 2018). Therefore, accurate measurement of the moisture content in starch plays a vital role in subsequent experiments.

Table 4.1.1 Moisture content of treated and untreated starches

		Quinoa	Amaranth	Taro	Potato	Maize
Moisture content (%)	Control	10.93±0.49	13.39±0.69	9.65±0.44	12.23±0.48	10.62±0.34
	Annealing	12.81±0.43 #	10.85±0.37 #	11.98±0.58 #	17.99±0.25 #	13.71±0.45 #

Data are displayed as mean values ± standard deviation values with different symbols after the treated result indicate significant differences * ($p<0.05$), extremely significant differences # ($p<0.01$).

The moisture content of starch before and after annealing can be seen in Table 4.1.1. The starch moisture content of the control group was between 9.7 - 13.4%, and the starch moisture content of the annealed group was between 10.9 - 18.0%.

In addition, the starch content of purchased natural potato and maize starch is above 86.4%, and the starch content of extracted natural quinoa, amaranth and taro starch is all above 88.3%, of which amaranth starch has the highest starch content at 93.5%. The protein content of purchased potato starch and maize starch was lower than 1.6%, the protein content of extracted natural quinoa starch was lower than 1.3%, and the protein content of amaranth and taro starch was lower than 0.4%.

4.2 Particle Size

The particle size of starch has an essential effect on starch in food and non-food applications. Because it can affect starch, starch has unique physicochemical properties (Falade & Ayetigbo, 2022). The starch granules before and after the five treatments were therefore measured.

Table 4.2.1 Particle size of treated and untreated starches

Result		Quinoa	Amaranth	Taro	Potato	Maize
d (0.5) μm	Control	1.72±0.01	1.93±0.00	3.91±0.03	40.18±0.06	15.12±0.03
	Annealing	1.72±0.02	1.98±0.01 #	4.09±0.04 #	40.90±0.07 #	15.26±0.01 #
D [3, 2] μm	Control	1.65±0.01	1.86±0.00	2.54±0.01	36.70±0.05	14.26±0.06
	Annealing	1.66±0.02	1.88±0.01 #	3.07±0.09 #	37.10±0.06 #	14.41±0.01 #
D [4, 3] μm	Control	2.23±0.02	2.00±0.00	4.11±0.03	43.25±0.08	15.84±0.03
	Annealing	2.32±0.03 #	2.10±0.01 #	4.39±0.05 #	44.10±0.08 #	15.96±0.01 #
Span	Control	1.28±0.02	0.73±0.00	1.58±0.00	1.12±0.00	0.86±0.03
	Annealing	1.26±0.07	0.89±0.04 #	1.34±0.06 #	1.15±0.00 #	0.84±0.00 #
Uniformity	Control	0.55±0.01	0.23±0.00	0.45±0.00	0.35±0.00	0.27±0.01
	Annealing	0.59±0.02 #	0.28±0.01 #	0.41±0.01 #	0.35±0.00 #	0.26±0.00 #

d (0.5): numerical median diameter; D [3,2]: surface area moment mean diameter; D [4,3]: mass moment mean diameter. Data are displayed as mean values ± standard deviation values with different symbols after the treated result indicate significant differences * ($p<0.05$), extremely significant differences # ($p<0.01$).

The experiment method of particle size is shown in Chapter 3, and the results are shown in Table 4.2.1. The plant source determines the size of starch granules

(Jayakody & Hoover, 2008). This is determined by the genes and cultivation of the plant (Singh et al., 2003; Sui & Kong, 2018). It can be seen from the table that amaranth starch has the smallest particle size among those five starches, and its D [4, 3] is 2.00 μm. Quinoa starch granules have a slightly larger particle size than amaranth starch, with a D [4, 3] of 2.23 μm. And the D [4, 3] of taro starch was 4.11 μm. Among those five starches, potato starch had the largest particle size with D [4, 3] of 43.25 μm, followed by maize starch (D [4, 3] =15.84 μm). Therefore, quinoa starch, amaranth starch and taro starch are consistent with the small granular starches described by Lindeboom, Chang & Tyler (2004) with a diameter of less than 10 μm, so they are small granular starches. Among them, quinoa and amaranth are obvious. Potato and maize starch are large granular starches. In general, the five starches have different granule sizes and are similar in size to Lu et al. (2008), Kong et al. (2012), Li et al. (2019), Vamadevan & Bertoft (2015), Ek, Brand-Miller & Copeland (2012) with the same results. The distribution uniformity of quinoa starch was the highest, followed by taro starch and potato starch. The distribution of amaranth starch was the most uneven, and the distribution of maize starch was slightly more uniform than that of amaranth starch.

Annealing treatment affects the particle size of starch. After annealing, the particle size of five starch granules was slightly increased, and the increase ranged from 0.09 - 0.85. Among them, the particle size of potato starch granules varies the most, which may be related to their particle size. That means there is a slight irreversible swelling of starch granules caused by annealing (Wang, Jin & Yu, 2013; Zhang et al., 2015). This may be because of moisture incorporated through the amorphous regions of starch granules while annealing (Zavareze & Dias, 2011; Zhang et al., 2015). The variation of starch granule size after annealing treatment may be determined by treatment temperature (Jayakody & Hoover, 2008).

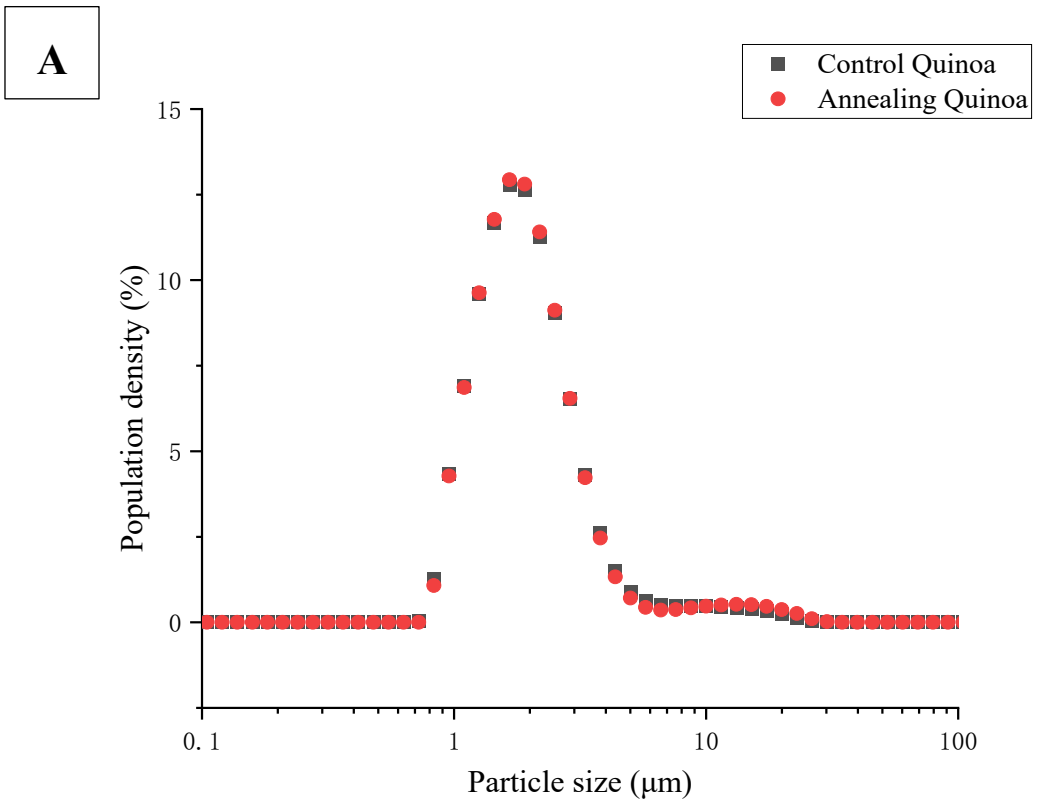
A
Control Quinoa
Annealing Quinoa
Population density (%)
15
10
5
0
0. 1
1
10
100
Particle size (μm)

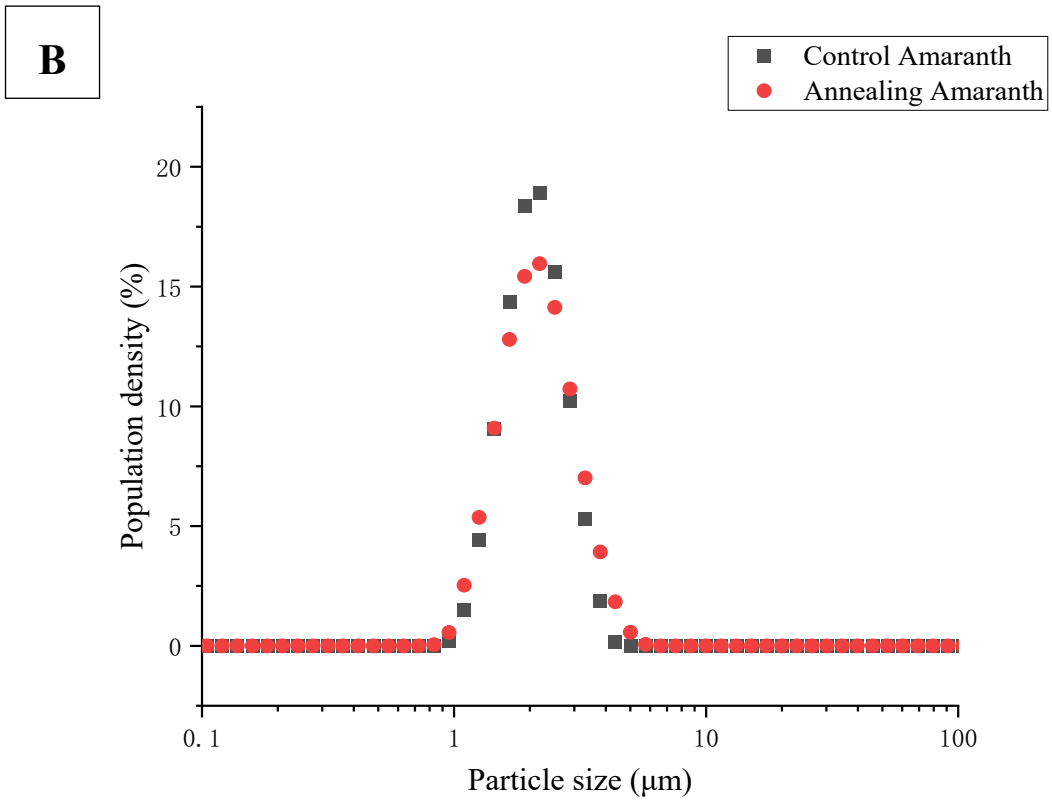
B
Control Amaranth
Annealing Amaranth
Population density (%)
20
15
10
5
0
0. 1
1
10
100
Particle size (μm)

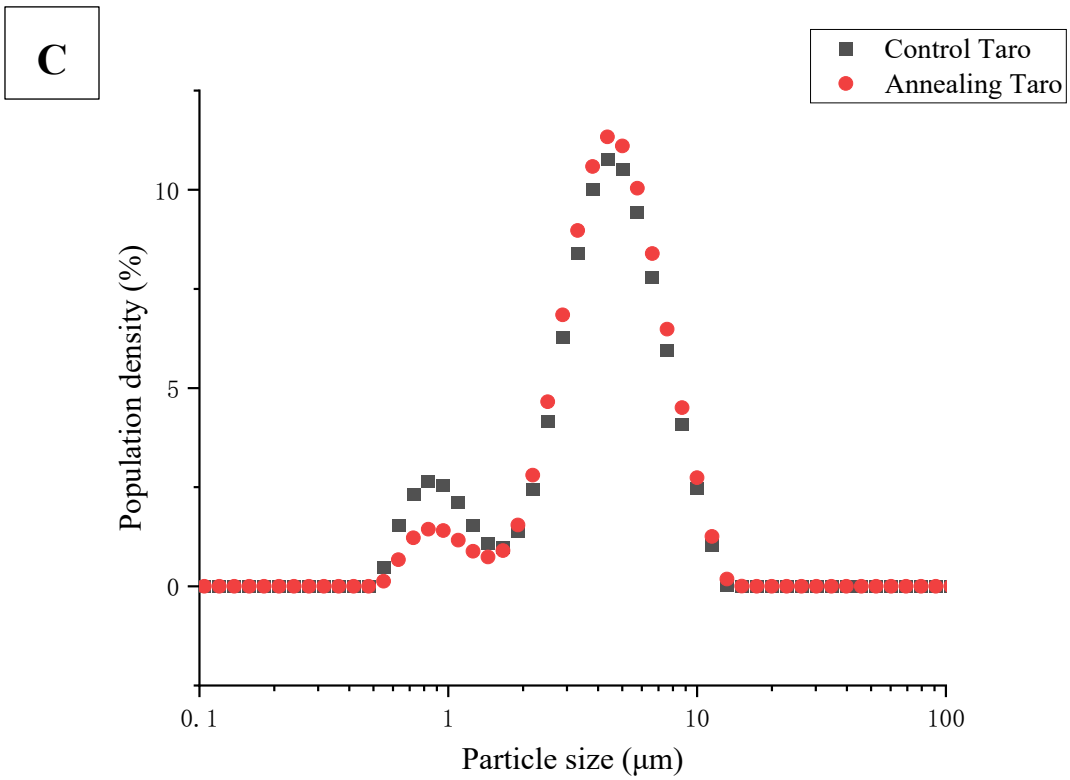
C
Control Taro
Annealing Taro
Population density (%)
10
5
0
0. 1
1
10
100
Particle size (μm)

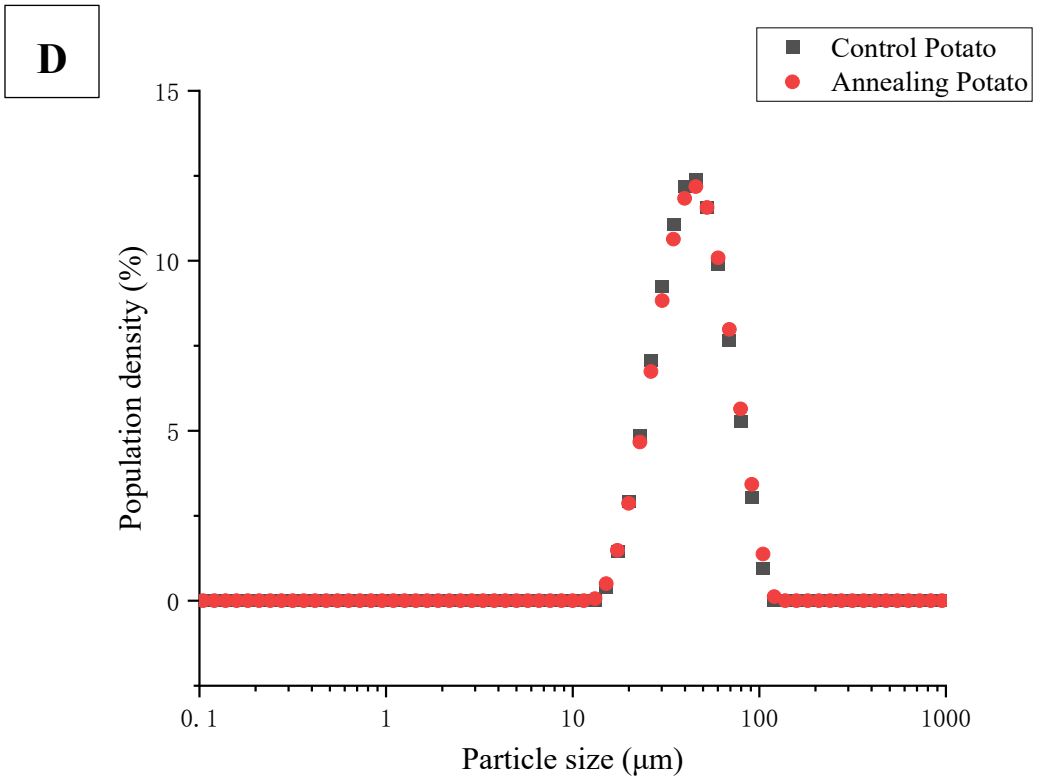
D
Control Potato
Annealing Potato
Population density (%)
15
10
5
0
0. 1
1
10
100
1000
Particle size (μm)

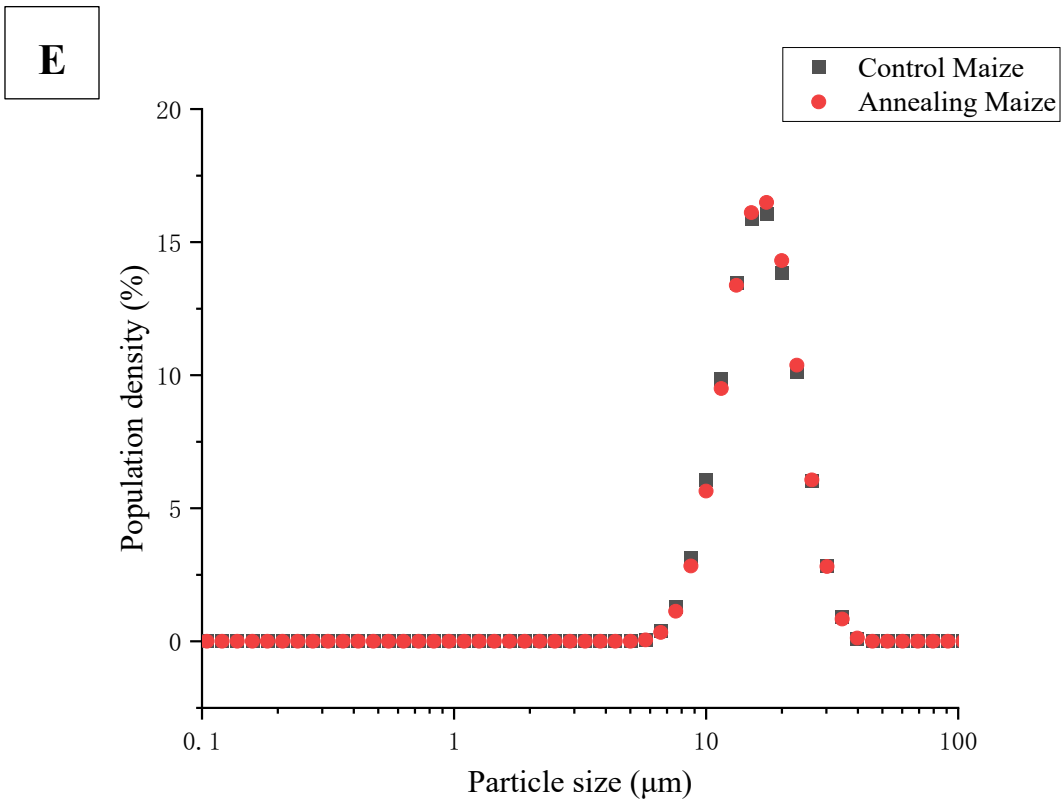

Figure 4.2.1 Particle size distribution of five starches before and after treatment

(A) Quinoa starch, (B) Amaranth starch, (C) Taro starch, (D) Potato starch, (E) Maize starch

It can be seen from the figure that the particle size distribution of untreated starch granules is mostly unimodal, obeying a normal distribution, and the distribution is dense. The granules of quinoa, amaranth and taro were distributed between 1 - 5 μm, 1 - 4 μm and 2 - 10 μm, respectively, and the granules of potato and maize starch were between 10 - 100 μm and 7 - 40 μm. In general, the distribution range of small granular starch is narrower than that of large granular starch. Taro starch had a small peak at 0.8 μm, which may be caused by the damage of intact starch granules during starch extraction (Das & Sit, 2021). Annealing treatment had no apparent effect on the particle size, distribution range and distribution of starch granules. In Figure 4.2.1, the annealing treatment slightly expanded the particle size distribution of amaranth starch, and the rest had no obvious effect.

4.3 Scanning electron microscopy (SEM)

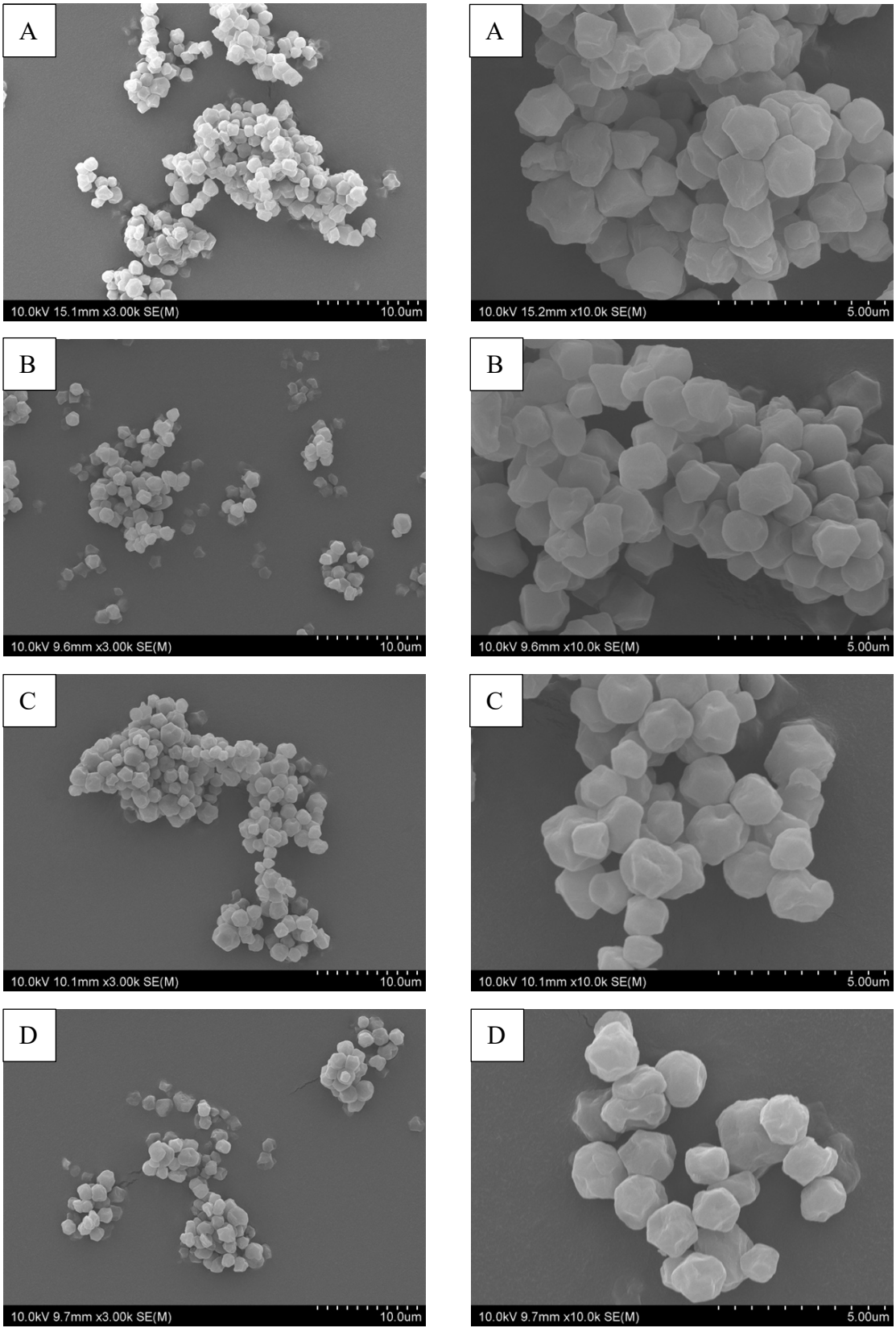

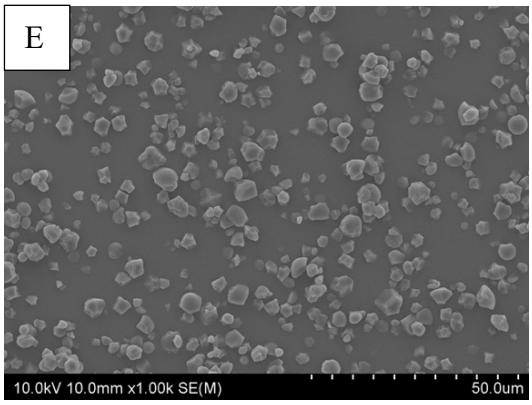
E
10.0kV 10.0mm x1.00k SE(M)
50.0um

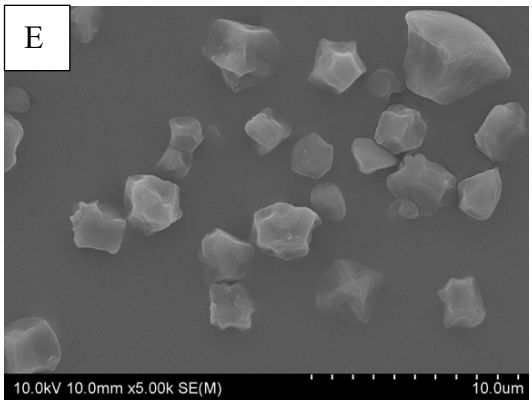
E
10.0kV 10.0mm x5.00k SE(M)
10.0um

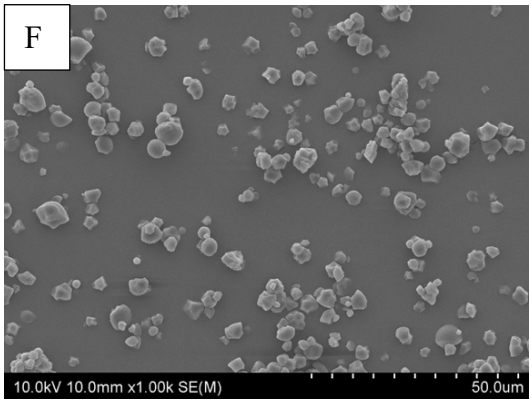
F
10.0kV 10.0mm x1.00k SE(M)
50.0um

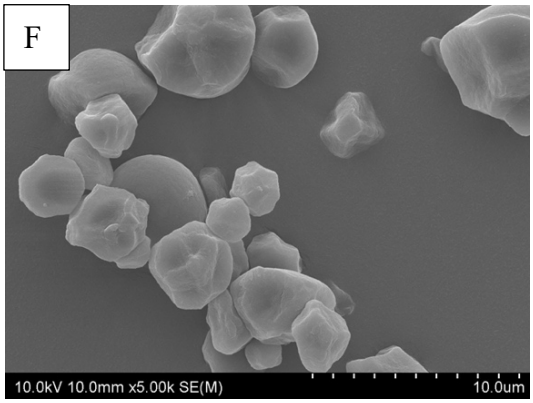
F
10.0kV 10.0mm x5.00k SE(M)
10.0um

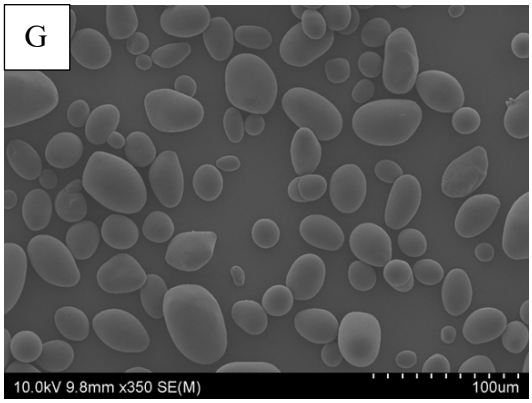
G
10.0kV 9.8mm x350 SE(M)
100um

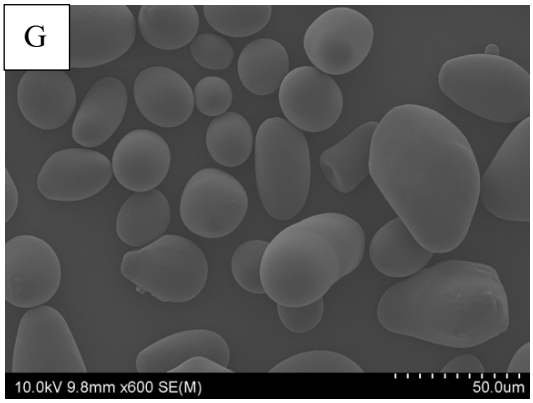
G
10.0kV 9.8mm x600 SE(M)
50.0um

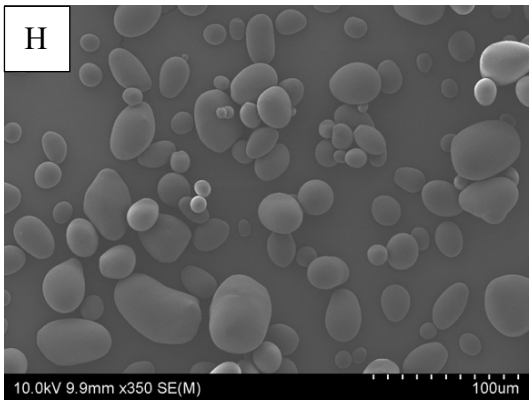
H
10.0kV 9.9mm x350 SE(M)
100um

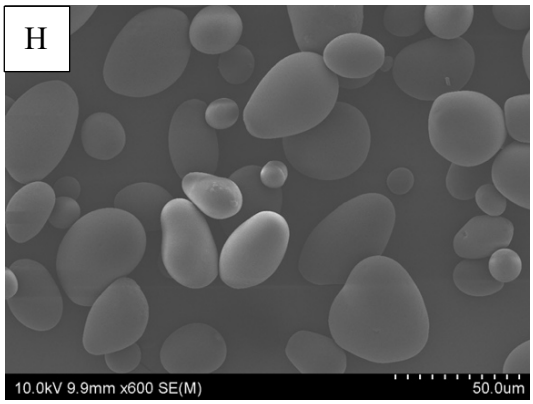
H
10.0kV 9.9mm x600 SE(M)
50.0um

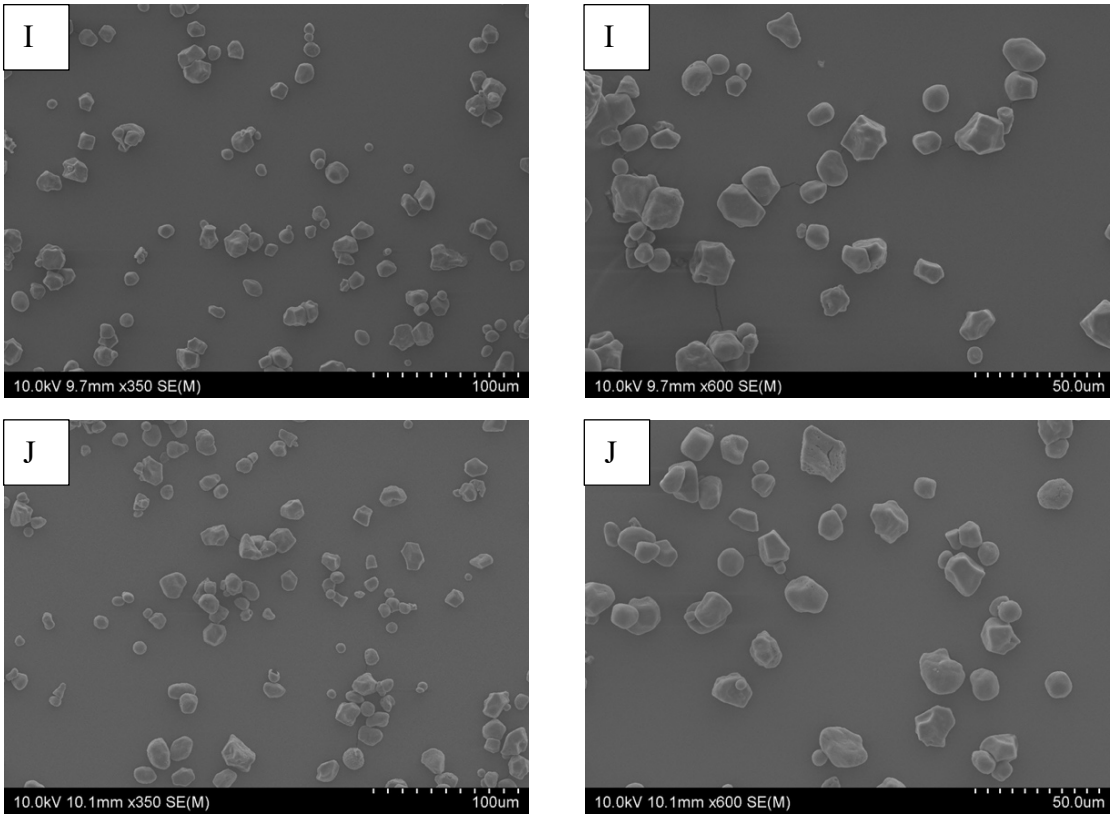

Figure 4.3.1 Scanning electron micrographs of control and annealed starches

(A) Control quinoa starch; (B) Annealing quinoa starch; (C) Control amaranth starch; (D) Annealing amaranth starch; (E) Control taro starch; (F) Annealing taro starch; (G) Control potato starch; (H) Annealing potato starch; (I) Control maize starch; (J) Annealing maize starch

By observing the results of scanning electron microscopy, it was found that the quinoa starch granules were small and irregular spheres or polyhedrons. The starch granules were uniform in size. The surface of starch granules was uneven, with many protrusions and depressions. The results are consistent with Li & Zhu (2018). The annealed quinoa starch had no noticeable difference in shape and size, and the surface was rough. In addition, the quinoa starch granules, both before and after treatment, adhered to each other, forming aggregates.

Untreated amaranth starch granules were small and uniform, most of them were irregular spheres, and a few particles were irregular in shape. The surface of starch was rough and had many wrinkles. The size and shape of annealed starch granules

were basically unchanged, but the surface was rougher than before, and the number of textures increased. Both before and after treatment, amaranth starch had the characteristics of mutual adhesion and aggregation.

For the untreated taro starch, the granule size was larger but uneven. The shape of starch granules was a mixture of spherical, polyhedral and irregular shapes. The surface of most starch granules is rough and has many protrusions and depressions. A small number of starch granules have a partially smooth surface, while the rest of the surface is bumpy. The size and shape of the treated starch granules were almost unchanged. However, the surface of some starch granules was more irregular, almost all the smooth surfaces were lost, and more depressions appeared. The distribution of untreated taro starch granules was relatively dispersed, and fewer individuals were adhering to each other. The adhesion of starch granules was slightly increased after treatment.

Potato starch granules were the largest of the five starches and were not uniform in size. Most of the starch granules are ellipsoid, and a few are spherical. Most of the particles had a smooth surface, and a few were slightly rough. The size and shape of the treated potato starch granules were basically unchanged, and some starch granules kept their original appearance. However, some particles had a rougher surface with more bumps and dents. The untreated starch granule distribution was dispersed with little aggregation, with a slight increase in the aggregation after treatment.

Untreated maize starch granules were smaller than potato starch granules and were not uniform. Starch granules were spherical and polyhedral. The surface was smooth, but there were some depressions and bumps. The size and shape of the treated maize starch granules remained almost unchanged, but a certain number of depressions and pores appeared on the surface. The distribution of starch granules before and after treatment was relatively dispersed, with little adhesion.

In conclusion, the size and morphology of five different plant-derived starches were different, and the results were the same for particle size. The morphology of native starch granules is determined by plant physiology and starch biochemistry (Singh et al., 2003). Different sources have different compositions, structures, and physicochemical properties (Jayakody & Hoover, 2008). Furthermore, the clustering phenomenon of small-granular starch is more evident than that of large-granular starch.

The annealing treatment does not change the shape of starch granules (Shen et al., 2021). Annealing resulted in a rougher surface of part of some starches and the agglomeration of starch granules, possibly due to a slight irreversible swelling of the starch granules (Wang, Jin & Yu, 2013; Zhang et al., 2015). This may be due to the excessive water absorption by starch granules during the annealing process, which causes the distance between clusters in starch granules to expand, forming a rough surface (Sui & Kong, 2018). The surface change of starch granules may also be caused by the heat in the annealing treatment, which leads to the recombination of amylose and amylopectin in starch, making the amorphous region of starch denser and the amorphous region more stable, resulting in an increase in the internal pressure of starch granules (Liu et al., 2015; Su et al., 2020). Another explanation is that annealing leads to the leaching of amylose from starch granules, and the enhanced activity of endogenous amylases causes changes in the surface of starch granules (Xu et al., 2018b).

Particle morphology is also affected by processing conditions. Annealing had different effects on the surface of different plant-derived starches, as stated by Su et al. (2020). Hu et al. (2020) found that the surface of starch annealed for a longer time (5 days) was smoother than that of sweet potato starch annealed for a short time (3 days). They believe this may be due to annealing resulting in slight fragmentation of starch

crystals (Hu et al., 2020). However, as annealing progresses, the fragmented and loose crystallites are transformed into stable and denser ones (Hu et al., 2020). However, Su et al. (2020) showed that grooves and cracks on the surface of wheat starch increased with increasing annealing time and were more pronounced in starches with lower amylose content. The moisture content and treatment temperature were the same for both sets of experiments, possibly due to the different properties of starches from different plant sources. Almeida et al. (2020) found that the starch granule characteristics of Prata banana were not affected by annealing and annealing temperature after annealing at different temperatures, which they said was the same as yam starch, but different from wheat starch (Almeida et al., 2020). This evidence also proves that the annealing of different starches from plant sources has different effects on the surface.

4.4 Gelatinization

Thermal properties of the samples were measured using the Differential scanning calorimeter using the methods of Chapter 3.

Table 4.4.1 DSC results of treated and untreated starches

Result		Quinoa	Amaranth	Taro	Potato	Maize
T_o (°C)	Control	53.37±0.20	55.75±0.03	72.34±0.20	58.00±0.11	68.94±0.31
	Annealing	57.97±0.27 #	60.42±0.06 #	78.13±0.07 #	65.33±0.10 #	74.30±0.08 #
T_p (°C)	Control	63.10±0.51	61.99±0.24	76.17±0.30	61.35±0.03	72.76±0.10
	Annealing	65.22±0.10 #	64.53±0.05 #	80.74±0.16 #	67.76±0.08 #	76.67±0.06 #
T_c (°C)	Control	73.10±0.69	70.96±0.23	86.07±1.09	68.81±0.21	78.57±0.19
	Annealing	73.32±0.19	73.13±0.33 #	89.56±0.88 #	73.22±0.41 #	81.29±0.13 #
Δ T (°C)	Control	19.73±0.59	15.21±0.21	13.73±1.04	10.81±0.25	9.63±0.39
	Annealing	15.36±0.44 #	12.71±0.37 #	11.43±0.81 *	7.90±0.49 #	6.99±0.19 #
Δ H (J/g)	Control	12.84±0.24	16.21±0.27	18.81±0.77	21.27±0.25	16.19±0.26
	Annealing	13.43±0.45	16.59±0.47	19.87±0.06 *	22.85±0.45 *	16.46±0.08

T_o: onset temperature; T_p: peak temperature; T_c: conclusion temperature; ΔH: the change of enthalpy; ΔT: gelatinization temperature range. Data are displayed as mean values ± standard deviation values with different symbols after the treated result indicate significant differences * ($p<0.05$), extremely significant differences # ($p<0.01$).

The DSC results for the Control Group and the annealing group are listed in Table 4.4.1. The gelatinization properties of starches from different plant sources were significantly different. Among them, quinoa starch had the lowest gelatinization onset temperature (53.4°C), followed by amaranth starch (55.8°C) and potato starch

(58.0°C), taro starch (72.3°C) was higher than maize starch (68.9°C), which was the highest among the five starches. For peak gelatinization temperature, quinoa starch is higher than amaranth starch and potato starch, which are 63.1°C, 62.0°C, and 61.4°C, respectively. In addition, taro has the highest gelatinization peak temperature, 76.2°C, followed by maize starch, 72.8°C. The gelatinization temperature ranges of the five starches were different, among which the gelatinization range of quinoa starch was the widest at 19.7°C, followed by amaranth starch and taro starch, which were 15.2 and 13.7°C, respectively, and the gelatinization range of maize starch was the narrowest at 9.6°C, followed by potato starch at 10.8°C. In general, the starch gelatinization peak temperature with the highest gelatinization onset temperature is also the highest, and the two trends are basically the same. In addition, among the five starches, the gelatinization range of small-granular starch was more significant than that of large-granular starch. For gelatinization enthalpy, the number of double helices melted and unraveled during starch gelatinization is shown (Hoover, 2008). It can be seen from the table that different starches behave differently. Among them, the gelatinization enthalpy of amaranth starch and maize starch are similar, approximately 16.2 J/g. The gelatinization enthalpy of potato starch was the highest, reaching 21.3 J/g. The gelatinization enthalpy of quinoa starch was the lowest among the five starches, which was 12.8 J/g. The gelatinization enthalpy of taro starch is higher than that of amaranth starch and maize starch, which is 18.8 J/g.

The gelatinization temperature and enthalpy of different plant-derived starches in the control group differed. The results are the same as Wu et al. (2016), Jayakody and Hoover (2008), Wang et al. (2017b), Kim et al. (1995), and Xu et al. (2018b). The swelling and hydration of amorphous regions in starch granules determine the gelatinization of starch granules (Marboh et al., 2022). The onset temperature represents the gelatinization temperature of the crystal with the weakest structure in starch granules, and the conclusion temperature represents the gelatinization temperature of the crystal with the strongest structure (Xu et al., 2018a; Wang et al., 2014; Singh et al., 2003; Kim et al., 1995). Therefore, the order of the crystal structure

and the degree of crystallinity may be the factors affecting the thermal transition temperature of different plant-derived starches (Xu et al., 2018a; Wang et al., 2014; Singh et al., 2003; Kim et al., 1995). It may be caused by the different properties of starch granules from different plant sources, such as chemical composition (Singh et al., 2003; Kim et al., 1995). The higher the degree of crystallinity, the higher the transition temperature, resulting in different gelatinization properties of different plant-derived starches (Barichello et al., 1990). In addition, different varieties and plant parts also affect the gelatinization temperature of starch (Karlsson & Eliasson, 2003). This may be due to the difference in gelatinization temperature and heat transfer rate due to different starch granule sizes and dry matter content (Karlsson & Eliasson, 2003). The molecular structure of the crystalline region and the granular structure of starch may also affect the gelatinization properties of starch (Singh et al., 2003).

The annealing treatment increased the gelatinization onset temperature, peak temperature and conclusion temperature of the five starches. The increases were 4.6 - 7.3°C, 2.1 - 6.4°C and 0.2 - 4.4°C, respectively. Among them, the gelatinization of potato starch started. The temperature increased the most, and the quinoa starch increased the least. At the same time, the gelatinization peak temperature and conclusion temperature of potato starch and quinoa starch were also the most obvious and least obvious, respectively. The gelatinization temperature range decreased by 2.3 - 4.3°C. Among them, quinoa starch decreased the most and taro starch decreased the least.

The effect of annealing treatment on the gelatinization onset temperature is greater than the gelatinization conclusion temperature (Jayakody & Hoover, 2008). An increase in the thermal transition temperature and a decrease in the gelatinization temperature range suggest that annealing increases the uniformity and stability of crystallites in starch granules (Wang et al., 2014; Tester, Debon & Sommerville, 2000; Wang et al., 2017b; Jayakody & Hoover, 2008). Amylose molecular

rearrangement-induced enhancement of amylopectin clusters leads to increased amylose-amylose interactions in starch, improved starch quality, increased thermal transition temperature, and decreased gelatinization temperature range (Wang et al., 2014; Wang et al., 2017b; Jayakody & Hoover, 2008; Zhang et al., 2015). Interactions between amylopectin chains allow for increased mobility of starch in the amorphous region, recombining molecules (Jayakody & Hoover, 2008). In addition, studies have shown that annealing can increase the ordering of amorphous regions or produce a glassier state and also increase the thermal transition temperature (Wang et al., 2017b). Since amylose is sensitive to annealing (Guo et al., 2020), annealing can rearrange the amylose, making the starch more uniform and stable, thereby increasing the gelatinization temperature and reducing the thermal transition temperature range (Wang et al., 2014). The results of Wang, Jin & Yu (2013) suggest that annealing causes slight leaching of apparent amylose from starch granules and, thus, a slight decrease in amylose content. That potentially reduces long-range forces between amylopectin clusters and causes more free infiltration of water into the annealed particles (Wang, Jin & Yu, 2013). They showed that with less heat input than native starch, annealed starch granules appeared to exhibit slower heat input, thus leading to an increase in thermal transition temperature (Wang, Jin & Yu, 2013).

The gelatinization enthalpies of the five starches increased after treatment, ranging from 0.3 to 1.6°C. Among them, the gelatinization enthalpy of maize starch changed the least after annealing treatment, which was consistent with the results of Wang et al. (2014). Annealing Treatment increases the energy of the crystal structure in starch to disrupt the amylopectin double helix, thus increasing the enthalpy of gelatinization (Simsek et al., 2012). The gelatinization enthalpy of starch is related to the dissociation and reorganization of the double helix (Liu et al., 2016a; Hu et al., 2020). It is also affected by the amylose content and location of starch granules, as well as the location and distribution of amylopectin (Hoover, 2008). Hu et al. (2020) concluded that prolonged (five days) annealing might promote the formation of new double-helical structures in the amorphous region increase the gelatinization enthalpy.

Liu et al. (2009) showed that the annealing treatment is a purely physical process with no apparent effect on the amylose and amylopectin content, and the increase in enthalpy may be due to the formation of more hydrogen bonds.

In addition to the annealing conditions in Chapter 3, the annealing of five starches under other conditions was attempted, and the results are presented in the Appendix. For the factors affecting the thermal properties of annealed starch, comparing the attached table with the table shows that the annealing time has a more significant impact on the DSC results but has different effects on starch from different plant sources. The changes in thermal transition temperature of starch annealed for five days were more pronounced than those of starch annealed for two days. This result is the same as Zhang et al. (2015). In addition, the gelatinization enthalpy of starch varies with the annealing time (Hu et al., 2020). This is because the thermal transition temperature increases with the annealing, but the gelatinization enthalpy decreases first because short-time annealing (one day and three days) leads to the dissociation of the double helix in the amorphous and crystalline regions of starch granules (Hu et al., 2020). With the increase in annealing time, the thermal transition temperature and gelatinization enthalpy change of starch gradually increased (Zhang et al., 2015). Xu et al. (2018a) and Hoover & Vasanthan (1997) also showed that the thermal properties of starch increased with a longer annealing time. The same results were obtained by Xu et al. (2018b) by annealing red adzuki bean starch at different times. They explained that this might be due to enhanced amylose-amylose and amylose-amylopectin interactions in starch granules, forming microcrystalline melting, which inhibits swelling and makes the crystal structure more ordered (Zhang et al. al., 2015; Hu et al., 2020). Annealing treatment changes the thermal stability of starch. It delays the progress of gelatinization, which can be applied to cooked food, such as canned food, which is beneficial to the processing and production of food (Sui & Kong, 2018).

4.5 Retrogradation

The starch was gelatinized during the DSC assay and then retrograded during low-temperature storage. The thermal properties of the regenerated samples were tested according to the method in Chapter 3.

Table 4.5.1 Retrogradation of treated and untreated starches

Result		Quinoa	Amaranth	Taro	Potato	Maize
T_o (°C)	Control	35.55±0.30	35.61±0.31	38.20±0.78	45.22±0.18	39.63±0.59
	Annealing	33.88±0.60 #	35.01±0.21 *	38.08±1.77	41.58±0.36 #	38.21±0.09 #
T_p (°C)	Control	46.29±0.54	47.91±0.84	51.4±0.32	64.52±2.62	51.22±0.81
	Annealing	45.60±0.72	47.13±0.34	52.48±0.91	55.63±2.12	49.52±0.75 *
T_c (°C)	Control	57.34±0.43	56.55±0.13	63.36±0.22	70.59±1.57	62.55±0.67
	Annealing	56.44±0.46 *	56.36±0.13	66.60±0.55 #	71.70±0.68	62.37±0.63
ΔT (°C)	Control	21.79±0.71	20.94±0.37	25.17±0.74	25.37±1.39	22.92±0.79
	Annealing	22.56±0.90	21.35±0.08	28.52±1.86	30.12±0.67	24.17±0.68
ΔH (J/g)	Control	8.33±0.41	10.16±0.21	12.52±0.28	9.38±0.59	10.66±0.23
	Annealing	9.60±0.73 *	10.84±0.36	13.52±1.34	11.94±1.18 *	11.12±0.62
R (%)	Control	0.65±0.03	0.63±0.01	0.67±0.01	0.44±0.03	0.66±0.01
	Annealing	0.71±0.05	0.65±0.02	0.68±0.07	0.52±0.05	0.68±0.04

T_o: onset temperature; T_p: peak temperature; T_c: conclusion temperature; ΔH: the change of enthalpy; ΔT: gelatinization temperature range. Data are displayed as mean values ± standard deviation values with different symbols after the treated result indicate significant differences * ($p<0.05$), extremely significant differences # ($p<0.01$).

The differential scanning calorimeter measurement results of the retrograded samples are shown in Table 4.5.1. The gelatinization onset temperatures of the five starches ranged from 35.6 to 45.2°C, which was significantly lower than the 53,4 to 72.3°C of the starches before gelatinization. The gelatinization onset temperature of untreated quinoa starch (35.6°C) was still the lowest among the five starches, followed by slightly higher amaranth starch (35.6°C) and taro starch (38.2°C). Potato starch (45.2°C) had the highest gelatinization onset temperature, followed by maize starch (39.6°C). The gelatinization peak temperature and conclusion temperature of the retrograded samples also decreased significantly, as was the gelatinization onset temperature. From 61.4 - 76.2°C and 68.8 - 86.1°C to 46.3 - 64.5°C and 56.6 - 70.6°C. Compared with the starch before gelatinization, the transformation temperature and retrogradation enthalpy of retrogradation samples were significantly lower. The retrogradation characteristics of different plant-derived starches are different, which may be caused by the differences in the transformation temperature and gelatinization enthalpy of the starch itself, which are caused by the characteristics of plants, including amylose content and chain length, starch granule shape and size, etc. factors (Singh et al., 2003). In addition, the storage time of the samples affects the retrogradation results of starch. Karlsson & Eliasson (2003) explained that most of the internal recrystallization of the samples occurred in the early storage period, after which the retrogradation process continued, but the rate slowed down.

Compared with the unannealed starch, the retrogradation rate of the annealed starch increased, the transition temperature decreased, and the retrogradation enthalpy increased slightly. This may be due to the rearrangement of the crystal structure in starch granules due to annealing (Singh et al., 2011). Amylose content affects the retrogradation of starch, so it may also be caused by the leaching of small amounts of amylose due to annealing (Yu et al., 2016; Singh et al., 2003). The retrogradation of starch is also affected by annealing conditions such as moisture content and temperature (Yu et al., 2016). They found that a small amount of water can increase the flow of starch molecules, but an excess of water may increase amylose leaching

in shorter treatments (Yu et al., 2016). Therefore, Yu et al. (2016) concluded that longer treatment time and lower water content could lead to more stable starch.

4.6 Swelling power and water solubility

The swelling of starch is caused by the breaking of hydrogen bonds in starch when excess water and heat exist at the same time, the crystal structure is destroyed, and the water molecules are connected to the hydroxyl groups of amylopectin and amylose (Hoover, 2001; Singh et al. al., 2003). The experimental conditions for the determination of swelling power and solubility coefficient were chosen at 85°C because the difference in swelling power and solubility between annealed and unannealed starch was more pronounced at a heating temperature of 80 to 90°C (Dias et al., 2010; Zhang et al., 2015).

Table 4.6.1 Swelling power and water solubility of treated and untreated starches

Result		Quinoa	Amaranth	Taro	Potato	Maize
SP (g/g)	Control	24.25±0.40	55.00±3.63	28.07±0.53	63.31±3.10	14.54±0.16
	Annealing	22.79±1.68	44.52±5.64	27.54±0.08	62.36±1.53	12.03±0.18 #
WSI (%)	Control	37.07±3.56	96.10±0.16	77.21±1.35	82.05±3.94	12.10±0.05
	Annealing	53.28±4.03 #	95.74±0.61	76.64±1.99	73.62±3.31 *	11.84±0.47

SP: swelling power; WSI: water solubility. Data are displayed as mean values ± standard deviation values with different symbols after the treated result indicate significant differences * ($p<0.05$), extremely significant differences # ($p<0.01$).

It can be seen from Table 4.6.1 and Figure 4.6.1 that the swelling power of different starches is different. Among the starches before annealing, the potato had the highest swelling power of 63.3 (g/g), followed by amaranth and taro starch, with swelling powers of 55.0 (g/g) and 28.1 (g/g), respectively. Among the five starches, the swelling power of maize starch (12.0 g/g) was the lowest, and the swelling power of

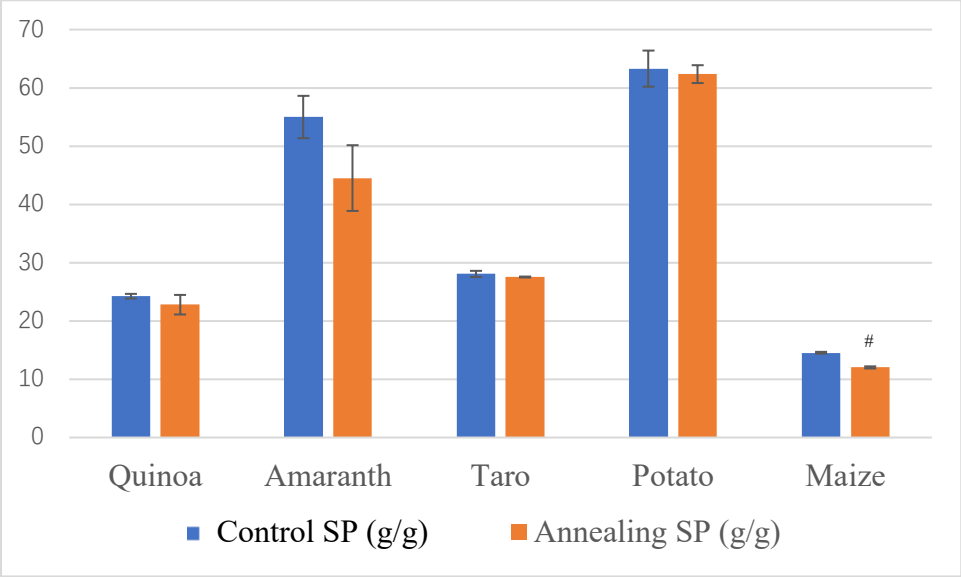

Figure 4.6.1 Swelling power of treated and untreated starches. Data are displayed as mean values ± standard deviation values with different symbols after the treated result indicate significant differences * ($p<0.05$), extremely significant differences # ($p<0.01$).

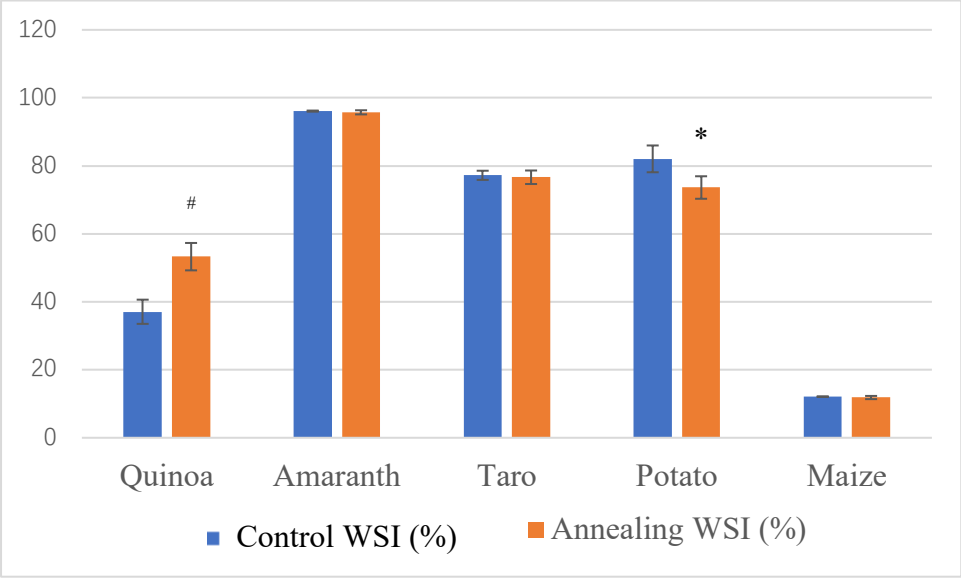

Figure 4.6.2 Water solubility index of treated and untreated starches. Data are displayed as mean values ± standard deviation values with different symbols after the treated result indicate significant differences * ($p<0.05$), extremely significant differences # ($p<0.01$).

quinoa starch (22.8 g/g) was greater than that of maize starch. For the solubility index, maize starch (12.1%) in the control group was the least soluble in water, and quinoa starch (37.1%) was more soluble than maize starch. Amaranth starch had the highest solubility (96.1%), followed by potato starch (82.1%) and taro starch (77.2%).

The swelling power and solubility of starch show the interaction of amylose and amylopectin chains in starch granules and are therefore affected by the content, chain length, ratio, and distribution of amylose and amylopectin in starch granules (Hoover, 2001; Singh et al., 2003). Phosphate groups in starch also affect the swelling power and solubility of starch by affecting the bonding of crystalline regions (Hoover, 2001). The content of phosphate groups in different plant-derived starches, especially potato starch, may be one of the reasons for the differences in swelling power and solubility of the five starches (Hoover, 2001; Singh et al., 2003). They suggest that potato starch has more phosphate groups on amylopectin, which may be the reason why potato starch has the highest swelling power of the five starches (Singh et al., 2003). The lipid in starch is also one of the factors affecting the swelling power of starch. Singh et al. (2003) indicated that the lowest solubility of maize starch might be due to the high lipid content in its starch granules. The shape of starch granules may be one of the influencing factors, the more irregular the shape of starch granules, the larger the volume will lead to lower swelling because the substances within the starch granules are easily fixed, resulting in difficult swelling (Singh et al., 2003).

From Table 4.6.1 and Figure 4.6.1, it can be seen that the annealing treatment reduces the swelling power of starch, the decrease range is between 0.53 and 10.48 (g/g), and the degree of change is related to the type of starch. This result is the same as Liu et al. (2016b), Yadav, Guleria & Yadav (2013). Among them, amaranth starch decreased the most, quinoa and maize starch decreased almost the same, but the swelling power of maize starch before and after treatment showed a very significant difference. Taro starch decreased the least, followed by potato starch. The structural integrity of amylopectin has a critical impact on the swelling power of starch granules

(Wang, Jin & Yu, 2013). The small decrease in swelling power indicates that the annealing treatment hardly breaks the amylopectin but slightly breaks the amylopectin molecules during the expansion of the starch granules (Wang, Jin & Yu, 2013). The crystal order can limit the swelling power of starch granules, and the interaction between amylose caused by annealing treatment, the perfection of crystallization and the small amount of starch water and interaction may also be the reasons for the slightly lower swelling power (Waduge et al., 2006; Liu et al., 2016b; Yadav, Guleria & Yadav, 2013; Liu et al., 2009). In addition, it is also possible that strong bonds are formed between amylopectin molecules after treatment, thereby reducing the swelling power (Liu et al., 2016a).

Annealing treatment reduced the solubility of four starches except for quinoa starch, ranging from 0.26% to 8.43%. Among the four declining starches, the solubility of potato starch decreased the most and was significant. Followed by taro starch and amaranth starch, and the solubility of maize starch decreased the least. Annealing treatment reduces the solubility of starch granules, possibly because the treatment strengthens the bonds between amylopectin molecules or between amylose and amylopectin, reducing the leaching of the granules (Zhang et al., 2015). Annealing makes the crystalline rearrangement and perfection of starch molecules and may also lead to a decrease in the hydration of the amorphous regions, thereby reducing the solubility of starch (Liu et al., 2016b; Xu et al., 2018b).

The solubility of quinoa starch increased after annealing treatment, possibly because the treatment reduced the association between polymers in starch granules (Liu et al., 2016b). Shen et al. (2021), Dias et al. (2010) annealing studies on wheat and rice showed increased starch solubility after treatment. The reason may be that solubility is more affected by amylose content (Xu et al., 2018a). At the higher assay temperature (85°C), the leaching of amylose was accelerated, resulting in increased solubility (Xu et al., 2018a).

4.7 Pasting

Methods for determination of starch Pasting properties are in Chapter 3. Below are figures of the pasting properties of starch before and after annealing.

A

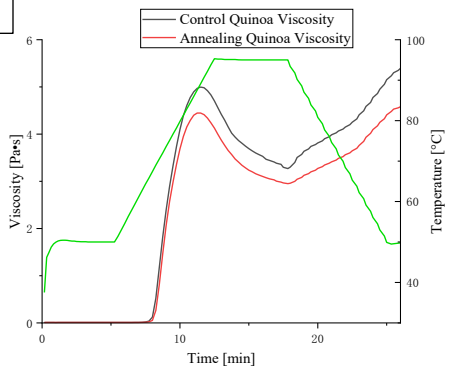

B

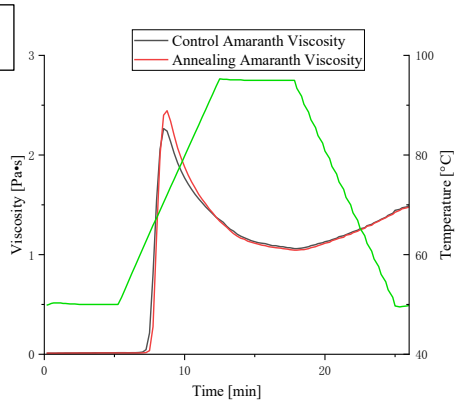

C

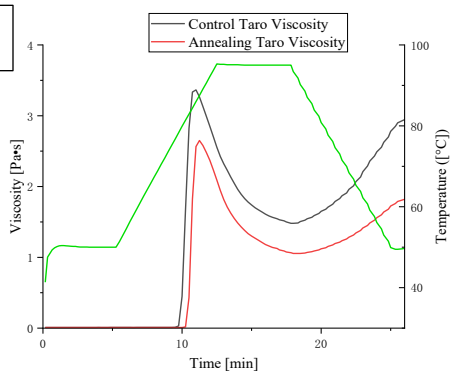

D

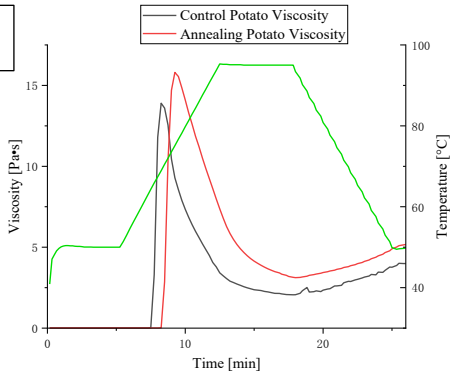

E

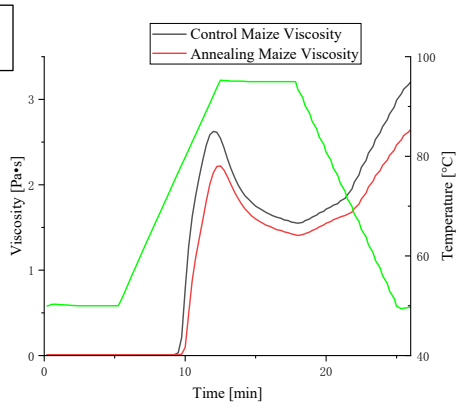

Figure. 4.7.1 The pasting profiles of control and annealed starches
(A) Quinoa starch; (B) Amaranth starch; (C) Taro starch; (D) Potato starch; (E) Maize starch

It can be seen from Figure 4.7.1 that there is no significant difference in the overall pasting trend of starches from different plant sources, and the gelatinization curves of the five starches all have obvious gelatinization peaks. During the heating process, the viscosity of the untreated starch first remained unchanged and then suddenly increased until the peak viscosity was reached. The viscosity decreased immediately when the peak viscosity was reached. Then there is the temperature holding stage, the viscosity continues to decrease until the hot paste viscosity turns, and the viscosity rises slowly. During the temperature drop stage, the viscosity of each starch gradually increased with the decrease in temperature. For different types of starch, the time when the viscosity starts to increase during the heating process is different. That is, the pasting temperature is different. It can be seen from Figure 4.7.1 that the viscosity of taro starch starts to rise at the latest as time increases, while amaranth starch is the earliest. The viscosity growth rate of starch is also different. The viscosity growth rate of amaranth starch, taro starch and potato starch are significantly higher than that of quinoa and maize starch. During the temperature holding stage, the hot paste viscosity of each starch was different, among which potato was the lowest, quinoa and maize the highest, which was caused by their different viscosity decline. The last is the viscosity cool paste viscosity at the end of the cooling process, which has the same trend as the hot paste viscosity in the image. The starch with higher hot paste viscosity also has higher cool paste viscosity. In addition, the cool paste viscosity of starch is larger because the viscosity increases faster in the cooling stage. The cool paste viscosity of quinoa starch and maize starch is higher than their peak viscosity.

Annealing treatment did not change the overall shape of the starch gelatinization curve, most starches shifted downward after annealing treatment, but amaranth starch and potato starch were different. The gelatinization curve of amaranth starch

before and after treatment almost overlapped, and the gelatinization curve of starch after treatment increased slightly. The gelatinization curve of annealed potato starch shifted upward to the right, and the viscosity of each inflection point was greater than that of control potato starch. The viscosity of quinoa starch and amaranth starch did not change significantly, but the viscosity of taro starch, potato starch and maize starch shifted to the right.

Table 4.7.1 Pasting of treated and untreated starches

Result		Quinoa	Amaranth	Taro	Potato	Maize
Pt (°C)	Control	65.30±0.87	61.10±0.00	78.30±0.00	65.10±1.13	76.75±0.07
	Annealing	65.83±0.06	64.30±0.00 #	83.00±0.00 #	69.80±1.13	79.9±0.00 #
Pv (Pa·s)	Control	5.00±0.18	2.27±0.01	3.37±0.01	13.90±0.00	2.63±0.01
	Annealing	4.45±0.01 *	2.45±0.01	2.65±0.01 #	15.80±0.28	2.22±0.02 #
Hpv (Pa·s)	Control	3.30±0.16	1.07±0.00	1.50±0.01	2.07±0.00	1.57±0.01
	Annealing	2.97±0.02	1.05±0.01	1.08±0.01 #	3.20±0.13	1.43±0.02 #
Cpv (Pa·s)	Control	5.39±0.11	1.49±0.01	2.95±0.01	3.99±0.03	3.21±0.01
	Annealing	4.58±0.02 #	1.48±0.01	1.82±0.01 #	5.17±0.06 #	2.65±0.02 #
Bd (Pa·s)	Control	1.70±0.14	1.20±0.01	1.87±0.02	11.83±0.00	1.06±0.00
	Annealing	1.48±0.03	1.40±0.02 *	1.58±0.01 *	12.61±0.15	0.79±0.01 #
Sb (Pa·s)	Control	2.10±0.12	0.42±0.01	1.45±0.01	1.92±0.03	1.64±0.00
	Annealing	1.61±0.01 *	0.43±0.00	0.75±0.01 #	1.98±0.08	1.22±0.00 #

Pt: pasting temperature; Pv: peak viscosity; Hpv: hot paste viscosity; Cpv: cool paste viscosity; Setback (SB = CPV − HPV); Breakdown (BD = PV − HPV). Data are displayed as mean values ± standard deviation values with different symbols after the treated result indicate significant differences * ($p<0.05$), extremely significant differences # ($p<0.01$).

The gelatinization properties of treated and untreated starches are summarized in Table 4.7.1, and it can be seen that the pasting properties of different starches are different. Pasting temperature is often related to gelatinization temperature. The pasting temperature of five starches before annealing treatment is between 61.1 and 78.3°C, the highest for taro starch and the lowest for amaranth starch. The peak viscosity ranges from 2.3 Pa·s to 13.9 Pa·s, among which the peak viscosity of potato starch is significantly higher than that of other starches, and amaranth starch has the lowest peak viscosity. The ranges of hot paste viscosity and cool paste viscosity are 1.1 - 3.3 Pa·s and 1.5 - 5.4 Pa·s, respectively. These two parameters of quinoa starch are higher than other starches, amaranth starch is lower than others starch. The breakdown and setback are from 1.1 Pa·s to 11.8 Pa·s, and from 0.4 Pa·s to 2.0 Pa·s. The breakdown of potato starch and the setback of quinoa starch are higher than other starches and the breakdown of maize and the setback of amaranth starch, respectively lower than other starches. The pasting characteristics of different plant-derived starches are different because the size of starch granules, the content of amylose, trace components and impurities in starch granules are different, which may affect the gelatinization characteristics of starch, and these are determined by the genes of plants (Sui & Kong, 2018; Ai & Jane, 2015). Lipids can inhibit swelling by affecting amylose by intertwining with amylopectin, and phospholipids can bind to amylose and inhibit pasting (Ai & Jane, 2015). Since the temperature of different plant-derived starches was different in this experiment, the different pasting properties may also be affected by the treatment temperature (Sui & Kong, 2018). In addition, parameters such as pH, shear rate, and sample concentration are all factors that may contribute to this result (Sui & Kong, 2018).

The effects of annealing on starch pasting properties are complex and vary among starches of different plant origins (Hoover, 2008). The pasting temperature of the annealed starch was increased, and the increase ranged from 0.5 to 4.7°C, which was consistent with the results of DSC. Among them, taro starch increased the most. Annealing treatments had different effects on peak viscosity, among which the peak

viscosity of quinoa starch, taro starch and maize starch decreased. The hot paste viscosity of starches other than potato starch decreased. The changing trend of cool paste viscosity is the same as that of hot paste viscosity. The changing trend of breakdown after five starch treatments was that all starches decreased except potato starch increased, and the change of setback was the same as that of breakdown.

It can be seen from the results that the annealing treatment improves the thermal stability of starch and delays the progress of gelatinization during the heating process. The increase in gelatinization temperature can delay the expansion of starch granules and affect the formation of pasting (Biduski et al., 2022). The increase in pasting temperature is due to the reduction of starch solubility and higher crystal melting temperature caused by the annealing treatment, which may be due to the partial microcrystalline structure caused by the treatment being more stable (Zhang et al., 2015; Hu et al., 2020).

The decrease in peak viscosity may be due to the increased crystallinity of starch, decreased swelling power and leaching of a small amount of amylose caused by annealing (Zhang et al., 2015; Liu et al., 2016). It may also be that the annealing treatment increases the interaction between starch molecular chains and improves the crystals, resulting in the limited hydrogen bonding force between starch molecules and water molecules, which reduces the swelling power and peak viscosity of starch granules (Xu et al. al., 2018a).

The result that the peak viscosity of potato starch increased after treatment was the same as Xu et al. (2018a), which showed that the peak viscosity of potato starch increased first with a shorter treatment time. This may be due to the enhanced ordering of amorphous regions in potato starch granules by annealing, resulting in higher resistance to shearing and heating in annealed potato starch (Wang et al., 2017b).

The cool paste viscosity and setback value are related to the retrogradation and hardness of starch gel, representing the stability of the cold paste (Zhang et al., 2019; Xu et al., 2018b). The leached amount of amylose and the long amylopectin content affected the values of these two parameters (Xu et al., 2018b; Liu et al., 2016a). Since the annealing treatment improved the crystal structure and reduced short amylopectin, the cool paste viscosity and setback value decreased (Xu et al., 2018b).

However, the increase in cool paste viscosity and setback value of potato starch after treatment may be due to the fact that the annealing treatment causes amylose to aggregate and rearrange during cooling, forming a starch network structure stabilized by hydrogen bonds (Zhang et al., 2019; Almeida et al., 2020; Su et al., 2020). This indicates that the treated starch cold paste is less stable and prone to gelation and retrogradation (Zhang et al., 2019; Xu et al., 2018a).

The Breakdown value shows the thermal and shear stability of starch paste at high temperatures (Su et al., 2020; Hu et al., 2020). Since the annealing treatment enhances the order of the amorphous region of starch granules, it is difficult for them to be destroyed, resulting in the reduced breakdown (Su et al., 2020; Xu et al., 2018a). Therefore, annealed starch has a stronger heat resistance and shear resistance of starch paste (Marboh et al., 2022). This indicates that the starch has a more stable conformation after annealing (Biduski et al., 2022), the same as the result of the swelling power above.

The hot paste viscosity of starch was reduced after treatment, the same as the results described by Singh et al. (2011) and Xu et al. (2018b). This is caused by the rearrangement of starch by annealing (Shen et al., 2021). The increase in hot paste viscosity of potato starch indicates that the annealing treatment slightly increases the size of starch granules and reduces the disintegration of starch granules, which may be related to the longer annealing time (Zhang et al., 2019).

Annealing reduces the peak viscosity of starch, so it can be used in foods that require heating during processing with lower viscosity, facilitating food processing and production (Marboh et al., 2022). In addition, it can also be applied to bread to give it a more unique texture (Sui & Kong, 2018).

4.8 Gel texture

See Chapter 3 for the method for determining the gel texture of starch. The results greatly impact the application of starch in food production.

Table 4.8.1 Gel texture of treated and untreated starches

Result		Quinoa	Amaranth	Taro	Potato	Maize
Hardness (g)	Control	25.19±2.29	2.92±0.27	14.93±0.36	40.61±0.00	67.59±0.89
	Annealing	34.24±2.95 #	3.06±0.19	17.14±1.13 *	64.9±6.10 #	76.62±6.91 *
Adhesiveness (g·s)	Control	-222.19±19.46	-25.98±0.93	-132.81±7.81	-351.72±27.61	-168.57±3.75
	Annealing	-284.49±18.63 #	-23.79±1.85	-124.97±8.55	-409.88±25.79	-306.03±18.72 #
Cohesiveness	Control	0.63±0.04	0.62±0.04	0.62±0.02	0.59±0.05	0.39±0.04
	Annealing	0.62±0.05	0.58±0.04	0.62±0.05	0.53±0.05	0.43±0.04 *

Data are displayed as mean values ± standard deviation values with different symbols after the treated result indicate significant differences * ($p<0.05$), extremely significant differences # ($p<0.01$).

The gel properties of the five starches before and after treatment are shown in Table 4.8.1. The hardness shows the hardness of the starch gel, and the adhesion represents the ability of the starch gel to adhere to other objects, which is due to the adhesion of the heavier water-soluble amylopectin bundles to the probes after the first compression (Iftikhar & Dutta, 2019), cohesion indicates the extent to which the structure of the starch gel is disrupted by the first compression during testing (Zhang et al., 2017). Refrigeration treatment increases the strength of starch gels as it promotes the retrogradation of starch gels and the tight arrangement of starch chains into three-dimensional complexes (Majzoobi et al., 2012).

It can be seen from Table 4.8.1 that among the five starches, maize starch has the highest gel hardness, and amaranth starch has the lowest gel hardness. In general, among the five starches, the gel hardness of large-granular starch is higher than that of small-granular starch gel. The gel of potato starch is the easiest to adhere to other items among the five starches, and the amaranth is the least easy to adhere to. The deformability of swollen particles and the size of the gel network formed by amylose are the main factors affecting the gel strength of starch (Steffolani, León & Pérez, 2013). Therefore, the lowest gel hardness of amaranth starch may be due to its low amylose content (Steffolani, León & Pérez, 2013). The cohesiveness of the gel of quinoa starch is the highest, the cohesiveness of the gel of amaranth, taro and potato starch is slightly lower than that of quinoa starch, and the cohesiveness of maize starch is the lowest, indicating that the reduced ability of maize starch gel is the worst after being compressed. In addition, the molecular weight of amylopectin also affects the gel properties of starch (Sui & Kong, 2018).

Annealing treatment increased the hardness of five starch colloids to different degrees, which was consistent with the results of Singh et al. (2011), Yadav, Guleria & Yadav (2013) and Chung, Moon & Chun (2000). Among them, the colloid hardness of quinoa starch and potato starch increased significantly, and the colloid hardness of taro and maize starch increased significantly. Annealing treatment can improve the crystallinity of starch granules and affect the gel properties by increasing the mobility of the amorphous region and ordering the double helix (Majzoobi et al., 2012). The increase in starch gel hardness may be due to the rearrangement of starch molecules caused by annealing treatment, which reduces the swelling power and solubility of starch, thereby reducing the proportion of gel volume and increasing gel hardness (Zavareze & Dias, 2011; Majzoobi et al., 2012; Singh et al., 2011; Wang et al., 2018).

For the adhesiveness, the annealing treatment significantly improved the gel adhesion of quinoa and maize starch, slightly increased the gel adhesion of potato

starch, and slightly decreased the gel adhesion of amaranth and taro starch. Among them, the reason for the decreased gel adhesion may be that the annealing treatment improves the stability of starch granule conformation, increases the interaction between starch chains, and reduces the leaching of amylose and the swelling of starch granules, thereby reducing the amaranth and taro starch gel viscosity, reducing its adhesion (Biduski et al., 2022). Yu et al. (2016) found that the adhesiveness of maize starch gel was affected by the annealing temperature and had different trends. Adhesiveness decreased at higher treatment temperatures (55°C) and increased at relatively low temperatures (45°C). Therefore, the difference in the changes of the five starches after annealing treatment may be directly caused by different treatment temperatures and different effects of amylose leaching (Yu et al., 2016).

Annealing treatment resulted in reduced cohesiveness of quinoa, amaranth and potato starches, as described by Molavi & Razavi (2018) and Biduski et al. (2022). The cohesiveness of maize starch was significantly increased after the annealing treatment. This result is in agreement with a previous study by Yu et al. (2016). However, the changes in the cohesiveness of maize starch gels were different at different annealing temperatures, the cohesiveness decreased at 55°C, and the cohesiveness increased at 45°C, which may be affected by the leached amylose (Yu et al., 2016). The texture characteristics of these gels before and after starch modification can be ideally applied to food and non-food products to achieve target hardness and viscosity (Iftikhar & Dutta, 2019; Steffolani, León & Pérez, 2013; Sui & Kong, 2018).

4.9 X-ray diffraction

See Chapter 3 for the experimental method of Xrd. The Xrd results show the long-range order information, those information are about the double helices form ordered crystalline structures (Marboh et al., 2022).

A

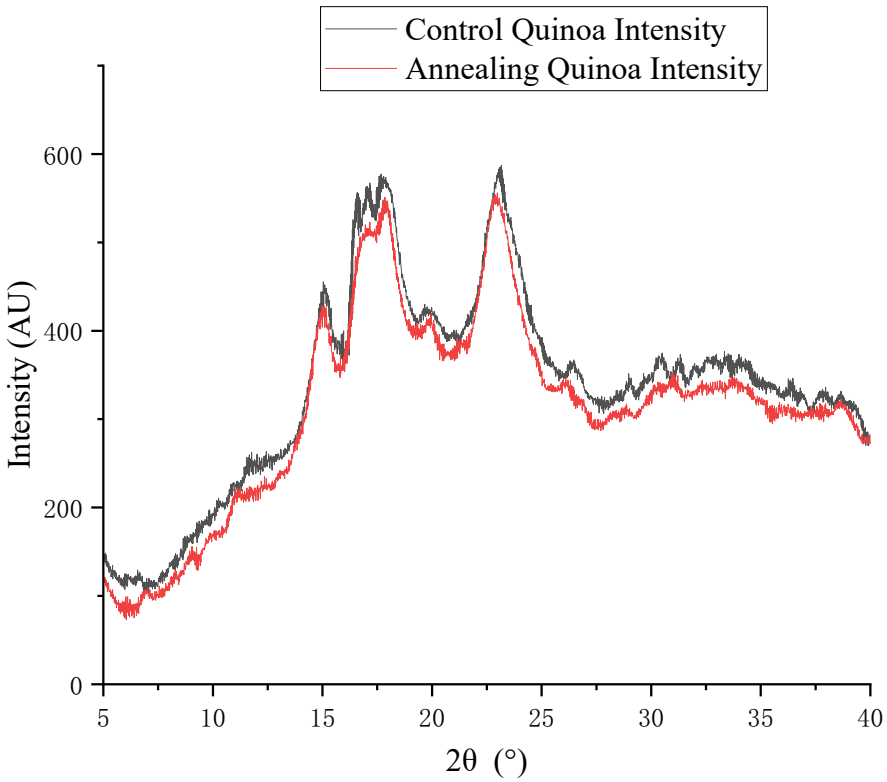

B

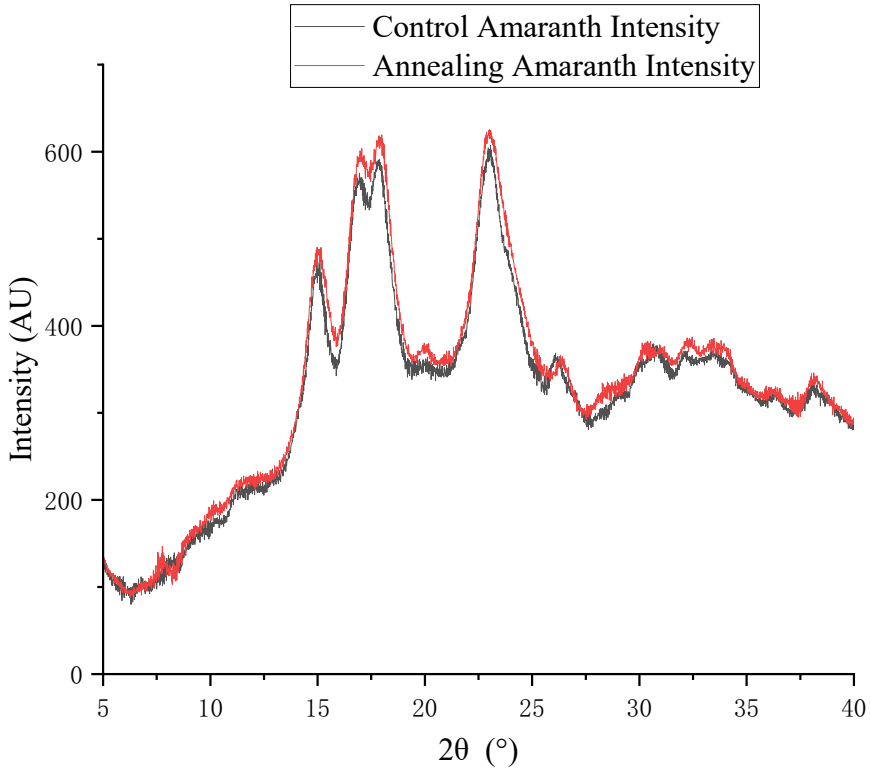
Control Amaranth Intensity
Annealing Amaranth Intensity
Intensity (AU)
0
200
400
600
5
10
15
20
25
30
35
40
2θ (°)

C

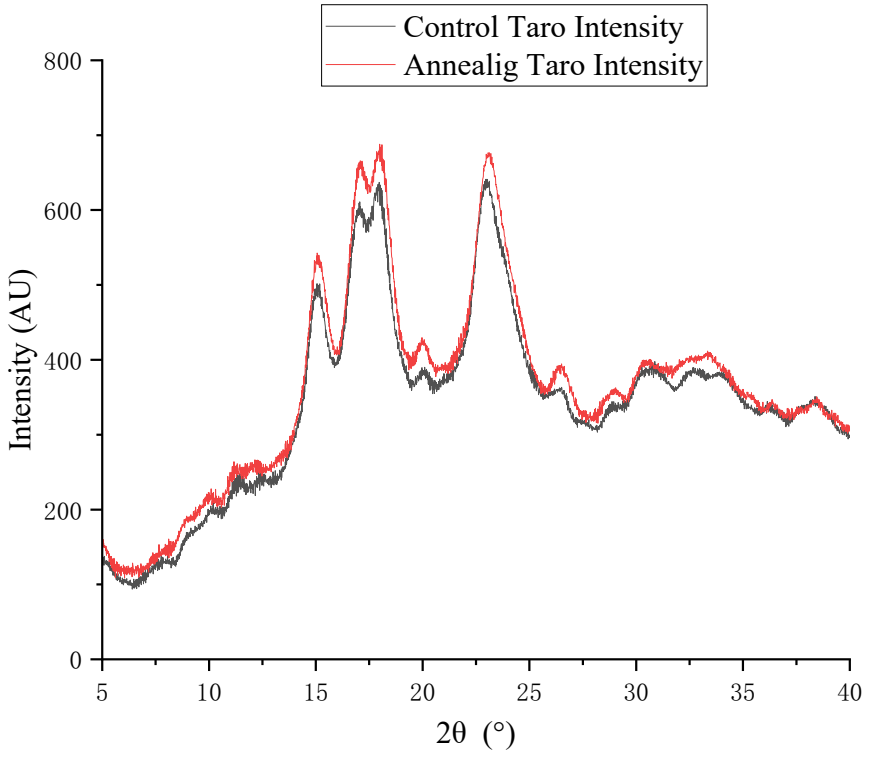
Control Taro Intensity
Annealig Taro Intensity
Intensity (AU)
0
200
400
600
800
5
10
15
20
25
30
35
40
2θ (°)

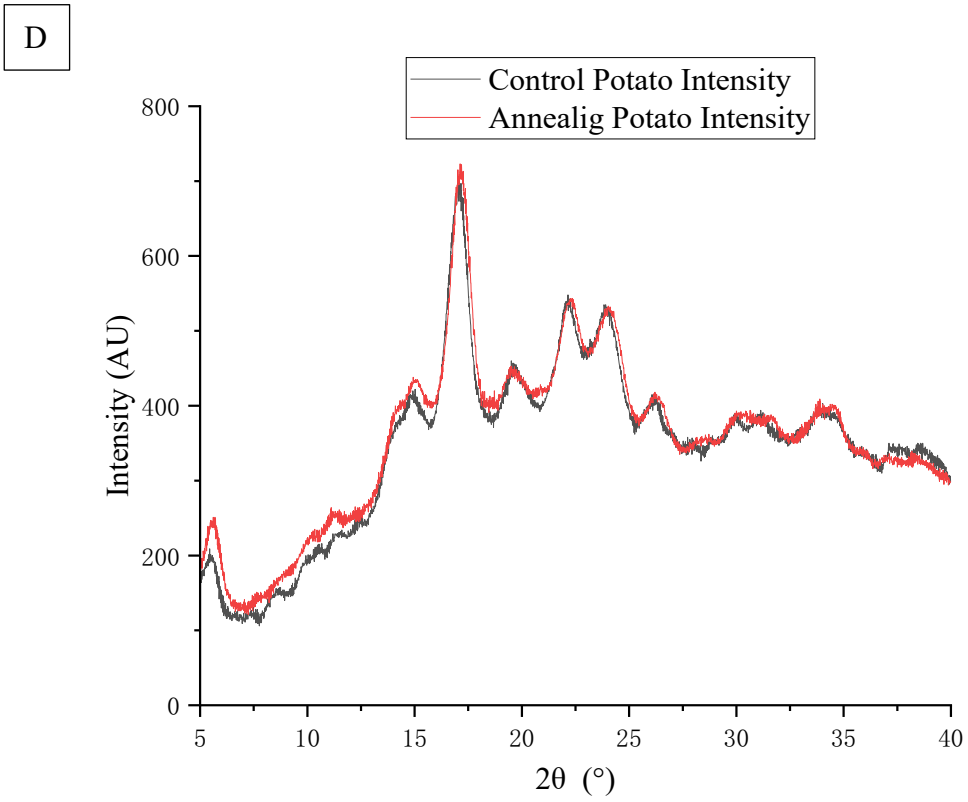

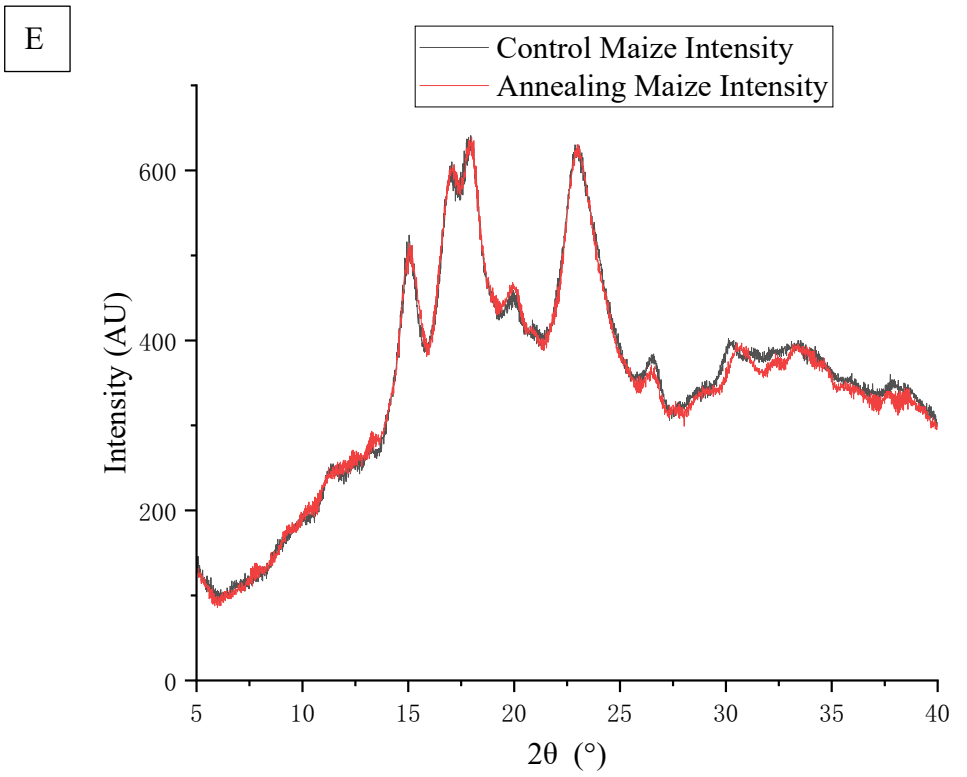

Figure. 4.9.1 The xrd result of control and annealed starches (A) Quinoa starch; (B) Amaranth starch; (C) Taro starch; (D) Potato starch; (E) Maize starch

There are three main crystalline types of starch. There are only four A-type crystallites with densely packed water molecules in the unit cell, an open B-type crystal containing thirty-six water molecules in the hydrated core, and both A-type and B-type crystals in the hydrated core. Form crystalline polymorphic mixture, C-starch (Zhang et al., 2015; Wang, Jin & Yu, 2013; Tester, Karkalas & Qi, 2004). Among them, A-type starch has lower water content, compact double helix structure, shorter amylopectin, and B-type starch has a looser structure (Tester, Karkalas & Qi, 2004; Srichuwong & Jane, 2007).

It can be seen from Figure 4.9.1 that quinoa, amaranth, taro and maize starch are typical A-type starches because they have two significant single peaks at Bragg angle (2θ) = 15°, 23°, and at Bragg angle (2θ) = 17°, there is a double peak at 18°, and a weak peak at Bragg angle (2θ) = 19°. Potato is B-starch because it has peaks at Bragg angle (2θ) = 5.6°, 15.0°, 17.0°, 19.5°, 22.0° and 24.0°, with the strongest peak at Bragg angle (2θ) = 17.0° consistent with Xu et al. (2018a).

In Figure 4.9.1, the change in the intensity of the diffraction peaks indicates that the annealing treatment has an effect on the relative crystallinity of the starch granules (Marboh et al., 2022; Zhang et al., 2015). Compared with the untreated quinoa starch, the X-ray diffraction pattern of the treated quinoa starch shifted slightly downward, and the diffraction intensity decreased. However, the spectra of amaranth, taro and potato starch can be seen to have a slight upward shift, and the diffraction intensity increases. Among them, the diffraction intensities of amaranth starch and taro starch were improved as a whole, and that of potato starch was mainly concentrated in the Bragg angle (2θ) = 5.0 - 17.0°. The profile of maize starch was almost unchanged, only slightly lower than that of untreated starch between Bragg angle (2θ) = 30.0 - 35.0°. There was no obvious change in the spectrum before and after treatment, indicating that the annealing treatment under this condition did not change the

structure types of the above five starches. The results are consistent with Wang, Jin & Yu (2013), Zhang et al. (2015) and Liu et al. (2009).

At Bragg angle (2θ) = 20.0°, the peaks of A-type starch, especially amaranth and taro starch, have obvious intensity changes, which may be due to the redirection of lipid molecules in the amorphous region to form an amylose-lipid complex (Sui & Kong, 2018; Waduge et al., 2006).

Table 4.9.1 Relative crystallinity of treated and untreated starches

Resule		Quinoa	Amaranth	Taro	Potato	Maize
Relative crystallinity	Control	0.25±0.01	0.30±0.01	0.32±0.00	0.25±0.01	0.32±0.02
	Annealing	0.24±0.01	0.34±0.01 *	0.35±0.01 *	0.27±0.01 *	0.33±0.01

Data are displayed as mean values ± standard deviation values with different symbols after the treated result indicate significant differences * ($p<0.05$), extremely significant differences # ($p<0.01$).

The crystallinity before and after starch treatment is shown in Table 4.9.1. Differences in relative crystallinity may be affected by differences in starch plant sources, extraction methods, and compositional differences such as fiber and protein content (Steffolani, León & Pérez, 2013). Relative crystallinity is associated with the formation of double helices from amylopectin branches, with amylopectin being the dominant influence (Marboh et al., 2022; Adebowale et al., 2009). The relative crystallinity of starch granules is also affected by the amylose content of the starch granules, the degree of amylose damage to the amylose crystallites, the number and degree of interaction between the double helices contained in the crystal array, and the crystallite size (Waduge et al., 2006; Dias et al., 2010; Biduski et al., 2022).

For untreated starch, the crystallinity of B-type starch is generally lower than that of A-type starch because the A-type starch granules contain a tight network structure (Sui & Kong, 2018).

From Table 4.9.1, it can be seen that the relative crystallinity of amaranth, taro and potato starch increased significantly after annealing treatment, which was consistent with Marboh et al. (2022), Zhang et al. (2015), Xu et al. (2018a) and Xu et al. (2018b). This may be due to the fact that the annealing treatment increases the crystal and double helix order in starch granules (Liu et al., 2016b; Yu et al., 2016). It is possible that annealing increases the size and integrity of starch granule crystals or that treatment induces the rearrangement of molten crystallites, resulting in more complete crystallization (Liu et al., 2016b; Hu et al., 2020; Yu et al., 2016; Marboh et al., 2022; Xu et al., 2018a). It is also possible that the previously unassociated starch chains formed new crystallites during the annealing process, slightly increasing the relative proportion of crystalline regions (Hu et al., 2020; Yu et al., 2016; Zhang et al., 2015; Xu et al., 2018a). It is also possible that the annealing treatment resulted in more amylose-amylose and amylose-amylopectin interactions in the starch (Marboh et al., 2022). The relative crystallinity of maize starch remained almost unchanged, with only a slight increase, which was the same as Rocha et al. (2012), Liu et al. (2009) and Xu et al. (2018a). Waduge et al. (2006) and Cheetham & Tao (1998) found that the relative crystallinity of maize starch decreased with increasing amylose content, so the reason for the slight increase in relative crystallinity of maize starch may be that the annealing treatment makes the amylose the starch is slightly leached, reducing the amylose content. However, they also indicated that this property might not apply to other starches (Waduge et al., 2006; Cheetham & Tao, 1998). The relative crystallinity of quinoa starch decreased slightly after annealing, but there was no significant difference. This may be due to the destruction or reorientation of very few crystallites during annealing (Hu et al., 2020; Wang et al., 2017b).

Annealing conditions also affect the crystalline properties of starch. For the annealing time, the relative starch crystallinity decreased and then increased during prolonged continuous annealing (Hu et al., 2020). They explain that during the whole process of annealing, starch first undergoes slight gelatinization, resulting in the destruction of crystalline regions, reducing relative crystallinity, and then annealing induces rearrangement of crystallites and the formation of new crystallites, thereby increasing relative crystallinity. However, Xu et al. (2018b) and Xu et al. (2018a) found that continuous annealing of red adzuki bean starch and potato starch resulted in a continuous increase in the relative crystallinity of starch. They explain that the annealing treatment may improve the perfection of the starch molecular crystallites, increase the mobility of the amorphous phase, and allow the crystals to pack efficiently (Xu et al., 2018a; Xu et al., 2018b). This result is consistent with Zhang et al. (2016) and Zhang et al. (2019).

4.10 Flow

See Chapter 3 for the steady flow determination method of starch. The study of starch flow properties contributes to the application of starch in food quality and senses (Devi & Sit, 2019).

The flow characteristics of the samples are shown in Table 4.10.1. The results were modeled using the Herschel-Bulkley model to describe the flow characteristics of starch before and after annealing. According to Equation 6, the shear stress increases with the increase of shear rate during the ascending and descending process of five starches. And the shear stress and shear rate do not have a linear relationship. Starch gel exhibits pseudo-plasticity, shear-thinning behavior. This is because the swollen particles deform and disintegrate under shear, disrupting the starch gel network (Hoover & Vasanthan, 1994; Li & Zhu, 2021). The flow behavior index n is a dimensionless constant, which represents the closeness of the flow of starch gel to Newtonian fluid, and the flow behavior index of Newtonian fluid is one (Zhou et al., 2017; Wu et al., 2016). The lower the n value, the higher the shear-thinning degree of starch (Li & Zhu, 2018; Devi & Sit, 2019). The n of starch gels is less than one, which indicates that the image is bent toward the abscissa axis during shearing (Wu et al., 2016; Zhou et al., 2017). This is due to shear breaking the entanglements in the starch gel network (Li & Zhu, 2021). In addition, although the upward and downward curves trended similarly, the downward curve for most starches was more sloping. The results are consistent with those reported by Zhou et al. (2017) and Wu et al. (2016).

Table 4.10.1 Herschel-Bulkley model for flow properties of treated and untreated starches

	Sample		Quinoa	Amaranth	Taro	Potato	Maize
Upward	K_0 (Pa)	Control	69.63±5.95	3.54±1.08	17.92±0.41	14.82±4.47	47.7±7.06
		Annealing	70.02±0.04	2.77±0.36	5.93±0.16 #	27.25±3.29	38.1±5.93
	K ($Pa \cdot s^n$)	Control	17.08±1.23	7.37±0.97	19.82±0.24	96.49±8.31	7.97±2.45
		Annealing	10.04±0.73 #	4.48±0.46	8.95±0.22 #	372.83±34.08 *	10.85±3.78
	n	Control	0.41±0.01	0.52±0.02	0.46±0.00	0.33±0.01	0.45±0.05
		Annealing	0.47±0.01 *	0.57±0.01	0.5±0.00 *	0.17±0.01 #	0.42±0.04
	Area	Control	270194.15±10819.61	174919.69±1857.62	335791.66±3999.19	720156.46±13419.44	164696.38±8366.17
		Annealing	245196.87±3202.59 *	146933.82±2189.44 #	196784.9±2148.78 #	839858.81±4236.92 *	171752.52±8058.28
	R^2	Control	0.99739	0.99875	0.99788	0.99622	0.98981
		Annealing	0.99371	0.99926	0.99992	0.99051	0.99314
Downward	K_0	Control	21.69±1.11	5.39±0.13	11.49±0.19	17.13±0.68	25.74±6.39

(Pa)	Annealing	18.86±0.30 *	2.84±0.09#	6.75±0.02 *	27.92±0.79 #	29.36±4.98
K ($Pa \cdot s^n$)	Control	14.99±0.53	10.01±0.02	5.83±0.11	27.65±0.61	10.51±1.89
	Annealing	13.84±0.11	8.16±0.18 *	4.14±0.17 *	24.41±0.14	11.19±1.74
n	Control	0.44±0.00	0.47±0.00	0.62±0.00	0.51±0.00	0.41±0.03
	Annealing	0.44±0.00	0.48±0.00	0.60±0.00	0.53±0.00 #	0.41±0.01
Area	Control	236346.08±9574.55	176646±4.71	273452.31±2849.78	630475.16±8141.07	153548.56±3882.96
	Annealing	220358.29±1178.38	152997.6±497.8 #	174393.81±2503.03 #	648157.55±1863.92	165105.08±6034.47
R^2	Control	0.99969	0.99998	0.99903	0.99984	0.99792
	Annealing	0.99977	0.99998	0.99882	0.99993	0.99730
Hysteresis loops (s^{-1} Pa·s)	Control	33848.07±1531.16	-1726.3±1852.91	62339.35±1149.41	89681.3±5278.37	11147.81±5769.17
	Annealing	24838.59±2024.21 *	-6063.78±1691.64	22391.09±354.25 #	191701.26±6100.84 #	6647.43±2023.81

K_0: yield stress; K: consistency coefficient; n: flow behavior index; Area: Curve integral with logarithmic abscissa; R^2: coefficient of determination; Hysteresis loops: the difference between upward area and downward area; Data are displayed as mean values ± standard deviation values with different symbols after the treated result indicate significant differences * ($p<0.05$), extremely significant differences # ($p<0.01$). Only part of the data was used for the upward yield stress fitting of annealed potato starch.

In the ascending region, amaranth starch had the lowest yield stress, followed by potato and taro starch, and quinoa starch had the highest yield stress, followed by maize starch. In the downside zone, the situation is similar to the upside zone. Amaranth still had the lowest yield stress, taro starch was higher than amaranth starch, and maize starch had the highest yield stress, but it was similar to quinoa and potato starch. This may be due to the different amylose content inside starch granules, and linear molecules such as amylose constitute the network of starch gels, which affect the yield stress (Li & Zhu, 2018; Li & Zhu, 2021). Amaranth starch has the least amylose content, so its gel has the lowest yield stress. Overall, shear reduced the yield stress of all starches except potato starch. Yield stress may also be affected by factors such as the ghost structure and its mechanical strength present in starch, starch granule size and the internal structure of amylopectin in starch (Li & Zhu, 2021).

Potato starch has the highest consistency coefficient in the ascending and descending regions. The consistency coefficient is affected by starch type, gel temperature and concentration (Wu et al., 2016). The swelling mode and the degree of contact between the swollen particles are also influencing factors, higher swelling leads to tighter packing between swollen particles and more frequent collisions (Hoover & Vasanthan, 1994). Therefore, the collisions between potato starch gel particles are frequent, which may make the consistency coefficient high (Hoover & Vasanthan, 1994). Shearing reduces the consistency coefficient of starches except for amaranth and maize starch, and the decrease is most obvious in taro and potato. The flow behavior index of potato starch in the ascending region is the lowest, which may be due to the fact that potato starch has the highest swelling power among the five starches (Table 4.6.1), and the sensitivity to shear deformation is proportional to the swelling power of starch granules (Hoover & Vasanthan, 1994).

A higher coefficient of determination ($R^2 \geq 0.989$) indicated that both the upward and downward curves fit the Herschel-Bulkley model well. Hysteresis loops represent the

extent to which starch gels lose resistance to shearing forces and damage their structures (Hoover & Vasanthan, 1994; Li & Zhu, 2021). Among them, maize starch was the highest, followed by potato starch and taro starch, and amaranth starch was the lowest among the five starches. A small upward-downward gap indicates weaker interactions, and the polymer and crosslink separate at higher shear rates but recombine at lower shear rates. It shows that the interaction force in amaranth starch gel is the weakest among the five starches, and it does not swell to deform or decompose under shear (Hoover & Vasanthan, 1994).

Annealing treatment reduced the yield stress of all starches except quinoa and potato starch on the upward curve and the downward curve of potato starch except potato and maize starch, among which the decrease of potato starch was the most obvious on the upward curve. The consistency coefficient of quinoa and taro starch decreased significantly after annealing treatment, the consistency coefficient of amaranth starch decreased, and potato starch increased significantly. This result is in agreement with a previous study by Hoover & Vasanthan (1994) and Devi & Sit (2019). The flow behavior index of quinoa and taro starch increased significantly, and the flow behavior index of amaranth starch increased, and the results were consistent with Devi & Sit (2019). It was shown that the annealing treatment reduced the pseudoplasticity of quinoa, amaranth and taro starch gels (Wu et al., 2016). In addition, the effect of annealing on the upward curve is greater than that on the downward curve. Annealing treatment reduced the Hysteresis loops of starches except potato starch to varying degrees, among which taro starch was significantly reduced, and quinoa starch was significantly reduced. It is shown that the annealing treatment reduces the degree of irreversible damage to the starch mentioned above. This may be due to the annealing treatment slightly changing the size of starch granules (Table 4.2.1), resulting in altered resistance of starch granules to disintegration and deformation (Hoover & Vasanthan, 1994).

4.11 Oscillation

The methods used in this section are described in Chapter 3 for determining starch oscillatory properties. The viscoelastic properties of starch can be analyzed and studied through the results of storage modulus (*G′*), loss modulus (*G″*) and the ratio of the loss modulus and the storage modulus (Sui & Kong, 2018). The dynamic shock results of starch can be found in Table 4.11.1. Its results show changes in starch structure as well as molecular structure (Molavi & Razavi, 2018). Its results are complemented with differential scanning calorimetry to understand starch gelatinization and retrogradation properties (Zhu, Bertoft & Li., 2016).

It can be seen from Figure 4.11.1 and Table 4.11.1 that the storage modulus of different samples varies with temperature rise. The figure shows that the storage modulus of quinoa starch starts to rise at around 53°C and reaches its highest value at 67°C, and the storage modulus of amaranth starch starts to rise at around 55°C and reaches its highest value at 63°C. The storage modulus of taro starch starts to rise around 73°C and reaches its highest value at 77°C. Among them, the storage modulus of quinoa starch and amaranth starch began to rise at a similar temperature, while taro starch was higher. For large-grain starch, the storage modulus of potato starch starts to rise at around 60°C and reaches the highest value at around 64°C. The storage modulus of maize starch begins to rise sharply at around 72°C and quickly reaches the highest value at 75°C, and the peak height is the highest among the five starches. Compared with the DSC results, it was found that the storage modulus of starch began to increase after the gelatinization start temperature, and the storage modulus reached the maximum value near the peak temperature. The results are consistent with Molavi & Razavi (2018) and Sinh et al. (2003). At the stage where the storage modulus remains unchanged, the amylose dissolves and the starch suspension transform into a sol (Hsu et al., 2000; Wu et al., 2016). The rapid increase in storage modulus may be due to the expansion of starch granules under the

influence of heat and water, filling the space, and the contact of the granules forms a three-dimensional network structure (Singh et al., 2003). It is also possible that the increase in gel volume and the formation of a tightly packed network of dissolved amylose molecules (Wu et al., 2016). Hsu et al. (2000) indicated that low molecular weight amylopectin and amylose might interact to form a gel.

After rising to a maximum value, the storage modulus of starch begins to decrease. This is because the gel structure of starch is destroyed during continuous heating due to the melting of the crystalline regions in the swollen starch granules, and the molecular mobility increases, so the starch granules become loose, the interchain interactions are weakened, and deformation occurs (Singh et al., 2003; Wu et al., 2016; Kong et al., 2010). It can be found from Figure 4.11.1 and Table 4.11.1 that the rheological properties of different starches are different. Same result as Singh et al. (2003). This is because the genotype and biological origin of starch determines the size, shape, and amylose-to-amylopectin ratio of starch granules, which affect the rheological properties of starch granules (Singh & Singh, 2001).

Table 4.11.1 Temperature sweep parameters of treated and untreated starches

			Quinoa	Amaranth	Taro	Potato	Maize
Heating	$T_{G' max}$ (°C)	Control	67.05±0.35	61.55±0.35	77.40±0.00	63.55±0.35	75.15±0.35
		Annealing	67.90±0.00	64.30±0.00	86.50±0.00	68.90±0.00 *	77.40±0.00
	G'_{max} (Pa)	Control	5480.00±14.14	293.00±1.41	1940.00±14.14	2960.00±42.43	7270.00±28.28
		Annealing	5010.00±42.43 *	159.00±4.24 #	425.00±1.41 #	2980.00±42.43	5895.00±35.36 #
	$T_{G'' max}$ (°C)	Control	63.80±0.00	61.30±0.00	77.15±0.35	62.05±0.35	73.40±0.00
		Annealing	63.80±0.00	64.3±0.00	89.10±0.00 *	66.80±0.00 *	75.40±0.00
	G''_{max} (Pa)	Control	321.50±2.12	71.00±2.69	277.50±0.71	916.00±43.84	1235.00±7.07
		Annealing	382.50±4.95 *	41.7±1.27 *	76.50±0.71 #	865.00±12.73	1050.00±14.14 *
	tan δmax	Control	0.06±0.00	0.24±0.01	0.14±0.00	0.31±0.01	0.17±0.00
		Annealing	0.08±0.00 #	0.26±0.00	0.18±0.00 *	0.29±0.00	0.18±0.00
	G'_{90} (Pa)	Control	2115.00±21.21	74.95±0.78	729.00±9.90	1025.00±21.21	3830.00±14.14
		Annealing	1820.00±70.71	63.45±1.34 *	882.50±14.85 #	1550.00±0.00 *	3285.00±7.07 #

	G''_{90} (Pa)	Control	168.50±3.54	28.25±0.35	118.50±2.12	165.00±4.24	244.50±0.71
		Annealing	159.00±4.24	24.70±0.42 *	144.00±2.83 *	270.50±2.12 #	244.00±1.41
	tan δ 90	Control	0.08±0.00	0.38±0.01	0.16±0.00	0.16±0.00	0.06±0.00
		Annealing	0.09±0.00	0.39±0.00	0.16±0.00 #	0.17±0.00 *	0.07±0.00 *
	G'_{25} (Pa)	Control	4490.00±113.14	89.70±0.14	875.50±0.71	1535.00±21.21	13000.00±0.00
		Annealing	4215.00±106.07	77.85±1.34 *	882.50±14.85	2270.00±28.28 #	12550.00±70.71
Cooling	G''_{25} (Pa)	Control	110.50±0.71	44.45±0.92	131.50±0.71	215.50±10.61	339.00±1.41
		Annealing	110.00±1.41	39.2±0.42 *	144.00±2.83	241.00±4.24	325.50±4.95
	tan δ 25	Control	0.02±0.00	0.50±0.01	0.15±0.00	0.14±0.00	0.03±0.00
		Annealing	0.03±0.00	0.50±0.00	0.16±0.00 *	0.11±0.00	0.03±0.00

$T_{G' max}$: the time of maximum storage modulus; G'_{max}: the maximum storage modulus; $T_{G'' max}$: the time of maximum loss modulus; G''_{max}:the maximum loss modulus; tan δmax: the ratio of the maximum loss modulus and the maximum storage modulus; G'_{90}: the storage modulus at 90°C; G''_{90}: the loss modulus at 90°C; tan δ 90: the ratio of the loss modulus and the storage modulus at 90°C; G'_{25}: the storage modulus at 25°C; G''_{25}: the loss modulus at 90°C; tan δ 25: the ratio of the loss modulus and the storage modulus at 25°C. Data are displayed as mean values ± standard deviation values with different symbols after the treated result indicate significant differences * ($p<0.05$), extremely significant differences # ($p<0.01$).

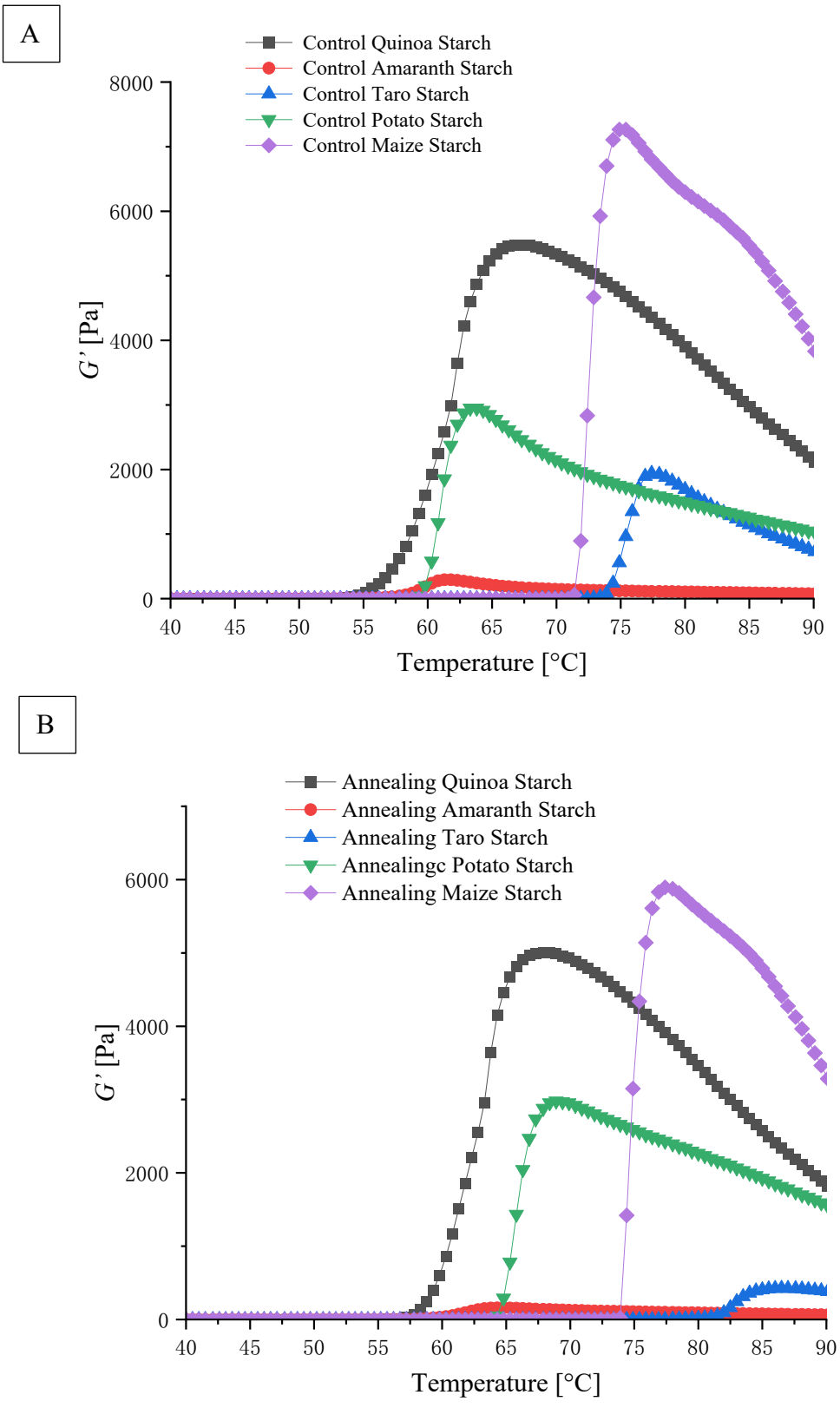

Figure 4.11.1 Changes of storage modulus (*G'*) of untreated starch (A) and annealed starch (B) with temperature change during the temperature rising stage

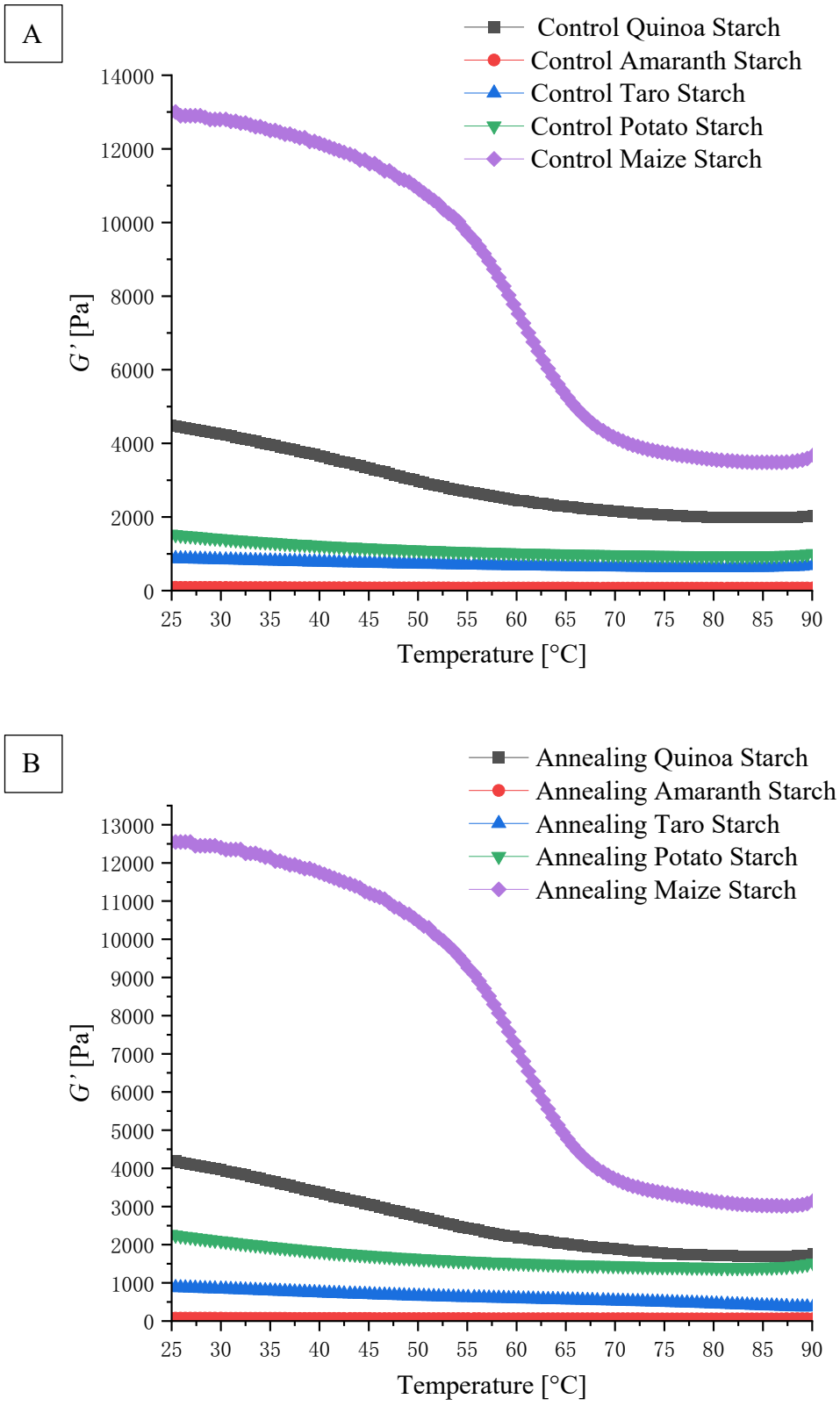

Figure 4.11.2 Variation of storage modulus (G') of untreated starch (A) and annealed starch (B) with temperature during the temperature drop stage

In the temperature drop stage, the storage modulus of the five starches gradually increased with the temperature decrease. In the higher temperature area (90 - 70°C), the storage modulus of the five starches increased slowly. In the area below 70°C, the storage modulus of starch increased rapidly, and the change of maize starch was the most obvious. The storage modulus of maize starch at 25°C is much higher than other starches. The storage modulus of amaranth, taro and potato starch is not much different at 25 and 90°C. This is due to the aggregation of amylose by intermolecular association and gel formation (Wu et al., 2016). It is found from Table 4.11.1 that tan δ decreases, which also proves the gel formation during cooling (Wu et al., 2016). The starch storage modulus after annealing treatment increased gradually with the temperature decrease. The difference between the storage modulus curves of taro starch and potato starch is more obvious.

The changing trend of the five types of starch loss modulus with temperature is the same as that of storage modulus. From the lower curve in Figure 4.11.1, Figure 4.11.3 and the tan δmax, an δ 90, and tan δ 25 in Table 4.11.1 are all less than 1. It can be seen that the storage modulus of starch is higher than the loss modulus, indicating that the samples are elastic (Osundahunsi & Mueller, 2011).

Table 4.11.1 shows that the storage modulus, loss modulus and loss tangent of the five starches are different. They are influenced by the shape of the starch granules, with irregularly shaped starches having smaller loss tangent and larger storage modulus, loss modulus than regular-shaped starches (Singh et al., 2003). The content of amylose in starch affects the results of storage modulus, loss modulus and loss tangent, and storage modulus and loss modulus increase with the increase of amylose content (Wu et al., 2016; Singh et al., 2003). In addition, the chain length of de-amylopectin has a high positive correlation with the storage modulus of starch (Kong et al., 2010). In addition, the phospholipid content, hardness and lipid content of starch granules may affect the storage modulus and loss modulus, the harder the

starch, the greater the storage modulus and loss modulus with more phospholipids (Singh et al., 2003).

The trend of starch storage and loss modulus after annealing did not change greatly in the temperature change stage. The storage modulus of most starches decreased after treatment, and the decrease in taro starch was the most obvious. However, the storage modulus of potato starch did not change greatly. Maize starch still has the highest storage modulus, and amaranth starch has the lowest storage modulus. But the temperature at which the storage modulus starts to rise increases, and the image shifts slightly to the right. Among them, taro starch and potato starch are the most obvious. This is consistent with the change in gelatinization onset temperature after starch treatment measured by DSC. As seen from the table, annealing reduced the storage modulus of starches except for potatoes, which is consistent with the results of Osundahunsi & Mueller (2011). This may be due to insufficient bond strength due to insufficient annealing time, resulting in decreased particle integrity. The storage modulus of potato starch increased after annealing. This result agrees with previous studies of Jacobs & Delcour (1998), Molavi & Razavi (2018). The loss tangent of annealed starch is similar to that of untreated starch. The loss tangent of some starch is slightly increased, the gel hardness and strength become larger, and it is difficult to recover after deformation, which is consistent with the gel texture results (Li & Zhu, 2018; Singh et al., 2003; Ai & Jane, 2015). There are also starches with slightly reduced loss tangent and reduced elasticity (Molavi & Razavi, 2018). Consistent with the results of Molavi & Razavi (2018).

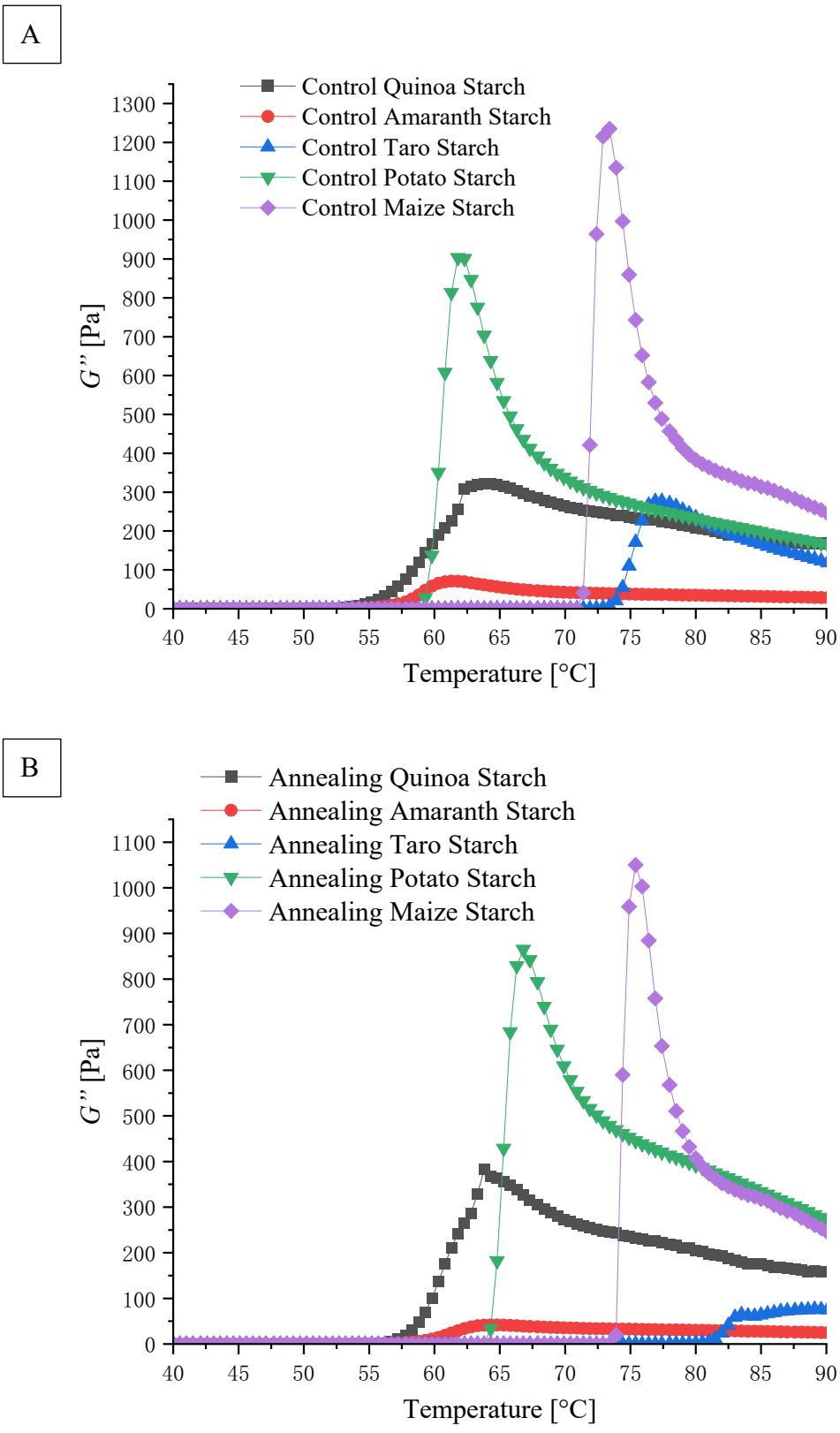

Figure 4.11.3 Changes of loss modulus (G″) of untreated starch (A) and annealed starch (B) with temperature change during the temperature rising stage

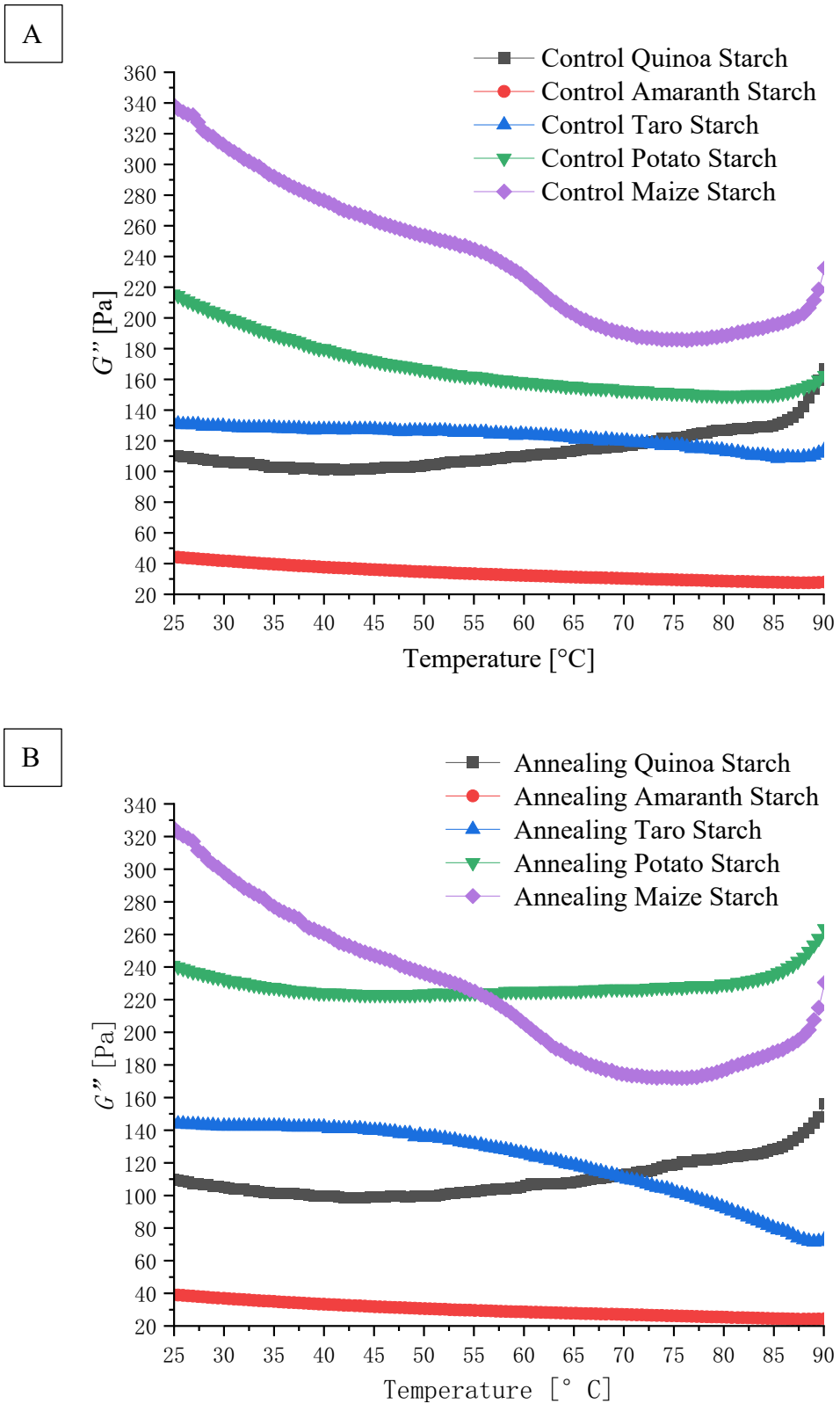

Figure 4.11.4 The change of loss modulus (G″) of untreated starch (A) and annealed starch (B) with temperature change during the temperature drop stage

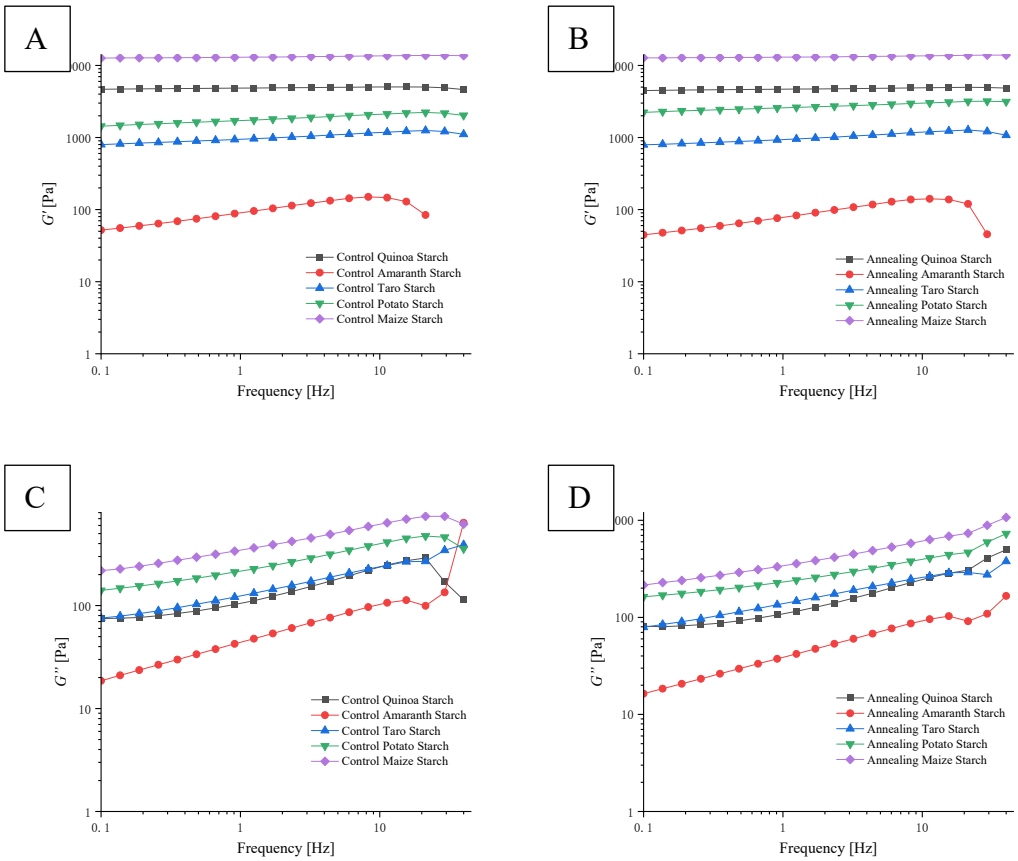

Figure 4.11.5 Changes of starch storage modulus (G'), loss modulus (G'') and frequency before and after annealing treatment.

A: The relationship between starch storage modulus (G') and frequency in the control group; B: The relationship between starch storage modulus (G') and frequency in the annealing group; C: relationship between starch loss modulus (G'') and frequency in control group; D: relationship between starch loss modulus (G'') and frequency in annealing group

Dynamic frequency sweeps can evaluate the viscoelasticity of the gels formed after the above heating and cooling phases (Wu et al., 2016). It can be seen from the figure that with the increase of frequency, the storage modulus of maize, potato, and taro starch increases, the storage modulus of quinoa starch first increases and then decreases, and the storage modulus of amaranth starch remains unchanged at first and then decreases. The image as a whole tends to be level with no noticeable change. After the annealing treatment, the changing trend of the storage modulus of each starch was basically unchanged, and the overall image was close to the level.

The upward trend of maize starch was more pronounced, the final downward trend of quinoa, taro and potato starch decreased and tended to be level, and the downward trend of amaranth starch moderated.

In the lower frequency range (0 - 25 Hz), the loss modulus shows an upward trend with increasing frequency, and the magnitude of the increase decreases gradually. Nevertheless, in the higher frequency (25 - 40 Hz) region, the loss modulus of quinoa, potato and maize starch gradually decreased. However, the loss modulus of amaranth and taro starch increased, and the increase of amaranth starch was pronounced. The starch loss modulus curve after annealing treatment is more stable, and the increase of the loss modulus in the lower frequency region is lower than before. However, in the areas with higher frequency, the loss modulus increased slightly, and the increase was relatively stable, except for the taro starch, which decreased slightly. This may be due to the annealing treatment changing the bond strength (Osundahunsi & Mueller, 2011).

Chapter 5. Conclusion and future work

5.1 Conclusion

In this experiment, by annealing small-grain quinoa, amaranth and taro starch and large-grain potato and maize starch, it was found that the properties of different plant-derived starches were different, and the effects of annealing on the properties of different starches were different. Annealing can slightly increase the particle size of starch, and the increase may be related to particle size. Annealing treatment can also reduce the smoothness of the starch granule surface. For thermal properties, annealing treatment increased the onset temperature and gelatinization enthalpy, which means annealing increased the thermal stability of starch, making it more wieldy use in cooked foods such as cans. However, there was no significant difference between large- and small-granular starches. In addition, annealing reduced the swelling power of five starches and the solubility of most starches. The difference in solubility effect may be due to the effect of the polymer. For pasting properties, the viscosity of most starches decreased after annealing. This can be used in foods that require heating during processing with low viscosity. However, the potato starch was different, which may be affected by the particle size. Annealing resulted in a more significant increase in particle diameter and reduced starch decomposition. The hardness of starch gels generally increases after annealing, which means annealed starch can be ideally applied to food and non-food products to achieve target hardness. Annealing did not affect the crystalline type of starch, and changes in relative crystallinity may not be related to starch granule size. Annealing has different effects on the flow and oscillation characteristics of different starches, and the influencing factors may not be related to the granule size of starch. Starch granule size has some influence on morphology and pasting caused by annealing but has little influence on crystallinity, gelatinization, flow and oscillation characteristics. Annealing

changed the physicochemical properties of starch to a certain extent, providing more possibilities for the application of starch.

5.2 Future work

In the future other large and small grain starches can be annealed to see the results and if there is a correlation with grain size.

The annealing conditions are difficult to determine when treating different plant-derived starches simultaneously, so a suitable annealing treatment condition for various starches can be determined in the future, including time, temperature and water content.

There are previous examples of co-modifying starch with other modification methods and annealing. However, other modification methods and annealing co-modify large-grain starch and small-grain starch, and few experiments compare the difference, so this may be a research direction.

Large- and small-granular starches with similar proportions of amylose and amylopectin were used for annealing modification to exclude their influence on the annealing results.

Modified starch has broad application prospects in the industry, and how to reduce the time cost of annealing in industrial production needs to be considered.

Taste and mouthfeel are essential properties of food, so annealed starch and its products are subjected to sensory evaluation to confirm their acceptability in food. In addition, its nutritional value and shelf life are also worth studying.

References

Adebowale, K. O., Henle, T., Schwarzenbolz, U., & Doert, T. (2009). Modification and properties of African yam bean (Sphenostylis stenocarpa Hochst. Ex A. Rich.) Harms starch I: Heat moisture treatments and annealing. *Food Hydrocolloids*, *23*(7), 1947-1957.

Adebowale, K. O., Olu-Owolabi, B. I., kehinde Olawumi, E., & Lawal, O. S. (2005). Functional properties of native, physically and chemically modified breadfruit (Artocarpus artilis) starch. *Industrial crops and products*, *21*(3), 343-351.

Agama-Acevedo, E., Garcia-Suarez, F. J., Gutierrez-Meraz, F., Sanchez-Rivera, M. M., San Martin, E., & Bello-Pérez, L. A. (2011). Isolation and partial characterization of Mexican taro (Colocasia esculenta L.) starch. *Starch-Stärke*, *63*(3), 139-146.

Ahamed, N. T., Singhal, R. S., Kulkarni, P. R., Kale, D. D., & Pal, M. (1996). Studies on Chenopodium quinoa and Amaranthus paniculatas starch as biodegradable fillers in LDPE films. *Carbohydrate Polymers*, *31*(3), 157-160.

Ai, Y., & Jane, J. L. (2015). Gelatinization and rheological properties of starch. *Starch-Stärke*, *67*(3-4), 213-224.

Akindahunsi, A. A. (2019). Investigation into the use of extracted starch from cassava and maize as admixture on the creep of concrete. *Construction and Building Materials*, *214*, 659-667.

Alcázar-Alay, S. C., & Meireles, M. A. A. (2015). Physicochemical properties, modifications and applications of starches from different botanical sources. *Food Science and Technology*, *35*, 215-236.

Almeida, M. C. B. D. M., Costa, S. D. S., Cavalcanti, M. T., & Almeida, E. L. (2020). Characterization of Prata Banana (Musa AAB-Prata) Starch: Native and Modified by Annealing. *Starch-Stärke*, *72*(3-4), 1900137.

Araujo-Farro, P. C., Podadera, G., Sobral, P. J., & Menegalli, F. C. (2010). Development of films based on quinoa (Chenopodium quinoa, Willdenow) starch. *Carbohydrate Polymers*, *81*(4), 839-848.

Baker, L. A., & Rayas-Duarte, P. (1998). Freeze-thaw stability of amaranth starch and the effects of salt and sugars. *Cereal Chemistry*, *75*(3), 301-307.

BARICHELLO, V., YADA, R. Y., COFFIN, R. H., & STANLEY, D. W. (1990). Low temperature sweetening in susceptible and resistant potatoes: starch structure and composition. *Journal of Food Science*, *55*(4), 1054-1059.

BeMiller, J. N., & Whistler, R. L. (Eds.). (2009). *Starch: chemistry and technology*. Academic Press.

Biduski, B., Werlang, S., Colussi, R., Pinto, V. Z., Zavareze, E. D. R., Gutkoski, L. C., & Bertolin, T. E. (2022). Starches Properties from Soft, Medium-Hard, and Hard Brazilian Wheat upon Annealing. *Starch-Stärke*, 2100267.

Biliaderis, C. G., Page, C. M., Maurice, T. J., & Juliano, B. O. (1986). Thermal characterization of rice starches: A polymeric approach to phase transitions of granular starch. *Journal of Agricultural and Food Chemistry*, *34*(1), 6-14.

Buléon, A., Gérard, C., Riekel, C., Vuong, R., & Chanzy, H. (1998). Details of the crystalline ultrastructure of C-starch granules revealed by synchrotron microfocus mapping. *Macromolecules*, *31*(19), 6605-6610.

Cao, X., Zhang, C., Dong, Y., Geng, P., Bai, F., & Bai, G. (2015). Modeling of cooked starch digestion process using recombinant human pancreatic α-amylase and maltase-glucoamylase for in vitro evaluation of α-glucosidase inhibitors. *Carbohydrate research*, *414*, 15-21.

Carlstedt, J., Wojtasz, J., Fyhr, P., & Kocherbitov, V. (2015). Understanding starch gelatinization: The phase diagram approach. *Carbohydrate Polymers*, *129*, 62-69.

Chandla, N. K., Saxena, D. C., & Singh, S. (2017). Amaranth (Amaranthus spp.) starch isolation, characterization, and utilization in development of clear edible films. *Journal of Food Processing and Preservation*, *41*(6), e13217.

Chaudhary, D. P., Kumar, S., & Langyan, S. (Eds.). (2014). *Maize: Nutrition dynamics and novel uses* (pp. 3-17). New Delhi: Springer India.

Cheetham, N. W., & Tao, L. (1998). Variation in crystalline type with amylose content in maize starch granules: an X-ray powder diffraction study. *Carbohydrate polymers*, *36*(4), 277-284.

Chung, K. M., Moon, T. W., & Chun, J. K. (2000). Influence of annealing on gel properties of mung bean starch. *Cereal Chemistry*, *77*(5), 567-571.

da Rosa Zavareze, E., & Dias, A. R. G. (2011). Impact of heat-moisture treatment and annealing in starches: A review. *Carbohydrate polymers*, *83*(2), 317-328.

Dai, L., Qiu, C., Xiong, L., & Sun, Q. (2015). Characterisation of corn starch-based films reinforced with taro starch nanoparticles. *Food chemistry*, *174*, 82-88.

Das, A., & Sit, N. (2021). Modification of taro starch and starch nanoparticles by various physical methods and their characterization. *Starch-Stärke*, *73*(5-6), 2000227.

Devi, R., & Sit, N. (2019). Effect of single and dual steps annealing in combination with hydroxypropylation on physicochemical, functional and rheological properties of barley starch. *International journal of biological macromolecules*, *129*, 1006-1014.

Dhital, S., Warren, F. J., Butterworth, P. J., Ellis, P. R., & Gidley, M. J. (2017). Mechanisms of starch digestion by α-amylase—Structural basis for kinetic properties. *Critical reviews in food science and nutrition*, *57*(5), 875-892.

Dias, A. R. G., da Rosa Zavareze, E., Spier, F., de Castro, L. A. S., & Gutkoski, L. C. (2010). Effects of annealing on the physicochemical properties and enzymatic susceptibility of rice starches with different amylose contents. *Food chemistry*, *123*(3), 711-719.

Ek, K. L., Brand-Miller, J., & Copeland, L. (2012). Glycemic effect of potatoes. *Food Chemistry*, *133*(4), 1230-1240.

Elkonin, L. A., Italianskaya, J. V., Fadeeva, I. Y., Bychkova, V. V., & Kozhemyakin, V. V. (2013). In vitro protein digestibility in grain sorghum: effect of genotype and interaction with starch digestibility. *Euphytica*, *193*(3), 327-337.

Englyst, K., Goux, A., Meynier, A., Quigley, M., Englyst, H., Brack, O., & Vinoy, S. (2018). Inter-laboratory validation of the starch digestibility method for determination of rapidly digestible and slowly digestible starch. *Food chemistry*, *245*, 1183-1189.

Ezekiel, R., Singh, N., Sharma, S., & Kaur, A. (2013). Beneficial phytochemicals in potato—a review. *Food Research International*, *50*(2), 487-496.

Falade, K. O., & Ayetigbo, O. E. (2022). Influence of physical and chemical modifications on granule size frequency distribution, fourier transform infrared (FTIR) spectra and adsorption isotherms of starch from four yam (Dioscorea spp.) cultivars. *Journal of Food Science and Technology*, *59*(5), 1865-1877.

Fonseca, L. M., El Halal, S. L. M., Dias, A. R. G., & da Rosa Zavareze, E. (2021). Physical modification of starch by heat-moisture treatment and annealing and their applications: A review. *Carbohydrate Polymers*, 118665.

Friedman, M. (1997). Chemistry, biochemistry, and dietary role of potato polyphenols. A review. *Journal of agricultural and food chemistry*, *45*(5), 1523-1540.

Giuri, A., Colella, S., Listorti, A., Rizzo, A., & Corcione, C. E. (2018). Biodegradable extruded thermoplastic maize starch for outdoor applications. *Journal of Thermal Analysis and Calorimetry*, *134*(1), 549-558.

Gordillo-Bastidas, E., Díaz-Rizzolo, D. A., Roura, E., Massanés, T., & Gomis, R. (2016). Quinoa (Chenopodium quinoa Willd), from nutritional value to potential health benefits: an integrative review. *J. Nutr. Food Sci*, *6*(497), 10-4172.

Gorinstein, S., Pawelzik, E., Delgado-Licon, E., Haruenkit, R., Weisz, M., & Trakhtenberg, S. (2002). Characterisation of pseudocereal and cereal proteins by protein and amino acid analyses. *Journal of the Science of Food and Agriculture*, *82*(8), 886-891.

Guo, B., Wang, Y., Pang, M., Wu, J., Hu, X., Huang, Z., ... & Liu, C. (2020). Annealing treatment of amylose and amylopectin extracted from rice starch. *International Journal of Biological Macromolecules*, *164*, 3496-3500.

Hoover, R. (2001). Composition, molecular structure, and physicochemical properties of tuber and root starches: a review. *Carbohydrate polymers*, *45*(3), 253-267.

Hoover, R., & Vasanthan, T. (1993). The effect of annealing on the physicochemical properties of wheat, oat, potato and lentil starches. *Journal of Food Biochemistry*, *17*(5), 303-325.

Hoover, R., & VASANTHAN, T. (1994). The flow properties of native, heat-moisture treated, and annealed starches from wheat, oat, potato and lentil. *Journal of Food Biochemistry*, *18*(2), 67-82.

Hormdok, R., & Noomhorm, A. (2007). Hydrothermal treatments of rice starch for improvement of rice noodle quality. *LWT-Food science and Technology*, *40*(10), 1723-1731.

Hsien-Chih, H. W., & Sarko, A. (1978). The double-helical molecular structure of crystalline A-amylose. *Carbohydrate Research*, *61*(1), 27-40.

Hsu, S., Lu, S., & Huang, C. (2000). Viscoelastic changes of rice starch suspensions during gelatinization. *Journal of food science*, *65*(2), 215-220.

Hu, A., Wang, X., Li, L., Xu, T., & Zheng, J. (2020). Effects of annealing time on structure and properties of sweet potato starch. *Cereal Chemistry*, *97*(3), 573-580.

Iftikhar, S. A., & Dutta, H. (2019). Status of polymorphism, physicochemical properties and in vitro digestibility of dual retrogradation-annealing modified rice starches. *International journal of biological macromolecules*, *132*, 330-339.

Jacobs, H., & Delcour, J. A. (1998). Hydrothermal modifications of granular starch, with retention of the granular structure: A review. *Journal of agricultural and food chemistry*, *46*(8), 2895-2905.

James, L. E. A. (2009). Quinoa (Chenopodium quinoa Willd.): composition, chemistry, nutritional, and functional properties. *Advances in food and nutrition research*, *58*, 1-31.

Jane, J., Shen, L., Chen, J., Lim, S., Kasemsuwan, T., & Nip, W. (1992). Physical and chemical studies of taro starches and flours1 2. *Cereal Chem*, *69*(5), 528-535.

Jayakody, L., & Hoover, R. (2008). Effect of annealing on the molecular structure and physicochemical properties of starches from different botanical origins–A review. *Carbohydrate polymers*, *74*(3), 691-703.

Ji, N., Ge, S., Li, M., Wang, Y., Xiong, L., Qiu, L., ... & Sun, Q. (2019). Effect of annealing on the structural and physicochemical properties of waxy rice starch nanoparticles: Effect of annealing on the properties of starch nanoparticles. *Food chemistry*, *286*, 17-21.

Kapusniak, K., & Nebesny, E. (2017). Enzyme-resistant dextrins from potato starch for potential application in the beverage industry. *Carbohydrate polymers*, *172*, 152-158.

Karlsson, M. E., & Eliasson, A. C. (2003). Gelatinization and retrogradation of potato (Solanum tuberosum) starch in situ as assessed by differential scanning calorimetry (DSC). *LWT-Food Science and Technology*, *36*(8), 735-741.

Kim, Y. S., Wiesenborn, D. P., Orr, P. H., & Grant, L. A. (1995). Screening potato starch for novel properties using differential scanning calorimetry. *Journal of food science*, *60*(5), 1060-1065.

Kong, X., Kasapis, S., Bao, J., & Corke, H. (2012). Influence of acid hydrolysis on thermal and rheological properties of amaranth starches varying in amylose content. *Journal of the Science of Food and Agriculture*, *92*(8), 1800-1807.

Kong, X., Kasapis, S., Bertoft, E., & Corke, H. (2010). Rheological properties of starches from grain amaranth and their relationship to starch structure. *Starch-Stärke*, *62*(6), 302-308.

Kulshreshtha, Y., Schlangen, E., Jonkers, H. M., Vardon, P. J., & Van Paassen, L. A. (2017). CoRncrete: A corn starch based building material. *Construction and Building Materials*, *154*, 411-423.

Larsson, I., & Eliasson, A. C. (1991). Annealing of starch at an intermediate water content. *Starch-Stärke*, *43*(6), 227-231.

Lavoisier, A., & Aguilera, J. M. (2019). Starch gelatinization inside a whey protein gel formed by cold gelation. *Journal of Food Engineering*, *256*, 18-27.

Lawal, O. S., & Adebowale, K. O. (2005). Physicochemical characteristics and thermal properties of chemically modified jack bean (Canavalia ensiformis) starch. *Carbohydrate Polymers*, *60*(3), 331-341.

Li, G., & Zhu, F. (2017a). Physicochemical properties of quinoa flour as affected by starch interactions. *Food Chemistry*, *221*, 1560-1568.

Li, G., & Zhu, F. (2017b). Amylopectin molecular structure in relation to physicochemical properties of quinoa starch. *Carbohydrate Polymers*, *164*, 396-402.

Li, G., & Zhu, F. (2018). Effect of high pressure on rheological and thermal properties of quinoa and maize starches. *Food Chemistry*, *241*, 380-386.

Li, G., & Zhu, F. (2021). Physicochemical, rheological, and emulsification properties of nonenyl succinic anhydride (NSA) modified quinoa starch. *International Journal of Biological Macromolecules*, *193*, 1371-1378.

Li, G., Xu, X., & Zhu, F. (2019). Physicochemical properties of dodecenyl succinic anhydride (DDSA) modified quinoa starch. *Food chemistry*, *300*, 125201.

Li, Q., Shi, S., Dong, Y., & Yu, X. (2021). Characterisation of amylose and amylopectin with various moisture contents after frying process: effect of starch–lipid complex formation. *International Journal of Food Science & Technology*, *56*(2), 639-647.

Li, S., Zhang, B., Tan, C. P., Li, C., Fu, X., & Huang, Q. (2019). Octenylsuccinate quinoa starch granule-stabilized Pickering emulsion gels: Preparation, microstructure and gelling mechanism. *Food Hydrocolloids*, *91*, 40-47.

Li, W., Gao, J., Wu, G., Zheng, J., Ouyang, S., Luo, Q., & Zhang, G. (2016). Physicochemical and structural properties of A-and B-starch isolated from normal and waxy wheat: Effects of lipids removal. *Food Hydrocolloids*, *60*, 364-373.

Lindeboom, N., Chang, P. R., & Tyler, R. T. (2004). Analytical, biochemical and physicochemical aspects of starch granule size, with emphasis on small granule starches: a review. *Starch-Stärke*, *56*(3-4), 89-99.

Liu, H., Guo, X., Li, W., Wang, X., Peng, Q., & Wang, M. (2015). Changes in physicochemical properties and in vitro digestibility of common buckwheat starch by heat-moisture treatment and annealing. *Carbohydrate polymers*, *132*, 237-244.

Liu, H., Lv, M., Wang, L., Li, Y., Fan, H., & Wang, M. (2016a). Comparative study: How annealing and heat-moisture treatment affect the digestibility, textural, and physicochemical properties of maize starch. *Starch-Stärke*, *68*(11-12), 1158-1168.

Liu, H., Wang, L., Shen, M., Guo, X., lv, M., & Wang, M. (2016b). Changes in physicochemical properties and in vitro digestibility of tartary buckwheat and sorghum starches induced by annealing. *Starch-Stärke*, *68*(7-8), 709-718.

Liu, H., Yu, L., Simon, G., Dean, K., & Chen, L. (2009). Effects of annealing on gelatinization and microstructures of corn starches with different amylose/amylopectin ratios. *Carbohydrate Polymers*, *77*(3), 662-669.

Lu, T. J., Lin, J. H., Chen, J. C., & Chang, Y. H. (2008). Characteristics of taro (Colocasia esculenta) starches planted in different seasons and their relations to the molecular structure of starch. *Journal of agricultural and food chemistry*, *56*(6), 2208-2215.

Majzoobi, M., Sabery, B., Farahnaky, A., & Karrila, T. T. (2012). Physicochemical properties of cross-linked-annealed wheat starch. *Iranian Polymer Journal*, *21*(8), 513-522.

Malinski, E., Daniel, J. R., Zhang, X. X., & Whistler, R. L. (2003). Isolation of small starch granules and determination of their fat mimic characteristics. *Cereal chemistry*, *80*(1), 1-4.

Malumba, P., Massaux, C., Deroanne, C., Masimango, T., & Béra, F. (2009). Influence of drying temperature on functional properties of wet-milled starch granules. *Carbohydrate polymers*, *75*(2), 299-306.

Marboh, V., Gayary, M. A., Gautam, G., & Mahanta, C. L. (2022). Comparative Study of Heat-Moisture Treatment and Annealing on Morphology, Crystallinity, Pasting, and Thermal Properties of Sohphlang (Flemingia vestita) Starch. *Starch-Stärke*, 2100294.

Martuscelli, E., & Pracella, M. (1974). Effects of chain defects on the thermal behaviour of polyethylene. *Polymer*, *15*(5), 306-314.

Mizuno, A., Mitsuiki, M., & Motoki, M. (1998). Effect of crystallinity on the glass transition temperature of starch. *Journal of Agricultural and Food Chemistry*, *46*(1), 98-103.

Molavi, H., & Razavi, S. M. (2018). Dynamic rheological and textural properties of acorn (Quercus brantii Lindle.) starch: Effect of single and dual hydrothermal modifications. *Starch-Stärke*, *70*(11-12), 1800086.

Nakazawa, Y., & Wang, Y. J. (2004). Effect of annealing on starch–palmitic acid interaction. *Carbohydrate Polymers*, *57*(3), 327-335.

Osundahunsi, O. F., & Mueller, R. (2011). Dynamic rheological and physicochemical properties of annealed starches from two cultivars of cassava. *Carbohydrate Polymers*, *83*(4), 1916-1921.

Pachuau, L., Dutta, R. S., Devi, T. B., Deka, D., & Hauzel, L. (2018). Taro starch (Colocasia esculenta) and citric acid modified taro starch as tablet disintegrating agents. *International journal of biological macromolecules*, *118*, 397-405.

Ratnayake, W. S., & Jackson, D. S. (2009). Starch Gelatinization. In S. L. Taylor (Ed.), *Advances in Food and Nutrition Research,* 55 (pp. 221-268).

Ray, A., Inamdar, A. A., Sakhare, S. D., & Srivastava, A. K. (2021). Development of physical process for quinoa fractionation and targeted separation of germ with physical, chemical and SEM studies. *LWT*, *141*, 110957.

Rayner, M., Timgren, A., Sjöö, M., & Dejmek, P. (2012). Quinoa starch granules: a candidate for stabilising food-grade Pickering emulsions. *Journal of the Science of Food and Agriculture*, *92*(9), 1841-1847.

Rocha, T. S., Cunha, V. A., Jane, J. L., & Franco, C. M. (2011). Structural characterization of Peruvian carrot (Arracacia xanthorrhiza) starch and the effect of annealing on its semicrystalline structure. *Journal of agricultural and food chemistry*, *59*(8), 4208-4216.

Rocha, T. S., Felizardo, S. G., Jane, J. L., & Franco, C. M. (2012). Effect of annealing on the semicrystalline structure of normal and waxy corn starches. *Food Hydrocolloids*, *29*(1), 93-99.

Rouf Shah, T., Prasad, K., & Kumar, P. (2016). Maize—A potential source of human nutrition and health: A review. *Cogent Food & Agriculture*, *2*(1), 1166995.

Sadeghi, R., Daniella, Z., Uzun, S., & Kokini, J. (2017). Effects of starch composition and type of non-solvent on the formation of starch nanoparticles and improvement of curcumin stability in aqueous media. *Journal of Cereal Science*, *76*, 122-130.

Sáez-Plaza, P., Michałowski, T., Navas, M. J., Asuero, A. G., & Wybraniec, S. (2013). An overview of the Kjeldahl method of nitrogen determination. Part I. Early history, chemistry of the procedure, and titrimetric finish. *Critical Reviews in Analytical Chemistry*, *43*(4), 178-223.

Shen, H., Xu, M., Su, C., Zhang, B., Ge, X., Zhang, G., & Li, W. (2021). Insights into the relations between the molecular structures and physicochemical properties of normal and waxy wheat B-starch after repeated and continuous annealing. *International Journal of Food Science & Technology*, *56*(12), 6405-6419.

Shi, Y. C. (2008). Two-and multi-step annealing of cereal starches in relation to gelatinization. *Journal of agricultural and food chemistry*, *56*(3), 1097-1104.

Simsek, S., & El, S. N. (2012). Production of resistant starch from taro (Colocasia esculenta L. Schott) corm and determination of its effects on health by in vitro methods. *Carbohydrate polymers*, *90*(3), 1204-1209.

Simsek, S., Ovando-Martínez, M., Whitney, K., & Bello-Pérez, L. A. (2012). Effect of acetylation, oxidation and annealing on physicochemical properties of bean starch. *Food Chemistry*, *134*(4), 1796-1803.

Singh, H., Chang, Y. H., Lin, J. H., Singh, N., & Singh, N. (2011). Influence of heat–moisture treatment and annealing on functional properties of sorghum starch. *Food Research International*, *44*(9), 2949-2954.

Singh, J., & Singh, N. (2001). Studies on the morphological, thermal and rheological properties of starch separated from some Indian potato cultivars. *Food chemistry*, *75*(1), 67-77.

Singh, N., Singh, J., Kaur, L., Sodhi, N. S., & Gill, B. S. (2003). Morphological, thermal and rheological properties of starches from different botanical sources. *Food chemistry*, *81*(2), 219-231.

Song, H. Y., Lee, S. Y., Choi, S. J., Kim, K. M., Kim, J. S., Han, G. J., & Moon, T. W. (2014). Digestibility and physicochemical properties of granular sweet potato starch as affected by annealing. *Food Science and Biotechnology*, *23*(1), 23-31.

Srichuwong, S., & Jane, J. I. (2007). Physicochemical properties of starch affected by molecular composition and structures: a review. *Food science and biotechnology*, *16*(5), 663-674.

Steffolani, M. E., León, A. E., & Pérez, G. T. (2013). Study of the physicochemical and functional characterization of quinoa and kañiwa starches. *Starch-Stärke*, *65*(11-12), 976-983.

Stute, R. (1992). Hydrothermal modification of starches: The difference between annealing and heat/moisture-treatment. *Starch-Stärke*, *44*(6), 205-214.

Su, C., Saleh, A. S., Zhang, B., Zhao, K., Ge, X., Zhang, Q., & Li, W. (2020). Changes in structural, physicochemical, and digestive properties of normal and waxy wheat starch during repeated and continuous annealing. *Carbohydrate polymers*, *247*, 116675.

Sui, Z., & Kong, X. (Eds.). (2018). *Physical modifications of starch*. Springer.

Teli, M. D., Rohera, P., Sheikh, J., & Singhal, R. (2009). Application of germinated maize starch in textile printing. *Carbohydrate Polymers*, *75*(4), 599-603.

Tester, R. F., & Debon, S. J. (2000). Annealing of starch—a review. *International journal of biological macromolecules*, *27*(1), 1-12.

Tester, R. F., Debon, S. J. J., & Sommerville, M. D. (2000). Annealing of maize starch. *Carbohydrate Polymers*, *42*(3), 287-299.

Tester, R. F., Debon, S. J. J., Davies, H. V., & Gidley, M. J. (1999). Effect of temperature on the synthesis, composition and physical properties of potato starch. *Journal of the Science of Food and Agriculture*, *79*(14), 2045-2051.

Tester, R. F., Karkalas, J., & Qi, X. (2004). Starch—composition, fine structure and architecture. *Journal of cereal science*, *39*(2), 151-165.

Tester, R. F., Karkalas, J., & Qi, X. (2004). Starch—composition, fine structure and architecture. *Journal of cereal science*, *39*(2), 151-165.

Tsai, M. L., Li, C. F., & Lii, C. Y. (1997). Effects of granular structures on the pasting behaviors of starches. *Cereal Chemistry*, *74*(6), 750-757.

Vamadevan, V., & Bertoft, E. (2015). Structure-function relationships of starch components. *Starch-Stärke*, *67*(1-2), 55-68.

Velásquez-Barreto, F. F., Miñano, H. A., Alvarez-Ramirez, J., & Bello-Pérez, L. A. (2021). Structural, functional, and chemical properties of small starch granules: Andean quinoa and kiwicha. *Food Hydrocolloids*, *120*, 106883.

Waduge, R. N., Hoover, R., Vasanthan, T., Gao, J., & Li, J. (2006). Effect of annealing on the structure and physicochemical properties of barley starches of varying amylose content. *Food research international*, *39*(1), 59-77.

Wang, H., Wu, Y., Wang, N., Yang, L., & Zhou, Y. (2019). Effect of water content of high-amylose corn starch and glutinous rice starch combined with lipids on formation of starch–lipid complexes during deep-fat frying. *Food chemistry*, *278*, 515-522.

Wang, K., Wang, W., Ye, R., Xiao, J., Liu, Y., Ding, J., ... & Liu, A. (2017a). Mechanical and barrier properties of maize starch–gelatin composite films: effects of amylose content. *Journal of the Science of Food and Agriculture*, *97*(11), 3613-3622.

Wang, L., Zhang, C., Chen, Z., Wang, X., Wang, K., Li, Y., ... & Li, J. (2018). Effect of annealing on the physico-chemical properties of rice starch and the quality of rice noodles. *Journal of Cereal Science*, *84*, 125-131.

Wang, S., Jin, F., & Yu, J. (2013). Pea starch annealing: New insights. *Food and Bioprocess Technology*, *6*(12), 3564-3575.

Wang, S., Jin, F., & Yu, J. (2013). Pea starch annealing: New insights. *Food and Bioprocess Technology*, *6*(12), 3564-3575.

Wang, S., Wang, J., Wang, S., & Wang, S. (2017b). Annealing improves paste viscosity and stability of starch. *Food Hydrocolloids*, *62*, 203-211.

Wang, S., Wang, J., Yu, J., & Wang, S. (2014). A comparative study of annealing of waxy, normal and high-amylose maize starches: The role of amylose molecules. *Food Chemistry*, *164*, 332-338.

Wang, S., Wang, J., Yu, J., & Wang, S. (2014). A comparative study of annealing of waxy, normal and high-amylose maize starches: The role of amylose molecules. *Food Chemistry*, *164*, 332-338.

Wang, X., Yuan, Y., & Yue, T. (2015). The application of starch-based ingredients in flavor encapsulation. *Starch-Stärke*, *67*(3-4), 225-236.

Wang, Y., Ye, F., Liu, J., Zhou, Y., Lei, L., & Zhao, G. (2018). Rheological nature and dropping performance of sweet potato starch dough as influenced by the binder pastes. *Food Hydrocolloids*, *85*, 39-50.

Wang, Y., Zhan, J., Lu, H., Chang, R., Qiu, L., & Tian, Y. (2021). Amylopectin crystal seeds: Characterization and their effect on amylopectin retrogradation. *Food Hydrocolloids*, *111*, 106409.

Wani, A. A., Singh, P., Shah, M. A., Schweiggert-Weisz, U., Gul, K., & Wani, I. A. (2012). Rice starch diversity: Effects on structural, morphological, thermal, and physicochemical properties—A review. *Comprehensive Reviews in Food Science and Food Safety*, *11*(5), 417-436.

Wilpiszewska, K., & Czech, Z. (2014). Citric acid modified potato starch films containing microcrystalline cellulose reinforcement–properties and application. *Starch-Stärke*, *66*(7-8), 660-667.

Wu, K., Dai, S., Gan, R., Corke, H., & Zhu, F. (2016). Thermal and rheological properties of mung bean starch blends with potato, sweet potato, rice, and sorghum starches. *Food and Bioprocess Technology*, *9*(8), 1408-1421.

Xu, M., Saleh, A. S., Gong, B., Li, B., Jing, L., Gou, M., ... & Li, W. (2018a). The effect of repeated versus continuous annealing on structural, physicochemical, and digestive properties of potato starch. *Food Research International*, *111*, 324-333.

Xu, M., Saleh, A. S., Liu, Y., Jing, L., Zhao, K., Wu, H., ... & Li, W. (2018b). The changes in structural, physicochemical, and digestive properties of red adzuki bean starch after repeated and continuous annealing treatments. *Starch-Stärke*, *70*(9-10), 1700322.

Xu, Z., Song, L., Ming, S., Zhang, C., Li, Z., Wu, Y., ... & Corke, H. (2022). Removal of starch granule associated proteins affects annealing of normal and waxy maize starches. *Food Hydrocolloids*, *131*, 107695.

Yadav, B. S., Guleria, P., & Yadav, R. B. (2013). Hydrothermal modification of Indian water chestnut starch: Influence of heat-moisture treatment and annealing on the physicochemical, gelatinization and pasting characteristics. *LWT-Food Science and Technology*, *53*(1), 211-217.

Yu, K., Wang, Y., Wang, Y., Guo, L., & Du, X. (2016). Effects of annealing and additives on the gelatinization, structure, and textural characteristics of corn starch. *International Journal of Food Properties*, *19*(6), 1272-1281.

Yu, K., Wang, Y., Xu, Y., Guo, L., & Du, X. (2016). Correlation between wheat starch annealing conditions and retrogradation during storage. *Czech Journal of Food Sciences*, *34*(1), 79-86.

Zhang, B., Wu, C., Li, H., Hu, X., Jin, Z., Tian, Y., & Xu, X. (2015). Long-term annealing of C-type kudzu starch: Effect on crystalline type and other physicochemical properties. *Starch-Stärke*, *67*(7-8), 577-584.

Zhang, B., Wu, H., Gou, M., Xu, M., Liu, Y., Jing, L., ... & Li, W. (2019). The comparison of structural, physicochemical, and digestibility properties of repeatedly and continuously annealed sweet potato starch. *Journal of food science*, *84*(8), 2050-2058.

Zhang, L., Li, G., Wang, S., Yao, W., & Zhu, F. (2017). Physicochemical properties of maca starch. *Food chemistry*, *218*, 56-63.

Zhou, D. N., Zhang, B., Chen, B., & Chen, H. Q. (2017). Effects of oligosaccharides on pasting, thermal and rheological properties of sweet potato starch. *Food Chemistry*, *230*, 516-523.

Zhu, F. (2016). Impact of γ-irradiation on structure, physicochemical properties, and applications of starch. *Food Hydrocolloids*, *52*, 201-212.

Zhu, F. (2016). Structure, properties, and applications of aroid starch. *Food Hydrocolloids*, *52*, 378-392.

Zhu, F. (2017). Structures, physicochemical properties, and applications of amaranth starch. *Critical reviews in food science and nutrition*, *57*(2), 313-325.

Zhu, F. (2018). Modifications of starch by electric field based techniques. *Trends in Food Science & Technology*, *75*, 158-169.

Zhu, F. (2019a). Starch based Pickering emulsions: Fabrication, properties, and applications. *Trends in Food Science & Technology*, *85*, 129-137.

Zhu, F. (2019b). Recent advances in modifications and applications of sago starch. *Food Hydrocolloids*, *96*, 412-423.

Zhu, F., Bertoft, E., & Li, G. (2016). Morphological, thermal, and rheological properties of starches from maize mutants deficient in starch synthase III. *Journal of agricultural and food chemistry*, *64*(34), 6539-6545.

Zhu, L., Jones, C., Guo, Q., Lewis, L., Stark, C. R., & Alavi, S. (2016). An evaluation of total starch and starch gelatinization methodologies in pelleted animal feed. *Journal of animal science*, *94*(4), 1501-1507.

Appendix

Appendix Table 1 DSC results of annealed 48h and untreated starch

Result		Quinoa	Amaranth	Taro	Potato	Maize
T_o (°C)	Control	53.37±0.20	55.75±0.03	72.34±0.20	58.00±0.11	68.94±0.31
	Annealing	55.81±0.17 #	57.80±0.05 #	75.30±0.25 *	63.12±0.03 #	70.63±0.16 #
T_p (°C)	Control	63.10±0.51	61.99±0.24	76.17±0.30	61.35±0.03	72.76±0.10
	Annealing	63.65±0.29	62.42±0.18 *	78.51±0.31 *	66.29±0.04 #	73.68±0.24*
T_c (°C)	Control	73.10±0.69	70.96±0.23	86.07±1.09	68.81±0.21	78.57±0.19
	Annealing	73.40±0.52	70.92±0.05	86.18±0.19	71.49±0.18 #	78.76±0.44
Δ T (°C)	Control	19.73±0.59	15.21±0.21	13.73±1.04	10.81±0.25	9.63±0.39
	Annealing	17.59±0.35 #	13.12±0.08 #	10.88±0.06 #	8.37±0.21 #	8.13±0.48 *
Δ H (J/g)	Control	12.84±0.24	16.21±0.27	18.81±0.77	21.27±0.25	16.19±0.26
	Annealing	13.31±0.23 *	15.89±0.23	19.85±0.75	18.23±0.31 #	14.91±0.53 *

Data are displayed as mean values ± standard deviation values with different symbols after the treated result indicate significant differences * ($p<0.05$), extremely significant differences # ($p<0.01$).